VOLUME XLVI NUMBER 1

AUG 4 1917
UNIV. OF MICH. LIBRARY

THE ASTROPHYSICAL JOURNAL

AN INTERNATIONAL REVIEW OF SPECTROSCOPY AND ASTRONOMICAL PHYSICS

EDITED BY

GEORGE E. HALE
Mount Wilson Solar Observatory of the Carnegie Institution of Washington

EDWIN B. FROST
Yerkes Observatory of the University of Chicago

HENRY G. GALE
Ryerson Physical Laboratory of the University of Chicago

JULY 1917

SELECTIVE REFLECTION AND ABSORPTION IN THE ULTRA-VIOLET REGION OF THE SPECTRUM *E. O. Hulburt* 1

PHOTOGRAPHS OF NEBULAE WITH THE 60-INCH REFLECTOR 1911–1916 - - *Francis G. Pease* 24

LIGHT-CURVES AND ORBITAL ELEMENTS OF TT LYRAE AND Y CAMELOPARDALIS *Martha Betz Shapley* 56

STUDIES BASED ON THE COLORS AND MAGNITUDES IN STELLAR CLUSTERS *Harlow Shapley* 64

EFFECT OF A LONGITUDINAL MAGNETIC FIELD UPON GLOW-DISCHARGE *R. F. Earhart and C. B. Jolliffe* 76

MINOR CONTRIBUTIONS AND NOTES:
Note on the Southern Tail of Halley's Comet Seen May 17 and 18, 1910, E. E. Barnard, 83.

THE UNIVERSITY OF CHICAGO PRESS
CHICAGO, ILLINOIS, U.S.A.

Agents
THE CAMBRIDGE UNIVERSITY PRESS, London and Edinburgh
THE MARUZEN-KABUSHIKI-KAISHA, Tokyo, Osaka, Kyoto, Fukuoka, Sendai
THE MISSION BOOK COMPANY, Shanghai

THE ASTROPHYSICAL JOURNAL

AN INTERNATIONAL REVIEW OF SPECTROSCOPY AND ASTRONOMICAL PHYSICS

EDITED BY

GEORGE E. HALE
Mount Wilson Solar Observatory of the
Carnegie Institution of Washington

EDWIN B. FROST
Yerkes Observatory of the
University of Chicago

HENRY G. GALE
Ryerson Physical Laboratory of the
University of Chicago

WITH THE COLLABORATION OF

JOSEPH S. AMES, Johns Hopkins University
ARISTARCH BELOPOLSKY, Observatoire de Poulkova
WILLIAM W. CAMPBELL, Lick Observatory
HENRY CREW, Northwestern University
CHARLES FABRY, Université de Marseille
CHARLES S. HASTINGS, Yale University
HEINRICH KAYSER, Universität Bonn
ALBERT A. MICHELSON, University of Chicago
HUGH F. NEWALL, Cambridge University
ERNEST F. NICHOLS, Yale University
ALFRED PEROT, Paris
EDWARD C. PICKERING, Harvard College Observatory
ANNIBALE RICCÒ, Osservatorio di Catania
CARL RUNGE, Universität Göttingen
ARTHUR SCHUSTER, The University, Manchester
FRANK SCHLESINGER, Allegheny Observatory

The Astrophysical Journal is published by the University of Chicago at the University Press during each month except February and August. ¶ The subscription price is $5.00 a year; the price of single copies is 65 cents. Orders for service of less than a half-year will be charged at the single-copy rate. ¶ Postage is prepaid by the publishers on all orders from the United States, Mexico, Cuba, Porto Rico, Panama Canal Zone, Republic of Panama, Hawaiian Islands, Philippine Islands, Guam, Samoan Islands, Shanghai. ¶ Postage is charged extra as follows: For Canada, 30 cents on annual subscriptions (total $5.30), on single copies, 3 cents (total 68 cents); for all other countries in the Postal Union, 62 cents on annual subscriptions (total $5.62), on single copies, 11 cents (total 76 cents). ¶ Patrons are requested to make all remittances payable to The University of Chicago Press in postal or express money orders or bank drafts.

The following agents have been appointed and are authorized to quote the prices indicated:

For the British Empire: The Cambridge University Press, Fetter Lane, London, E.C. 4. Yearly subscriptions, including postage, 23*s.* each; single copies, including postage, 3*s.* 3*d.* each.

For Japan and Korea: The Maruzen-Kabushiki-Kaisha, 11 to 16 Nihonbashi Tori Sanchome, Tokyo, Japan. Yearly subscriptions, including postage, Yen 11.25 each; single copies, including postage, Yen 1.50 each.

For China: The Mission Book Company, 18 Peking Road, Shanghai. Yearly subscriptions $5.00; single copies, 65 cents, or their equivalents in Chinese money. Postage extra, if mailed direct outside of Shanghai, on yearly subscriptions 62 cents, on single copies 11 cents.

Claims for missing numbers should be made within the month following the regular month of publication. The publishers expect to supply missing numbers free only when losses have been sustained in transit, and when the reserve stock will permit. Deliveries are not guaranteed in the war zones of Europe nor in other countries where transportation is disturbed by conditions incident to war.

Business correspondence should be addressed to The University of Chicago Press, Chicago, Ill.

Communications for the editors and manuscripts should be addressed to the Editors of THE ASTROPHYSICAL JOURNAL, Yerkes Observatory, Williams Bay, Wisconsin.

The cable address of the Editorial Office is "Arcturus, Chicago."

The articles in this Journal are indexed in the *Readers' Guide Supplement*, White Plains, N.Y.

Entered as second-class matter, January 17, 1895, at the Post-office at Chicago, Ill., under the act of March 3, 1879.

CONTENTS

NUMBER I

PAGE

SELECTIVE REFLECTION AND ABSORPTION IN THE ULTRA-VIOLET REGION OF THE SPECTRUM. E. O. Hulburt 1

PHOTOGRAPHS OF NEBULAE WITH THE 60-INCH REFLECTOR 1911–1916. Francis G. Pease 24

LIGHT-CURVES AND ORBITAL ELEMENTS OF TT LYRAE AND Y CAMELOPARDALIS. Martha Betz Shapley 56

STUDIES BASED ON THE COLORS AND MAGNITUDES IN STELLAR CLUSTERS. Harlow Shapley 64

EFFECT OF A LONGITUDINAL MAGNETIC FIELD UPON GLOW-DISCHARGE. R. F. Earhart and C. B. Jolliffe 76

MINOR CONTRIBUTIONS AND NOTES: Note on the Southern Tail of Halley's Comet Seen May 17 and 18, 1910, E. E. Barnard . 83

NUMBER II

THE MATHEMATICAL STRUCTURE OF BAND SERIES. Raymond T. Birge 85

A METHOD OF INVESTIGATING THE STARK EFFECT FOR METALS, WITH RESULTS FOR CHROMIUM. J. A. Anderson 104

A DETERMINATION OF THE GALACTIC CONDENSATION FROM CERTAIN ZONES OF THE *Astrographic Catalogue*. Frederick H. Seares . 117

THE ELIMINATION OF POLE-EFFECT FROM THE SOURCE FOR SECONDARY STANDARDS OF WAVE-LENGTH. Charles E. St. John and Harold D. Babcock 138

THE MINIMUM RADIATION VISUALLY PERCEPTIBLE. Prentice Reeves 167

PRELIMINARY EXAMINATION OF THE PLANETARY NEBULAE FOR PREFERENTIAL MOTION. C. D. Perrine 175

NOTICE 179

324689

NUMBER III

PAGE

BAND AND LINE SPECTRA OF IODINE. R. W. Wood and M. Kimura 181

ZEEMAN-EFFECT FOR COMPLEX LINES OF IODINE. R. W. Wood and M. Kimura 197

PHOTOGRAPHIC EFFECTIVE WAVE-LENGTHS OF SOME SPIRAL NEBULAE AND GLOBULAR CLUSTERS. Knut Lundmark and Bertil Lindblad 206

A NEW FORM OF SPECTRO-COMPARATOR. Ralph E. De Lury . . 219

ON THE SPIRAL OF OBSCURATION IN THE STELLAR UNIVERSE. A REPLY TO MR. F. H. SEARES. H. H. Turner 226

THE SPIRAL OF OBSCURATION. COMMENTS ON PROFESSOR TURNER'S REPLY. Frederick H. Seares 232

REVIEWS: Collected Papers on Spectroscopy, G. D. Liveing and Sir J. Dewar (H. C.) 238

NUMBER IV

THE VARIATION WITH TIME OF THE CHARACTERISTICS OF A POTASSIUM PHOTO-ELECTRIC CELL AS TO SENSIBILITY ACCORDING TO WAVE-LENGTH. Herbert E. Ives 241

THE PRINCIPLE OF GENERALIZED RELATIVITY AND THE DISPLACEMENT OF FRAUNHOFER LINES TOWARD THE RED. Charles E. St. John 249

RELATION TO PROPER MOTION OF PREFERENTIAL MOTION AND OF THE PROGRESSIONS OF SPECTRAL CLASS AND MAGNITUDE-VELOCITY. C. D. Perrine 266

NOTES ON THE COLOR-CURVE AND LIGHT-ELEMENTS OF W URSAE MAJORIS. Harlow Shapley and J. Van der Bilt 281

BAXANDALL'S EXPLANATION OF AN "ABNORMAL" SOLAR SPECTRUM. George E. Hale 291

THE MINIMUM RADIATION VISUALLY PERCEPTIBLE. Henri Buisson 296

SOLAR HYDROGEN "BOMBS." Ferdinand Ellerman 298

REVIEWS: The Principles of Aërography, Alexander McAdie (W. I. M.) 301

NUMBER V

PAGE

A DIFFERENTIAL SPECTRO-PHOTOMETER. G. A. Shook . . . 305

THE LUMINOSITIES AND PARALLAXES OF FIVE HUNDRED STARS. FIRST LIST. Walter S. Adams and A. H. Joy 313

THE STRUCTURE OF THE MERCURY LINE, λ 2536. Lucy Wilson . 340

MINOR CONTRIBUTIONS AND NOTES: On the Temperature and Radiation of the Sun, Felix Biscoe, 355; Wave-Lengths of the Stronger Lines in the Helium Spectrum, Paul W. Merrill, 357.

COMMUNICATION. W. S. Eichelberger 366

INDEX 367

THE
ASTROPHYSICAL JOURNAL
AN INTERNATIONAL REVIEW OF SPECTROSCOPY
AND ASTRONOMICAL PHYSICS

VOLUME XLVI JULY 1917 NUMBER 1

SELECTIVE REFLECTION AND ABSORPTION IN THE ULTRA-VIOLET REGION OF THE SPECTRUM

By E. O. HULBURT

1. *Introductory.*—The phenomenon of selective reflection from the surface of certain liquids for monochromatic radiation of wave-length below 400 $\mu\mu$ has been observed by P. G. Nutting,[1] F. F. Martens,[2] and E. Flatow.[3]

Carbon disulphide, cassia oil, and monobromnaphthalene were found to exhibit traces of selective reflection for ultra-violet light. By photographic methods the positions of the maxima of reflection were determined, and the regions of absorption of thin films of the substances were mapped.

In the present investigation quantitative measurements of the reflecting powers of these and other substances have been made at various wave-lengths in the region from 210 $\mu\mu$ to 450 $\mu\mu$ by means of a grating spectrograph with a sodium photo-electric cell. At the same time the percentage transmission of thin films of the substances pressed between quartz plates has been determined. The liquids chosen for investigation were those possessing strong absorption bands and high values of the refractive index, for it is

[1] *Physical Review*, **13**, 193, 1901.

[2] *Annalen der Physik*, **6**, 603, 1901. [3] *Ibid.*, **12**, 85, 1903.

only in such cases that appreciable reflecting powers, i.e., values above 5 per cent, were to be expected.

The values of the reflecting power found in the present work, combined with the values of the refractive index, have been introduced into the formulae of the generalized dispersion theory to compute the optical constants of the substances.

2. *Theoretical.*—The three most important electron theories of dispersion—that of Helmholtz-Reiff-Drude, that of H. A. Lorentz, and that of M. Planck (first form)—differ only in respect to the interpretation of the meaning of the constants of the equations. The final formulae for n, the refractive index, and K, the extinction coefficient, obtained from these three theories are of the same form and are obtained by introducing a frictional term into the equation of motion of the dispersion electron.

Let ϵ be the base of natural logarithms, and let all independent variables contain the time only in the factor $\epsilon^{i\frac{2\pi c}{\lambda}t}$, where $\frac{2\pi c}{\lambda}$ is the frequency, λ the wave-length of the vibration, and c is the velocity of light *in vacuo*. Then the complete dispersion formula is

$$\frac{1}{\sigma+\frac{1}{[n(1-iK)]^2-1}}=\sum\frac{C_s\lambda_s^2\lambda^2/4\pi^2c^2}{\lambda^2-\lambda_s^2-ib_s\lambda_s^2\lambda/2\pi c}. \qquad (1)$$

$\frac{2\pi c}{\lambda_s}$ is the frequency of the natural undamped vibration of the s'th electron. σ is a constant; two special types are obtained by making it zero, or $\frac{1}{3}$.

$$C_s=4\pi N_s\frac{e_s^2}{m_s},$$

where e_s is the charge, m_s the mass of the electron, and N_s is the number of such electrons per unit volume. b_s denotes absorption; if b_s is zero, K is zero, and (1) simplifies to the Sellmeier type of dispersion formula.

We assume that we are concerned with a region of absorption which is far removed from other similar regions, so that in the summation of (1) all the terms except one may be replaced by a

quantity independent of λ; hence in the vicinity of wave-length λ we write

$$\frac{1}{\sigma+\dfrac{1}{[n(1-iK)]^2-1}}=q_1+\frac{C_1\lambda_1^2\lambda^2/4\pi^2c^2}{\lambda^2-\lambda_1^2+ib_1\lambda_1^2\lambda/2\pi c}. \tag{2}$$

Separating real and imaginary parts, we find

$$\left.\begin{aligned}\frac{n^2(1-K^2)}{q_1'}&=1+\frac{g\lambda^2(\lambda^2-\lambda_1'^2)}{(\lambda^2-\lambda_1'^2)^2+g'^2\lambda^2}\\ \frac{2n^2K}{q_1'}&=\frac{gg'\lambda^3}{(\lambda^2-\lambda_1'^2)^2+g'^2\lambda^2}\end{aligned}\right\} \tag{3}$$

where q_1', g_2 λ_1', and g' are defined by the following equations,

$$\left.\begin{aligned}q_1'&=\frac{1+q_1(1-\sigma)}{1-q_1\sigma},\quad g=\frac{C_1}{(1-q_1\sigma)^2}\cdot\frac{\lambda_1'^2}{q_1'4\pi^2c^2}\\ \frac{4\pi^2c^2}{\lambda_1'^2}&=\frac{4\pi^2c^2}{\lambda_1^2}-\frac{C_1\sigma}{1-q_1\sigma},\quad g'=\frac{b_1\lambda_1'^2}{2\pi c}\end{aligned}\right\}. \tag{4}$$

We obtain the special case of no absorption by making b_1 zero. In that case (3) becomes

$$\frac{n^2}{q_1'}=1+\frac{g\lambda^2}{\lambda^2-\lambda_1'^2}. \tag{5}$$

The reflecting power at normal incidence, R, of the substance in contact with a medium of refractive index n' and extinction coefficient K′ is given by the formula

$$R=\frac{(n-n')^2+(nK-n'K')^2}{(n+n')^2+(nK+n'K')^2}.$$

In the present work the measurements of the reflecting powers were made on the surface of the substances in contact with quartz. We can take the extinction coefficient K' for quartz for the region from 210 to 450 $\mu\mu$ to be zero. Hence we write

$$R=\frac{(n-n')^2+n^2K^2}{(n+n')^2+n^2K^2}. \tag{6}$$

We shall be concerned with the reflecting power of the substance *in vacuo*, of the substance in contact with quartz, and of the substance in contact with fluorite. These reflecting powers are denoted by R_o, R_q, and R_f, respectively.

For many of the ideas used in the application of these formulae to the experimental results the writer is indebted to two papers by T. H. Havelock.[1]

3. *Apparatus and experimental details.*—A hydrogen end-on discharge tube, Fig. 1, served as the source of light. The tube

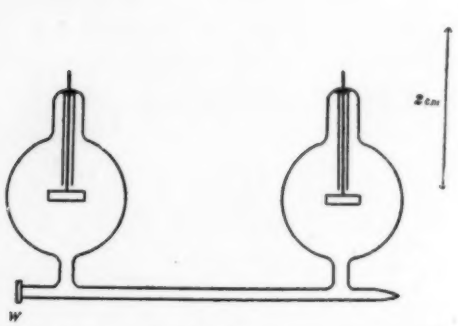

FIG. 1

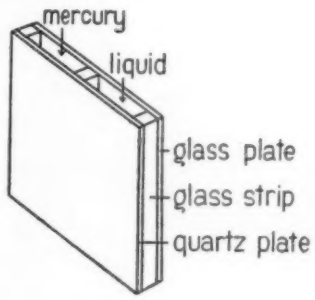

FIG. 3

was made by fusing two glass bulbs containing aluminum electrodes on to a small glass tube 14 cm in length and of 4 mm bore, and filling with hydrogen at a pressure of about 1 mm of mercury. This form of tube possessed the desirable qualities of being simple to construct and of being able to absorb considerable energy without becoming unduly heated around the quartz window, *W*, Fig. 1, which was fastened on with red sealing-wax. The tube was operated by a 250-to-1 transformer run on 60-cycle, 110-volt, alternating current, and taking 5–7 amperes in the primary circuit. The primary current was turned on and off with a contact key operated by a pendulum with a period of 5 seconds. By this means the hydrogen tube could be lighted for accurately known time-intervals of 5, 10, 15, etc., seconds.

The light from the hydrogen tube was focused on the slit *B* of the spectrograph by a quartz lens, *L*, Fig. 2, 2.8 cm in diameter

[1] *Proc. Roy. Soc.*, A, 84, 492, 1911; A, 86, 1, 1912.

and of focal length 15.8 cm. The spectrograph consisted of the Rowland mounting of a concave speculum metal grating, *C*, of 16 cm radius of curvature, ruled 15,000 lines to the inch, the area of ruling being 15 mm × 24 mm. The spectrum was brought to a focus at slit *A*, back of which was placed the sodium photo-electric cell, *P*, with a quartz window. Slit *A* and the cell were on a movable arm so that various wave-lengths could be reached. The

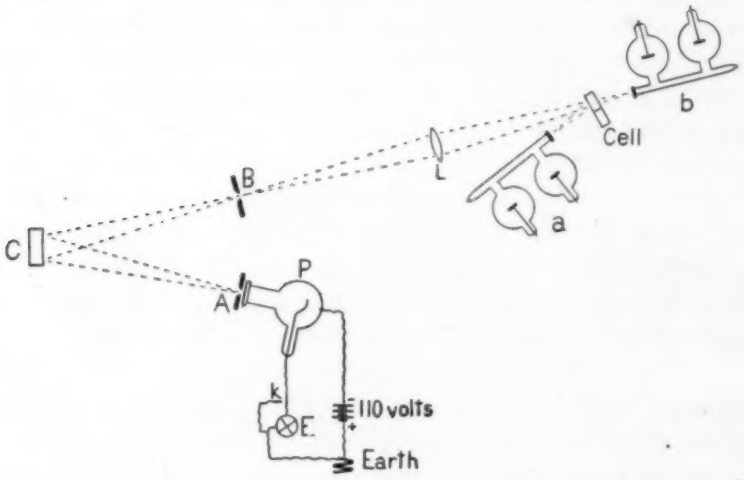

FIG. 2

dispersion was 106 A per mm. Each slit was 0.5 mm wide; the correction for finite width of slit was considered negligible. The photo-electric cell was connected to a Dolezalek quadrant electrometer, *E*, of sensibility 3600 mm per volt difference of potential between the quadrants, period 40 seconds. The deflections were observed by measuring the ballistic throw of the electrometer needle in a manner described by J. B. Nathanson.[1] The method consisted in first breaking the earth connection of those quadrants which were joined to the electrode of the photo-electric cell, then in turning on the light in the hydrogen tube for a convenient length of time, e.g., 10 seconds, and finally in observing the throw of the electrometer needle. In the present work this method had

[1] *Astrophysical Journal*, 44, 137, 1916.

especial advantage as a timesaver over the steady-deflection method because of the comparatively long period of the electrometer needle.

Single measurements of the reflecting powers, which were for the most part below 0.20, varied by as much as 25 per cent. Therefore the final recorded values were the means of many determinations and were considered accurate to perhaps 10 per cent.

The grating used in the present work was the same as the one described in a previous paper.[1] In that paper mention was made of the effect of scattered light produced by this grating and of how corrections were made for this effect. In the present case the correction for scattered light has been considered negligible, because a reflection measurement was the ratio of the intensity of a direct and a reflected beam, each of which contained probably nearly the same proportion of light of foreign wave-lengths. The spectrum produced by this grating was not particularly strong in the extreme ultra-violet, the deflections for an exposure of 15 seconds were less than 50 mm for wave-lengths below 210 $\mu\mu$. Therefore no trustworthy measurements were obtainable below 210 $\mu\mu$.

4. *Measurement of transmission.*—When the transmission (or absorption) of a liquid was to be studied, the liquid was pressed into a thin film between two plane plates of quartz. In the cases of the volatile substances the edges of the plates were surrounded by cotton wool which was kept saturated with the liquid. This insured the permanence of a film during the course of a measurement. The hydrogen tube was placed in position *b*, Fig. 2, and the absorption cell—i.e., the quartz plates and film—was placed close to the end of the tube. A measurement of transmission consisted in observing the deflection produced by the unscreened beam and that produced by the beam after passing through the cell. The ratio of the two deflections, increased by 20 per cent to correct for the transmission of the cell, gave the transmission, t, of the film; the values of the transmission at each wave-length plotted as ordinates against wave-lengths as abscissae formed the transmission curve.

5. *Measurement of reflection.*—For the purpose of the measurements of reflection a cell was constructed as shown in Fig. 3. This

[1] *Astrophysical Journal*, 45, 152, 1917.

cell had two compartments, one of which was filled with mercury and the other with the liquid under examination. The front face of the cell was a plane quartz plate 1 mm in thickness. The other parts were of glass; the cell was cemented with water-glass.

In the case of the reflection measurement the hydrogen tube was placed in position *a*, Fig. 2, and the light was reflected on the slit *B* of the spectrograph from the face of each compartment in turn at an angle of incidence of 7°. The cell was supported on a sliding carriage so arranged that the cell could be moved in its own plane, allowing either compartment to be placed in the path of the beam of light without displacement of the image of the source on the slit. The measurement consisted in observing d' and d, the deflections produced by light of a specified wave-length when reflected from the mercury and the liquid compartments, respectively. The ratio d/d' has been plotted in the figures on the same scale of ordinates as was used for the transmission t. Although the angle of incidence was 7°, all the reflection measurements have been treated as if they had been made for normal incidence. The error resulting from this was inappreciable in comparison with the error of experiment. The reflecting power, R_q, of the liquid surface in contact with quartz has been computed from the approximate relation

$$R_q=\frac{\frac{d}{d'}\times R'-r}{(1-r)^2}. \qquad (7)$$

R' is the reflecting power of the face of the mercury compartment; r is the reflecting power of quartz, computed from the formula $r=\left(\frac{n-1}{n+1}\right)^2$, the values of n, the refractive index of quartz, for each wave-length being interpolated from the measurements of Martens (*loc. cit.*).

Before R_q could be computed, R' had first to be determined. This is described in the next section.

6. *Mercury.*—The refractive index n and the extinction coefficient K for mercury have been determined by W. Meier[1] for wave-lengths in the visible region of the spectrum and in the ultra-violet

[1] *Annalen der Physik*, 31, 1017, 1910.

as far as 325.5 $\mu\mu$, using the katoptric method of R. S. Minor.[1] P. Erochin[2] has continued the work, obtaining measurements at wave-lengths 295, 275, and 257 $\mu\mu$. In Fig. 4 the values of R_q computed by means of (6) from the values of n and K given by Meier and Erochin are shown by crosses and circles, respectively. The values of R_o are about 13 per cent greater than the corresponding values of R_q; these have not been plotted in Fig. 4.

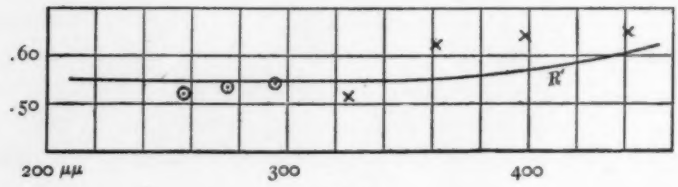

FIG. 4

The mercury used in the present work was freshly distilled according to the method of G. A. Hulett.[3] The reflecting power, R', of the face of the mercury compartment was equal to the deflection produced by the direct beam, with the hydrogen tube in position b, Fig. 2, divided into the deflection produced by the beam reflected from the face of the mercury compartment when the tube was swung around into position a, Fig. 2. The reflection cell was placed so that the optical path from the source to slit B was the same in each case.

The values of R' are shown by the smooth curve of Fig. 4; the curve represents the means of several measurements. The values of R' from this curve have been used in the subsequent calculations.

If we assume that there was no air film between the mercury and the quartz, then, approximately, for normal incidence

$$R_q = \frac{R' - r}{(1-r)^2},$$

where r is the reflecting power of the quartz. The values of R_q computed from this relation were found to be about 1 per cent greater than the values of R' shown in Fig. 4. It is seen that there

[1] *Annalen der Physik*, **10**, 581, 1903.

[2] *Ibid.*, **39**, 213, 1912.

[3] *Physical Review*, **21**, 388, 1905.

is fair agreement between these values of R_q and the values computed from the data of Meier and Erochin. This is evidence of the correctness of our assumption.

If, on the other hand, we assume that an air film existed between the mercury and the quartz, then, approximately, for normal incidence

$$R_o = \frac{R' - r - r(1-r)^2}{(1-r)^4}.$$

The values of R_o computed from this relation were found to be about 1.5 per cent greater than the values of R'. These values of R_o disagree unmistakably with those computed from the data of Meier and Erochin. Therefore it is concluded that the first assumption was correct—namely, that there was no appreciable air film between the mercury and the quartz.

7. *Carbon disulphide.*—The optical properties of this substance in the ultra-violet have been studied by Flatow,[1] Martens,[1] and W. Fricke.[2] The refractive index was found to increase with decrease in wave-length, showing a slight anomaly at 325 $\mu\mu$ (Fricke, *loc. cit.*), and then to increase rapidly for wave-lengths below 320 $\mu\mu$, the limit of the observations being at 266 $\mu\mu$. Absorption spectrograms of thin films of the pure substance, pressed between quartz plates, showed a region of minor absorption, with a maximum of absorption at about 320 $\mu\mu$ corresponding to the dispersion anomaly mentioned above, and a band of metallic absorption setting in below 250 $\mu\mu$. Martens found that a film of carbon disulphide diluted ten times with alcohol absorbed only the wave-lengths from 228 to 190 $\mu\mu$. He concluded that the pure substance probably became transparent again below 185 $\mu\mu$, and he pointed out that the dispersion-curve indicated another region of absorption at a still shorter wave-length. By a method of continued reflection from carbon disulphide in contact with fluorite, Flatow concluded that there was a band of selective reflection with its maximum at about 230 $\mu\mu$.

In the present work carbon disulphide, freshly purified by distillation, was used. The transmission-curve for a thin film of

[1] *Loc. cit.*

[2] *Annalen der Physik*, **16**, 865, 1905.

the substance is given in Fig. 5. The values of the ratio d/d' (see sec. 5), determined from 210 $\mu\mu$ to 340 $\mu\mu$, are shown in Fig. 5; from these values R_q, Fig. 6, for each wave-length has been computed by means of (7). R_q has a maximum value of 0.092 at about 230 $\mu\mu$. We cannot as yet compare this result with Flatow's similar result upon the position of the maximum of reflection, because in the one case the reflection has occurred in quartz and in the other case in fluorite.

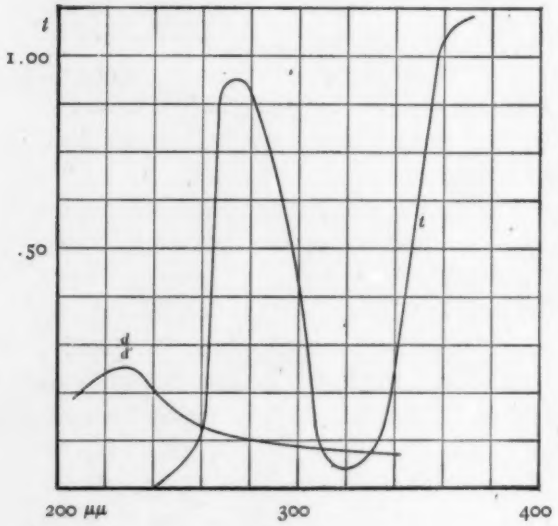

FIG. 5

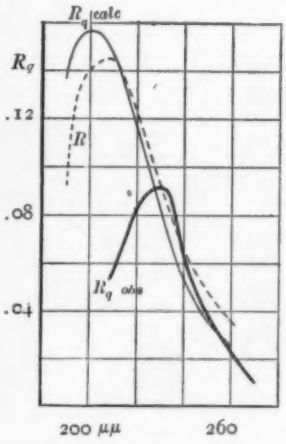

FIG. 6

In order to introduce these experimental results into the complete dispersion formula (3), only approximate methods are available. Following the method of Havelock, we ignore the region of minor absorption near 325 $\mu\mu$ and assume that we are dealing with a single principal frequency in the ultra-violet. We take the values of the refractive index as determined at 20° by Flatow—namely,

λ	441.6 $\mu\mu$	508.6	589.3
n	1.67180	1.64586	1.62806

We consider the absorption of carbon disulphide inappreciable at these wave-lengths, and hence use the simplified formula (5).

Substituting the above values of λ and n in this formula to determine the constants, we find

$$q_1'=1.7544 \qquad g=0.434 \qquad \lambda_1'=228.4\,\mu\mu.$$

Formula (5) with these constants gives too high a value for n at $267\,\mu\mu$; e.g., $n=2.39$, as compared with the index $n=2.08884$ observed by Flatow. This is due to the fact that absorption has been neglected, i.e., g' has been taken to be zero. Havelock has proceeded by giving a value 0.2284×10^{-5} to g' such as to give $n=2.0904$ at $267\,\mu\mu$ (using [3] for the calculation), which agreed sufficiently well with the observed value. In the present instance we make use of the reflection measurements to determine g'. From formula (3) at wave-length λ_1', we have

$$n^2(1-K^2)=q_1', \tag{8}$$

$$2n^2K=\frac{q_1'g\lambda_1'}{g'}. \tag{9}$$

Eliminating n^2K^2 between (6) and (8), and solving for n, gives

$$n=\frac{n'}{2}\,\frac{1+R_q}{1-R_q}\pm\sqrt{\frac{n'^2}{4}\left(\frac{1+R_q}{1-R_q}\right)^2-\frac{n'^2-q_1'}{2}}. \tag{10}$$

At wave-length $\lambda_1'=228\,\mu\mu$ the observed value of R_q was 0.087. Taking the refractive index of quartz at this wave-length, n', to be 1.622 (the mean between $n_\omega=1.616$ and $n_\epsilon=1.628$, which have been found by interpolation from the data given by Martens (*loc. cit.*), and using the previously determined value of $q_1'=1.7544$, we find, from (10), $n=1.66846$ at $228\mu\mu$. Substituting this value in (8) gives $K=0.60810$. Using these values for n and K in (9) gives

$$g'=0.5136\times10^{-5}.$$

We retain the above values of q_1', g, and λ_1', unaltered, for simplicity; this means that we regard K as inappreciable at the wave-lengths for which these constants were determined.

With the values of the constants thus determined n and nK have been computed by means of (3). With these values of n and nK, and with the values for the refractive index of quartz and fluorite from Martens' data, R_q and R_f have been computed for

each wave-length by means of (6); their graphs are shown in Fig. 6. The difference in R_q produced by using n_ω and n_ϵ, the indices for the ordinary and the extraordinary rays, respectively, is too slight to be of importance. The computed curve for R_q does not agree with the observed curve, giving values of R_q much too great. The maximum of the computed curve lies at about 200 $\mu\mu$, whereas the observed maximum is at about 230 $\mu\mu$. The computed curve for R_f has its maximum at about 207 $\mu\mu$, which does not agree with Flatow's observation.

The reason for the discrepancies between the observed and computed values is to be found in the incomplete nature of the dispersion formula (3). If we were dealing with the simple case of a single principal frequency, q_1' would equal unity. The fact that q_1' is much greater than unity shows that the carbon disulphide possesses another characteristic frequency farther in the ultra-violet, and that λ_1' as computed above is too small. We then take $\lambda_1' = 240\ \mu\mu$. At this wave-length we have the observed value 0.063 for R_q. Using these values for λ_1' and R_q, and the former values of g and q_1', in (8), (9), and (10), we find

$$g' = 0.7135 \times 10^{-5}.$$

With this new set of constants, namely,

$$q_1' = 1.7544 \qquad g = 0.434 \qquad \lambda_1' = 240\ \mu\mu \qquad g' = 0.7135 \times 10^{-5},$$

the values of n, nK, R_o, R_q, and R_f, have been computed from (3) and (6). The graphs are shown in Fig. 7.

The computed curve for R_q shows tolerable agreement with the observed curve. The computed values for n agree closely with the observed values for wave-lengths greater than 380 $\mu\mu$. For wave-lengths less than this the computed index falls considerably below the observed index. To lessen the discrepancy would probably necessitate a complete readjustment of all the constants. Such a procedure would be of little value at present, in view of the fact that the dispersion formula (3) is only an approximate one. The formula should contain several terms, one term for the characteristic frequency at 325 $\mu\mu$ (which is perhaps of minor importance), a second term for the frequency near 230 $\mu\mu$, a third term for a fre-

quency corresponding to some wave-length below 190 $\mu\mu$, and perhaps others. Further investigation in the extreme ultra-violet is necessary before one can attempt to evaluate the constants entering in the various terms.

Although neither of the two sets of constants used above yielded values of the optical constants which agreed satisfactorily with the observed values, yet in both cases the maxima of R_q and R_f were

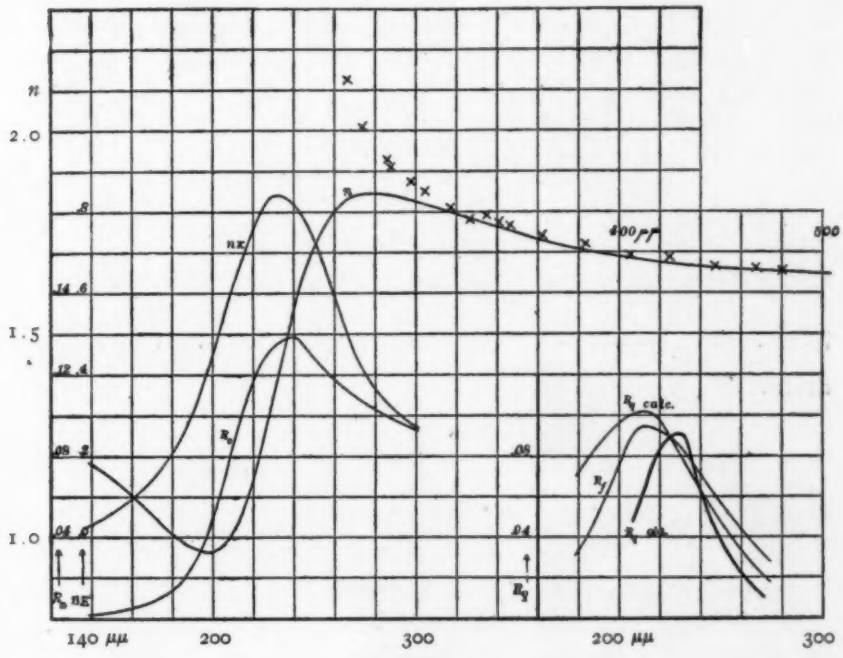

FIG. 7

found to occur at about the same wave-length (see Figs. 6 and 7). This indicates that if R_q and R_f had been computed from the true values of the optical constants their maxima would both have occurred at about the same wave-length. We conclude, therefore, that the observed maximum of R_q at about 230 $\mu\mu$ and Flatow's observed maximum of R_f also at 230 $\mu\mu$ are in accordance.

In the present instance we consider that the values of R_q and n, given in Fig. 7, which have been computed from equation (3) with the use of the second set of constants, agree sufficiently well with

the observed values to make it worth while to use the values of these constants to compute certain numerical facts concerning the dispersion electron which has its natural frequency near 230 $\mu\mu$. Putting the values for q_1', λ_1', g, and g', in equations (4), and using $\frac{1}{3}$ for σ, we obtain

$$q_1 = 0.603 \qquad b_1 = 2.33 \times 10^{15}$$
$$C_1 = 30 \times 10^{30} \qquad \lambda_1 = 219\ \mu\mu$$

We note that the natural frequency of the electron is at wave-length 219 $\mu\mu$, which is a shorter wave-length than λ_1', the critical frequency for the medium as a whole. We next compute p the number of dispersion electrons per molecule, after the manner of Drude. From Sec. 2 we have

$$C_1 = 4\pi N \frac{e^2}{m_1}.$$

Let M be the molecular weight and d the density of carbon disulphide; let $\frac{e}{m_H}$ be the ratio of the charge to the mass of the hydrogen atom. Then

$$N = \frac{pd}{Mm_H} \text{ and } p\frac{e}{m_1} = \frac{m_H}{e}\frac{M}{d}\frac{C_1}{4\pi}.$$

With $M = 76$, $d = 1.26$, $\frac{e}{m_H} = 9660$, we find

$$p\frac{e}{m_1} = 1.66 \times 10^7,$$

the charge being expressed in electro-magnetic units. This indicates one electron per molecule.

7. *α-monobromnaphthalene.*—The optical properties of this substance in the ultra-violet have been studied by Martens (*loc. cit.*). Absorption spectrograms showed that a thin film pressed between quartz plates transmitted no light of wave-length below 313 $\mu\mu$. Fourfold reflection from the substance in contact with fluorite showed only the lines 232 $\mu\mu$ and 228 $\mu\mu$.

The α-monobromnaphthalene used in the present work was obtained from Eimer and Amend, New York. The transmission-curve, given in Fig. 8, of a very thin film, between quartz plates,

shows complete absorption below 305 $\mu\mu$. The values of d/d' obtained from the reflection measurements are given in Fig. 8 for each wave-length in the region from 210 $\mu\mu$ to 290 $\mu\mu$. The values of R_q, computed from these values of d/d' by means of (7) are shown in Fig. 9; R_q has a maximum value of 0.092 at about 230 $\mu\mu$.

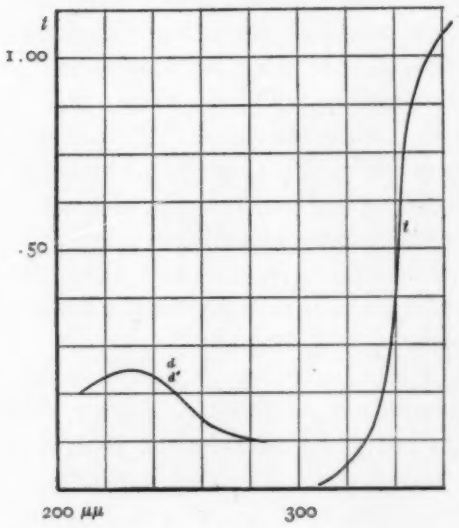

FIG. 8

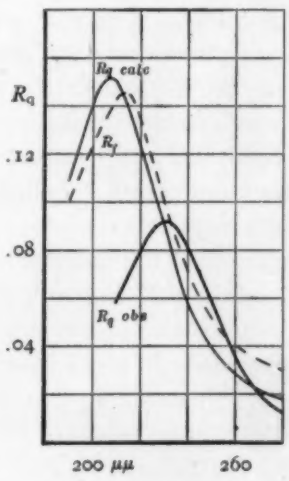

FIG. 9

We introduce these results into the dispersion formulae in a manner similar to the procedure used in the case of carbon disulphide. Using the values of the refractive index at 19°.4 C. determined by Brühl,[1] namely,

λ	434 $\mu\mu$	486	589
n	1.70433	1.68245	1.65876

to compute the constants of (5), we obtain

$$q_1' = 1.811 \qquad g = 0.439 \qquad \lambda_1' = 229\ \mu\mu.$$

As before, we make use of the reflection measurements to determine g'. At wave-length λ_1', the observed value of R_q was 0.091. With

[1] *Ber. Chem. Ges.*, **22**, 388, 1897.

this value of R_q and with $n'=1.622$, using (8), (9), and (10), we find

$$g'=0.5096\times10^{-5}.$$

With the constants thus determined, n, nK, R_o, R_q, and R_f have been computed from (3) and (6). The graphs are shown in Figs. 9 and 10.

It is seen that the computed values of R_q are greater than the observed values and that the maximum of the computed curve for R_q lies at a shorter wave-length than does the maximum of the observed curve. These discrepancies are of the same character as were those in the case of carbon disulphide. R_q and R_f, although computed from values of the optical constants, which are probably only approximately correct, possess maxima at about the same wave-length. Following out the same reasoning as was given in the similar case of carbon disulphide, we conclude that the maximum of R_q observed at about 230 $\mu\mu$ is in accordance with the maximum of R_f also at 230 $\mu\mu$ observed by Martens.

Since data concerning the refractive index of α-monobromnaphthalene in the ultra-violet were not available, no adjustment of the constants to give better agreement between the observed and computed values of R_q was carried out. The discrepancy here, as in the case of the carbon disulphide, may be attributed to the incompleteness of the dispersion formula (3). This formula assumes that we are dealing with the region of a single principal frequency near 229 $\mu\mu$, which is remote from other similar regions. The large value of $q_1'-1$ and the difference between the observed and computed values of R_q indicate that such an assumption is erroneous, and that there exist other characteristic frequencies in the more remote ultra-violet.

If we use the constants determined above to compute the number of dispersion electrons per molecule, and take 1.49 for the density, we find

$$p\frac{e}{m_1}=5.38\times10^{7},$$

which indicates three electrons per molecule.

8. *Cinnamic aldehyde.*—Pure cinnamic aldehyde, obtained from Eimer and Amend, New York, pressed between quartz plates trans-

mitted no light of wave-length below 340 $\mu\mu$. The transmission-curve, Fig. 11, of a film of the substance diluted fifteen times with ethyl alcohol showed a strong absorption band with a maximum at about 285 $\mu\mu$ and indicated another region of absorption below 210 $\mu\mu$. The curve for R_q, Fig. 12, computed by means of (7) from the values of d/d', shown in Fig. 11, has a maximum value of 0.043 at about 285 $\mu\mu$.

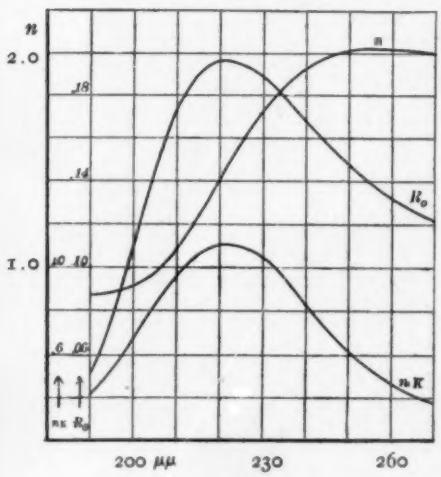

FIG. 10

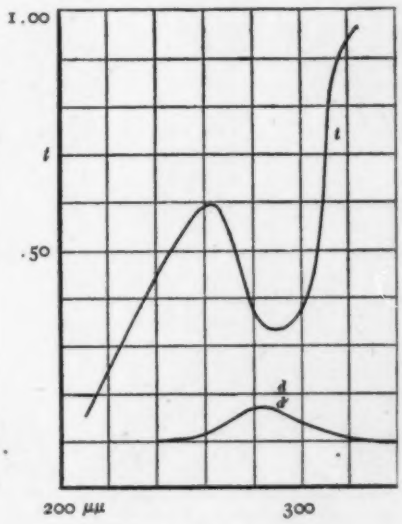

FIG. 11

Making use of the values of the refractive index determined at 20°C. by Brühl,[1] namely,

λ	434 $\mu\mu$	486	589
n	1.68295	1.65090	1.61949

to compute the constants of (5), we obtain

$$q_1'=1.940 \qquad g=0.275 \qquad \lambda_1'=275\ \mu\mu.$$

Using the observed value of $R_q=0.034$, and $n'=1.592$ at wave-length λ_1', together with formulae (8), (9), and (10), we find

$$g'=0.8475\times10^{-5}.$$

[1] *Liebigs Annalen*, **235**, 1, 1886.

With the constants thus determined, n, nK, R_o, and R_q, have been computed by means of (3) and (6). The graphs are shown in Figs. 11 and 12.

The discrepancies between the observed and computed values of R_q are of the same character as was noticed in the cases of carbon disulphide and α-monobromnaphthalene. This disagreement and the large value of $q_1'-1$ lead to the conclusion that the cinnamic

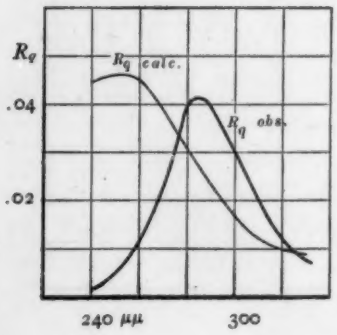

FIG. 12

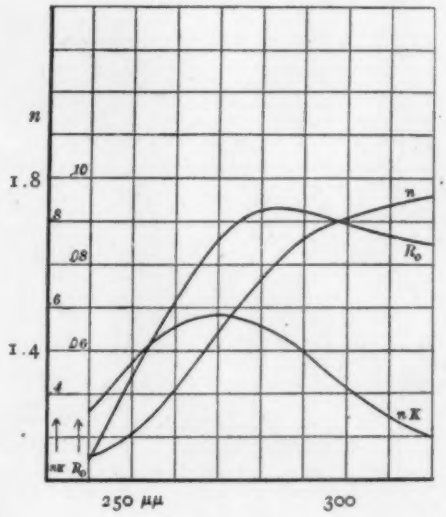

FIG. 13

aldehyde possesses other characteristic frequencies in the more remote ultra-violet.

Using the constants determined above, and with 1.05 for the density, we find

$$p\frac{e}{m_1}=1.97\times 10^7,$$

which indicates one electron per molecule.

9. *Cassia oil.*—This substance was given attention chiefly because it has been included by Martens in his investigations. Commercial cassia oil, such as was used in the present work, contained 75–80 per cent cinnamic aldehyde, the remainder being

cinnamic esters and terpenes. Whether this was the same as the substance used by the earlier investigators is unknown.

Martens (*loc. cit.*) found that pure cassia oil pressed between quartz plates was opaque below 336 $\mu\mu$. When diluted ten times with alcohol it was transparent as far as 305 $\mu\mu$ and at 256 $\mu\mu$ and 230 $\mu\mu$. Fourfold reflection from the substance in contact with fluorite showed only the line 274 $\mu\mu$, with no traces of the neighboring lines 257 $\mu\mu$ and 288 $\mu\mu$.

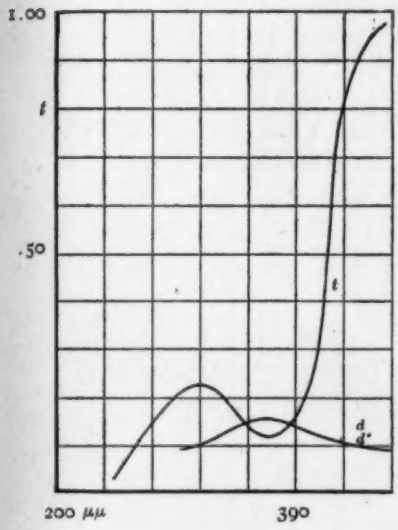

FIG. 14

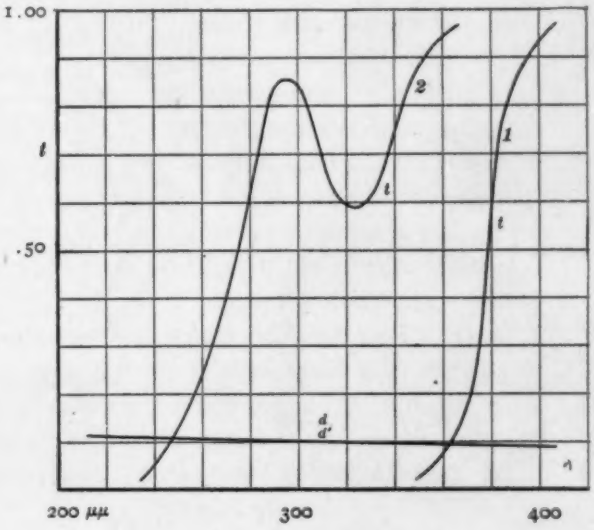

FIG. 15

The transmission-curve for a thin film of cassia oil diluted with ethyl alcohol, and the curve for d/d' (see Fig. 14), were very similar to the corresponding curves for the cinnamic aldehyde. This indicated that the cassia oil owed its ultra-violet optical properties to the presence of the cinnamic aldehyde.

10. *Barium mercury iodide.*—The transmission-curves for a thin film of a saturated aqueous solution of this salt, and for a film of a dilute solution, are given in Fig. 15, curves 1 and 2, respectively. There is a band of absorption with a maximum at about 325 $\mu\mu$; strong absorption begins again at 240 $\mu\mu$.

The refractive index of a saturated aqueous solution of this salt has been determined by C. Rohrbach.[1] Using his values—namely,

λ	486.15 $\mu\mu$	589.31	656.30
n	1.8488	1.7928	1.7752

to determine the constants of (5), we find

$$q_1'=2.368 \qquad g=0.2527 \qquad \lambda_1'=319\ \mu\mu.$$

The value of λ_1' occurs near the observed maximum of the absorption band. The large value of $q_1'-1$ indicates other critical frequencies farther in the ultra-violet.

Reflection measurements gave values of about 10 per cent for d/d', Fig. 15, throughout the region from 210 $\mu\mu$ to 350 $\mu\mu$. The values of R_q computed from (7) were less than 4 per cent, and therefore the substance showed no appreciable traces of selective reflection in this region. This was perhaps due to the fact, indicated by the absorption-curves, that the extinction coefficient did not attain a sufficiently great value in the regions of absorption at 325 $\mu\mu$ and below 240 $\mu\mu$.

11. *Phenol.*—The transmission-curve of a thin film of pure phenol, from Kahlbaum, is given in Fig. 16. There is a broad band of absorption in the region from 280 to 260 $\mu\mu$, with a maximum at about 270 $\mu\mu$. Strong absorption begins again at 230 $\mu\mu$.

Introducing the values of the refractive index determined at 40.6°C. by Eisenlohr,[2] namely,

λ	434 $\mu\mu$	486	589
n	1.56840	1.55581	1.54247

in formula (5) we obtain

$$q_1'=1.9566 \qquad g=0.1807 \qquad \lambda_1'=237.6\ \mu\mu.$$

The wave-length λ_1' lies between the two regions of absorption. This fact and, also, the large value of $q_1'-1$ indicate that we are concerned with at least two critical frequencies, one associated with the absorption band at 268 $\mu\mu$ and the other with the band beginning at 230 $\mu\mu$.

[1] *Wied. Ann.*, **20**, 172, 1883.

[2] *Ber. Chem. Ges.*, **44**, 3207, 1911.

The reflection measurements showed that phenol exhibited no marked selective reflection in the region from 210 $\mu\mu$ to 320 $\mu\mu$. The values of R_q computed by means of (7) from the value of d/d', given in Fig. 16, were less than 4 per cent throughout this region. The low reflecting power for wave-lengths in the neighborhood of the absorption bands was due more probably to a low value of the refractive index than to a low value of the extinction coefficient.

12. *Bromine.*—F. F. Martens[1] found that bromine possessed an absorption band in the blue from 450 $\mu\mu$ to 390 $\mu\mu$ and a band in the ultra-violet which began at about 309 $\mu\mu$. The refractive-index curve of bromine (Fig. 16), determined by W. Fricke,[2] showed an anomaly in the region of the blue absorption band, and then rose rapidly in the region of shorter wave-lengths, attaining a value of 1.851 at 309.19 $\mu\mu$.

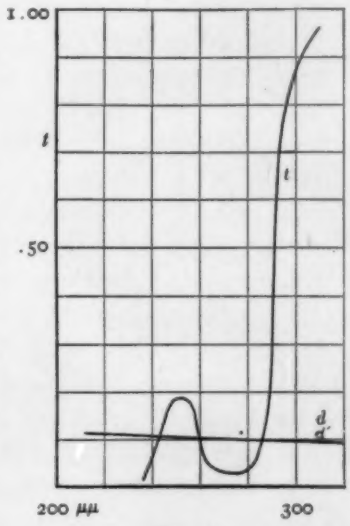

FIG. 16

In the present work the reflection measurements gave values of R_q computed from the values of d/d', Fig. 17, by means of (7), less than 4 per cent throughout the region from 210 $\mu\mu$ to 450 $\mu\mu$. The transmission-curve, Fig. 17, of a thin film of bromine water pressed between quartz plates showed that the blue absorption band is comparatively weak and indicated that bromine is very strongly absorbing below 300 $\mu\mu$. The absence of selective reflection in the region of the blue absorption band is due to the low values of the refractive index and the weak absorption. In the region of the ultra-violet band beginning at 300 $\mu\mu$ the data indicated high values of the refractive index and the extinction coefficient, which would imply values of the reflecting power greater than 4 per cent. There is no evident explanation for the low values actually observed.

[1] *Verhandl. d. Deutsch. Physik. Gesellsch.*, **4**, 139, 1902.

[2] *Annalen der Physik*, **16**, 865, 1905.

13. *Discussion.*—It has been demonstrated that a dispersion formula such as (2), which is of the Ketteler-Helmholtz type, does not serve to express in an entirely satisfactory manner the optical properties in the ultra-violet of the three liquids, carbon disulphide, α-monobromnaphthalene, and cinnamic aldehyde. This is not surprising. The dispersion formula (2), a special case of the more general formula (1), describes the propagation of light in an ideally simple medium, one which contains a single type of dispersion

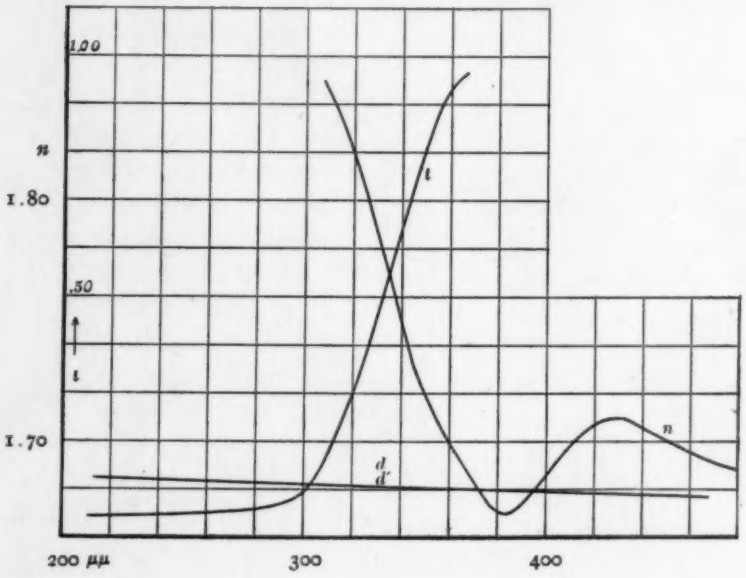

FIG. 17

electron actuated only by elastic and dissipative forces. The inapplicability of this formula in the case of the aforementioned three liquids merely goes to show that these substances cannot be considered ideal media of this kind. If we attempt to explain their optical properties by supposing them to contain additional types of electrons, each type controlled by a similar set of elastic and dissipative forces, but of varying magnitudes for each type, then (2) must be replaced by the more general formula (1), which contains a number of similar terms, one term for each type of electron. The

experimental data available at present are too meager to permit the applicability of (1) to be tested. Further, we know that in certain instances light of wave-length in the extreme ultra-violet causes the emission of electrons, etc., whereas light of longer wave-length does not. The absorption and dispersion in the substance of the short wave-lengths could not be represented by mathematical expressions of the same form as were used in the cases of the longer wave-lengths. It therefore seems probable that for the very short wave-lengths formula (1) is not a true, or at least not a complete, statement of the mechanism. At all events, further observations concerning the optical properties of these substances in the extreme ultra-violet are desirable.

The reflection coefficients of barium mercury iodide in aqueous solution, phenol, and bromine were found to be small for wave-lengths in the region of the strong ultra-violet absorption bands. The experimental data, although incomplete, have shown that, with one possible exception, the small reflectivity in these regions may be attributed to a small index of refraction, or to a small extinction coefficient, or to both.

14. *Summary.*—A grating spectrograph with a sodium photo-electric cell and electrometer has been used for quantitative measurements of monochromatic radiation in the region of the spectrum from 450 $\mu\mu$ to 210 $\mu\mu$.

In a preliminary experiment the reflecting power of mercury in contact with quartz has been determined.

The main portion of the work has consisted in a study of the selective reflection and absorption of seven liquids—carbon disulphide, α-monobromnaphthalene, cinnamic aldehyde, cassia oil, barium mercury iodide in aqueous solution, phenol, and bromine. The first four liquids have been found to exhibit traces of selective reflection; the last three have been found to show no such effect. The results have been discussed in connection with the electron theory of dispersion.

WESTERN RESERVE UNIVERSITY
CLEVELAND, OHIO
May 1917

PHOTOGRAPHS OF NEBULAE WITH THE 60-INCH REFLECTOR 1911–1916[1]

By FRANCIS G. PEASE

The 60-inch reflector with its aperture ratio of F/5 is well adapted for the photography of faint nebulae and all such objects as require great light-gathering power together with considerable scale in order to show their details. For the program of observations, of which some account is given in this paper, the objects selected were in general those whose real nature was unknown or those which possessed curious or questionable characteristics. Many photographs were made under very unfavorable observing conditions, and, in consequence, for these little more than the type is discernible. At times of good seeing, well-known objects were photographed for purposes of measurement. Exposures on several of the bright planetaries were made with the 80- and 100-foot focus, Cassegrain arrangements, with a corresponding increase in scale.

The double-slide plate-holder and its manipulation have been previously described,[2] and but few changes in the instrument or in its usage have been made since that time. Since the actual photographic image is many times the theoretical diameter of the diffraction image, small changes of focus are unimportant in their effect on the images, and intervals of an hour and more were permitted between refocusing. When the image of the guiding star vibrates rapidly, it is found advisable to neglect its excursions to and fro and to follow only the slow drift of its mean center. Both eyes were used alternately for guiding; and on long exposures two guiding stars were used, and correction was made for variation in size and rotation of the field produced by refraction and imperfect adjustment of the instrument. Changes in character of the guiding image during the exposure are responsible for as many plates with elongated images as are irregularities in the driving of the telescope.

[1] *Contributions from the Mount Wilson Solar Observatory*, No. 132.

[2] *Mt. Wilson Contr.*, No. 47; *Astrophysical Journal*, 32, 26, 1910.

PLATE I

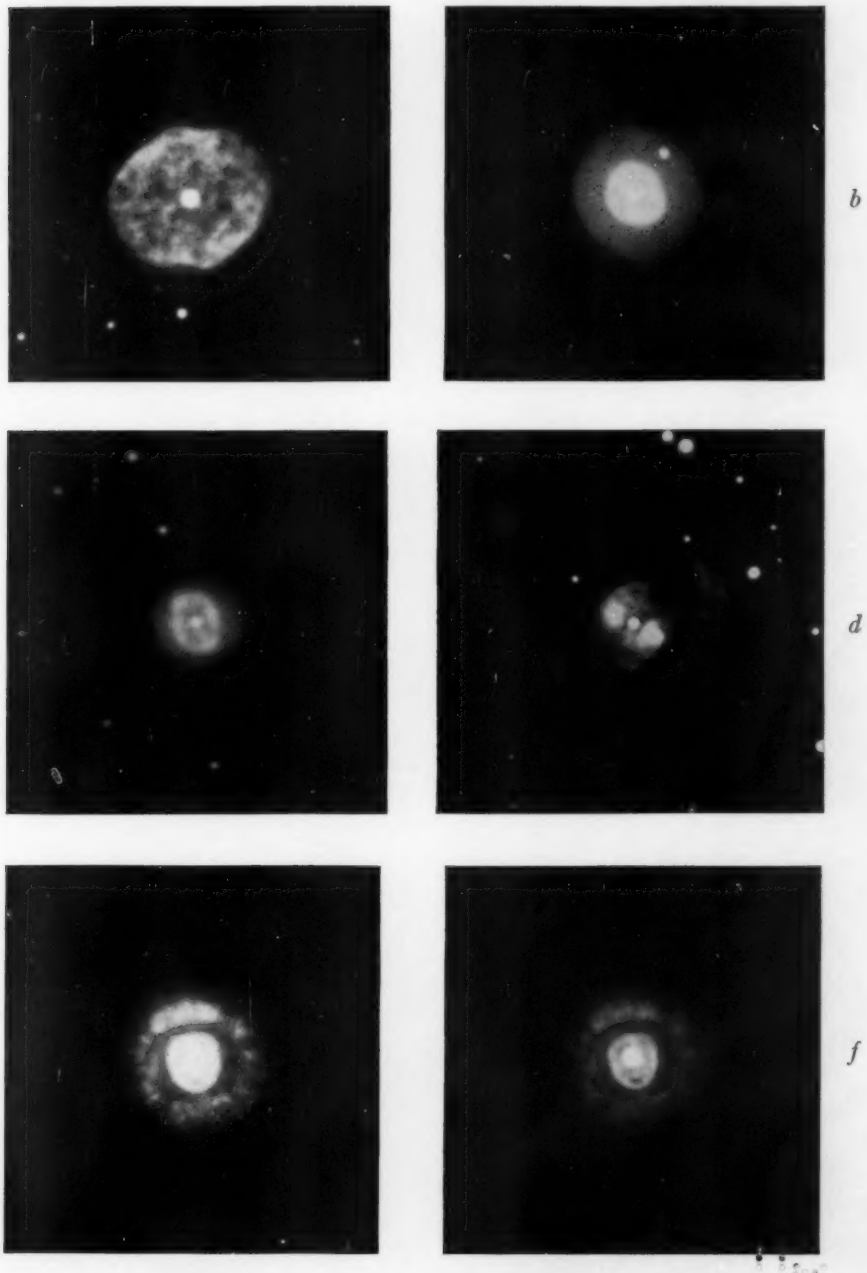

a	N.G.C. 1501	Exposure 120^{m},	Enlargement 10.0,	1 mm = 2.″7	
b	1535	85	11.2	2.4	
c	2022	60	11.1	2.5	
d	2371–2	221	5.2	5.2	
e and *f*	2392	120	4.0	2.1	80-ft. focus

e and *f* are reproduced from the same negative with differences in exposure and development.

PLATE II

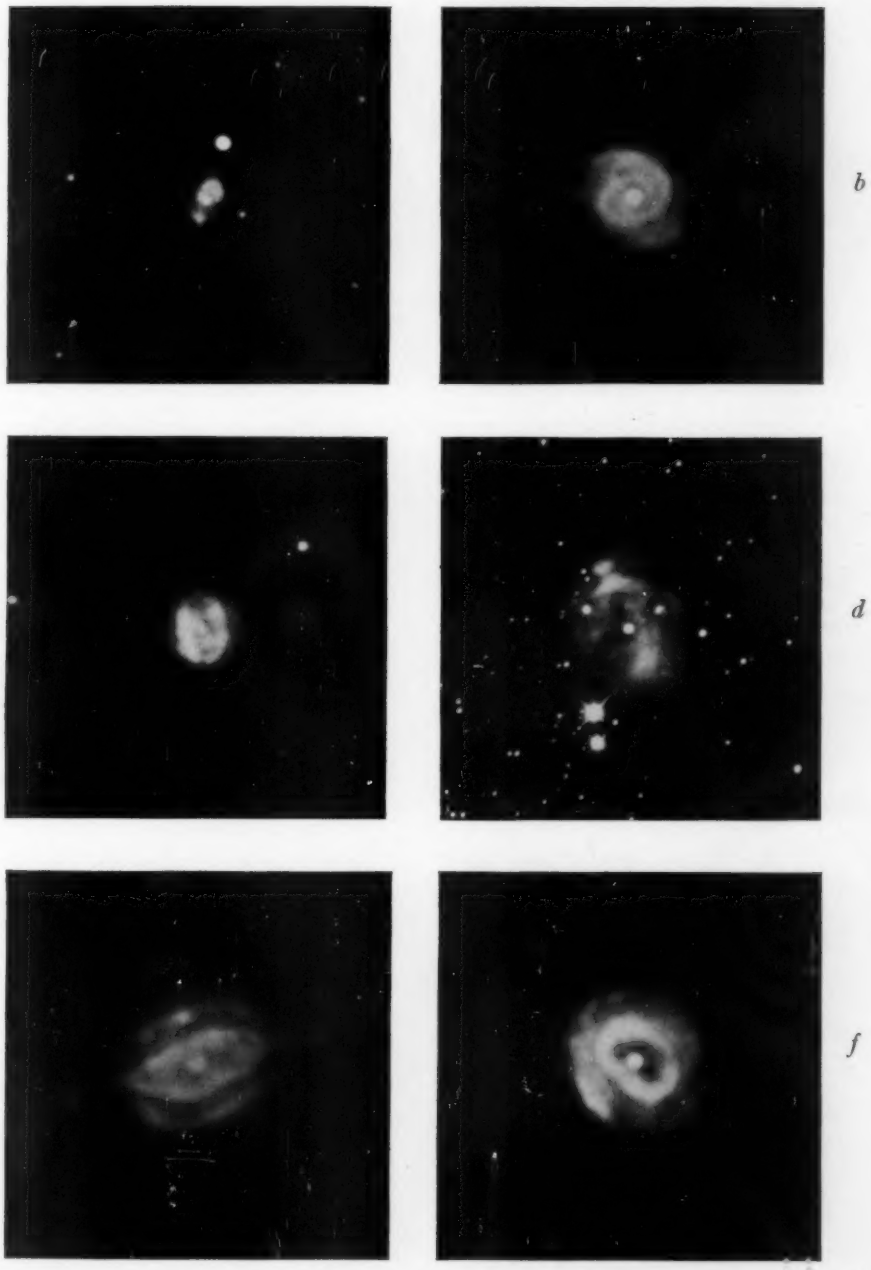

a	N.G.C. 6309	Exposure	90^{m},	Enlargement 9.6,	1 mm = 2″8	
b	6543		50	4.5	1.5	100-ft. focus
c	6818		75	2.8	2.4	100-ft. focus
d	7008		180	5.9	4.7	
e	7009		210	4.5	1.5	100-ft. focus
f	7662		90	4.5	1.5	100-ft. focus

PLATE III

a

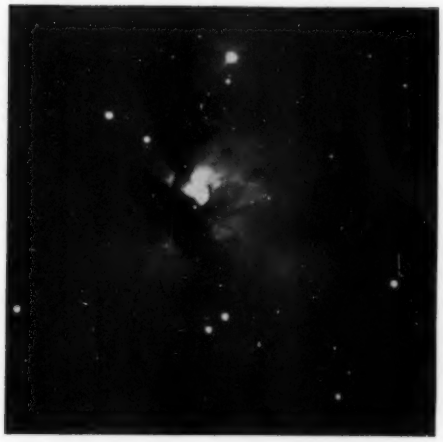

b

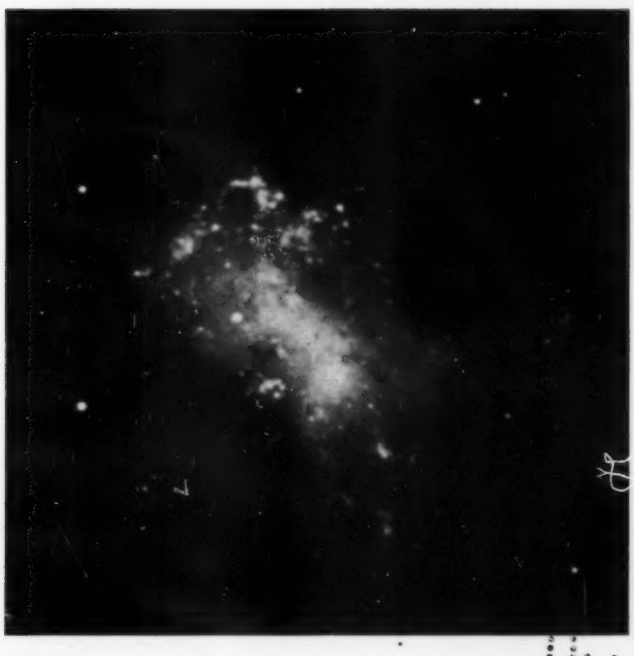

a N.G.C. 1579 Exposure 420^{m}, Enlargement 3.0, 1 mm = 9".1
b 4449 300 5.8 4".7

PLATE IV

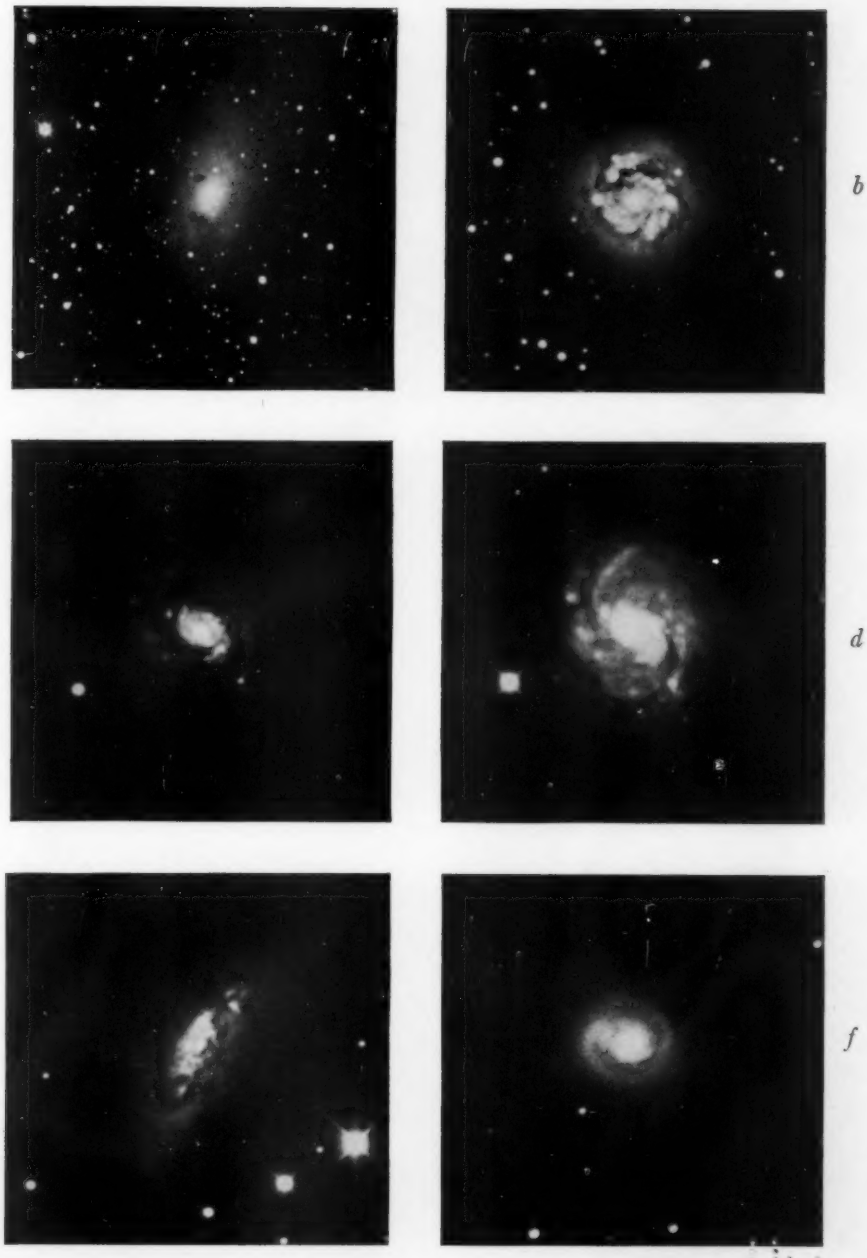

a	N.G.C. 205	Exposure 230^{m},	Enlargement 1.5,	1 mm = 19″.4
b	278	240	5.8	4.7
c	1068	22	5.5	5.0
d	1068	120	5.5	5.0
e	972	195	6.9	3.9
f	2681	190	7.9	3.4

PLATE V

a

b

c

a	N.G.C. 2841	Exposure 120^{m},	Enlargement 3.8,	1 mm =	7".2
b	2976	180	4.7		5.7
c	2403	210	2.7		10.0

PLATE VI

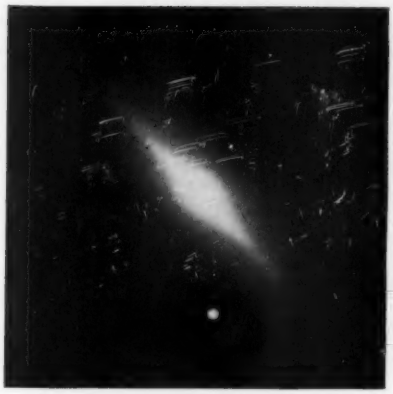

a

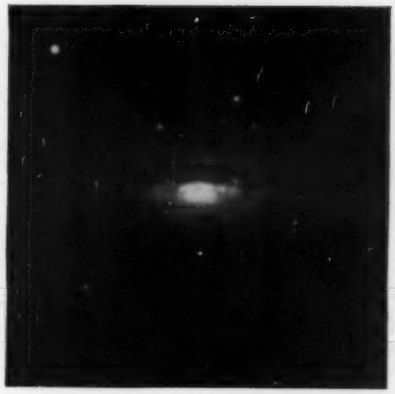

b

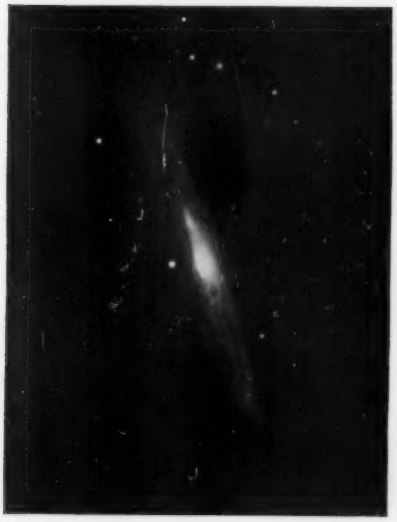

c

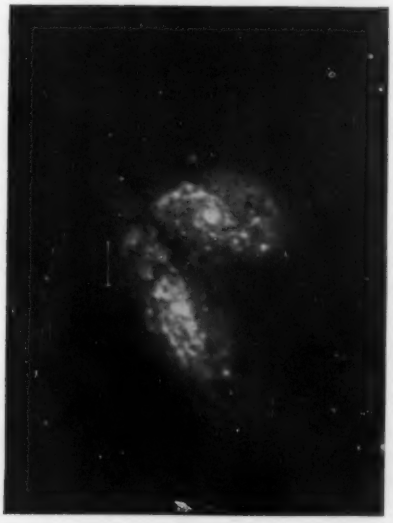

d

e

a	N.G.C. 3115	Exposure 100^{m},	Enlargement 5.5,	1 mm = 5^{s}.0
b	3593	210	5.5	5.0
c	4216	90	3.0	9.2
d	4567–8	360	4.9	5.6
e	4594	132	4.5	6.0

PLATE VII

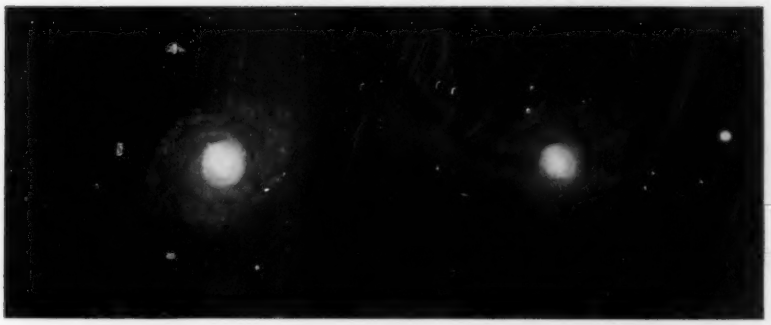

b *a*

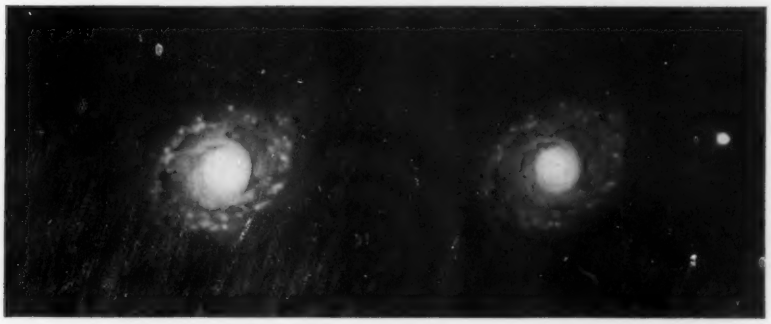

d *c*

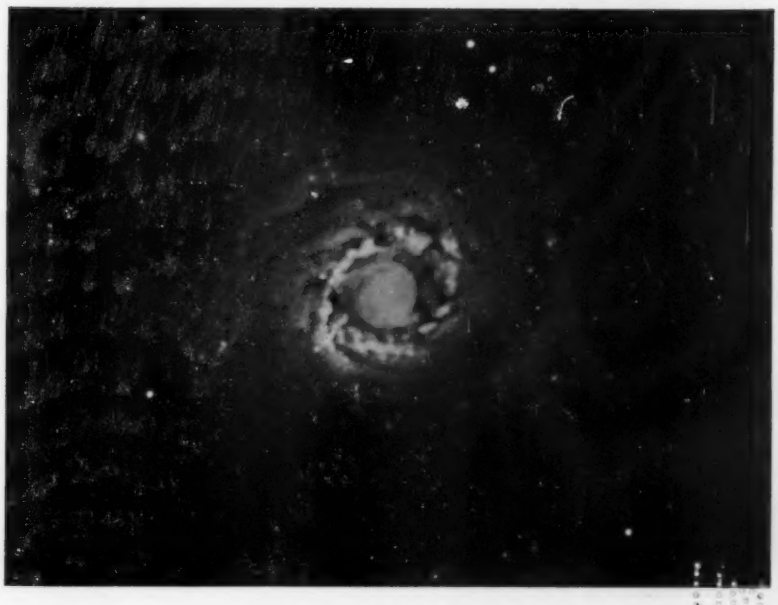

e

N.G.C. 4736 Exposure *a*, 5^{m}; *b*, 10^{m}; *c*, 20^{m}; *d*, 40^{m}; *e*, 225^{m}.
Enlargement 5.1, 1 mm = 5″.4

PLATE VIII

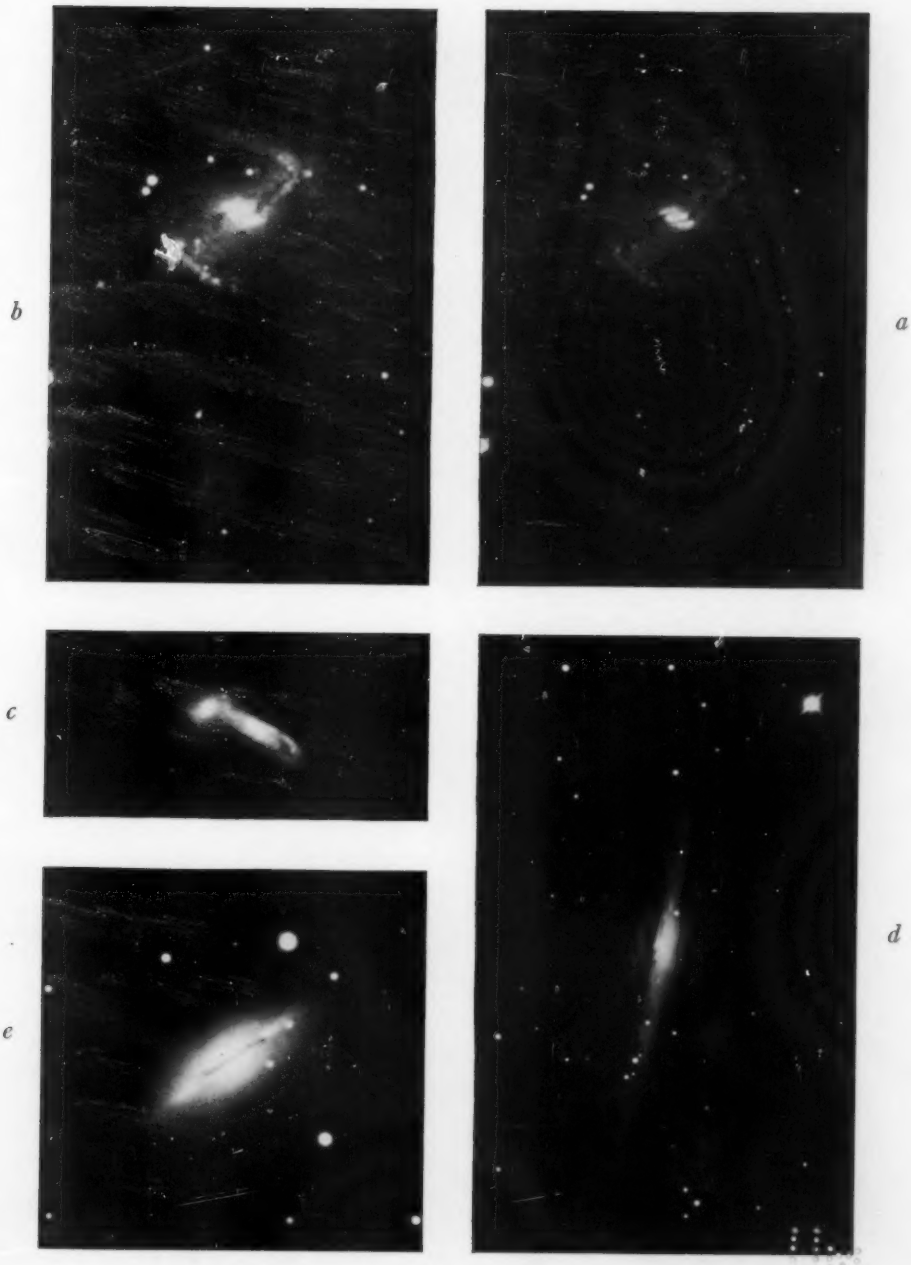

a	N.G.C. 5383	Exposure 180^m,	Enlargement 5.0,	1 mm = 5″.4
b	5383	360	4.9	5.5
c	5544–5	360	5.5	5.0
d	5746	360	3.4	7.9
e	5866	165	5.0	5.5

PLATE IX

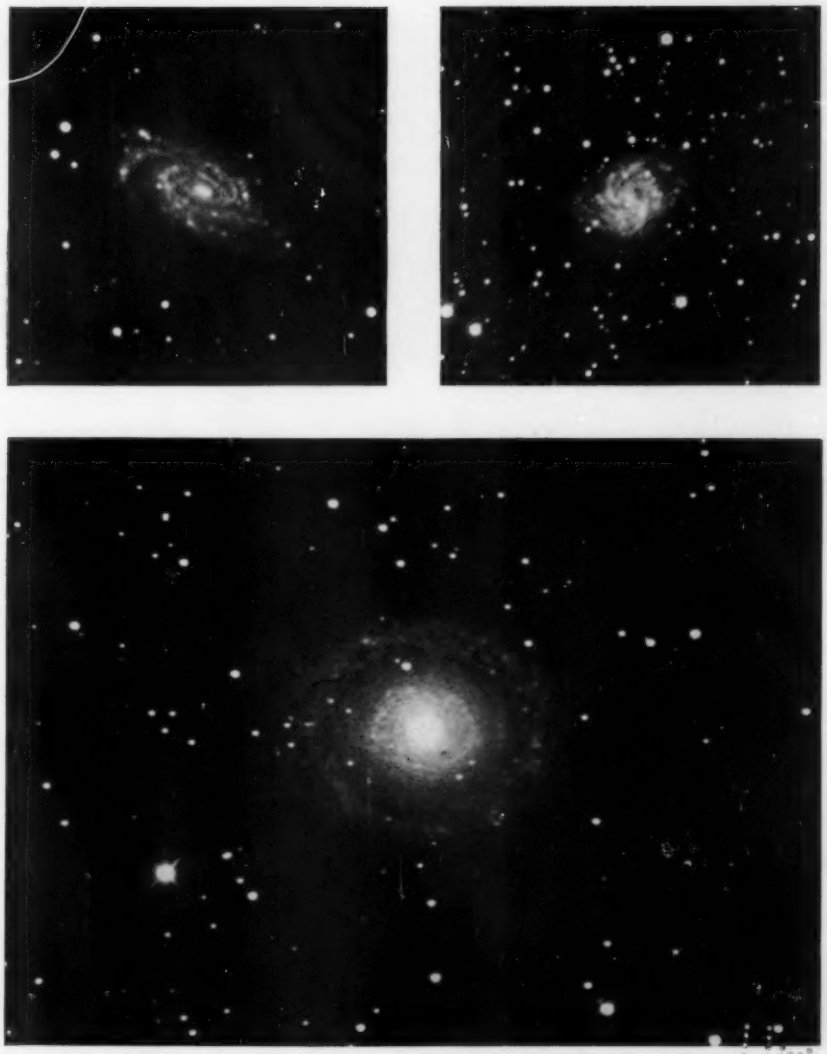

a	N.G.C. 6070	Exposure 150^{m},	Enlargement 4.2,	1 mm = 6.″5
b	6555	360	4.5	6.0
c	7217	330	5.5	5.0

Many objects are so situated as to place the observer in arduous positions for guiding, a difficulty now avoided by using a "goose-neck" microscope—a double-prism device which enables the guiding image to be viewed at a convenient angle.

All negatives were made on Seed 23 plates unless otherwise mentioned. For long exposures and for all those on fields containing bright stars the plates were backed. The usual development was with rodinal, of concentration 1/64 for 30 minutes at 20° C., though in some cases 1/32 for 15 minutes was used. All plates, except a few of early date and those otherwise noted, were taken with the full aperture of 60 inches, with a central stop of 23 inches diameter introduced to cut out the irregularly shaped cell of the Newtonian flat.

The appended list of the nebulae photographed gives (*a*) the approximate position for 1917 (the 1860 position of the *N.G.C.* corrected for precession); (*b*) the constellation; (*c*) the numbers assigned in various catalogues; (*d*) the type (El.=elliptical or elongated, Spl.=spiral, Plan.=planetary, Irr.=irregular, Spe.=spindle); (*e*) the 60-inch plate number, and (*f*), if illustrated, the number of the reproduction.

In the text following Table I is given the *N.G.C.* number of the nebula, its position for 1917, its galactic co-ordinates taken from a chart prepared by Professor Kapteyn, a list of the plates on which the object appears, and a brief description of its principal features. Much of the detail is faint and diffuse, unsuitable for comparator measures, so that the description is based on measures and estimates obtained with a magnifying glass of low power and a photographic reseau giving polar co-ordinates. The orientations have been derived from star trails, but as some of the plates are not provided with trails the results are approximate. Position angle (*p*) is measured from the north toward the east through 360°. The type of spectrum has been added wherever possible, a number of spectrograms, besides those by other observers, having been obtained with the focal-plane spectrograph of the 60-inch reflector.

A left-handed spiral has been defined as one in which an object traveling inward along one of the arms moves in a counter-clockwise direction. Many spirals which are inclined to the line of sight have

TABLE I

NEGATIVES WITH THE 60-INCH REFLECTOR

N.G.C.	α 1917	δ 1917	Constellation	G.C.	H and Others	h	Type	Plate Nos.	Illustrations
205	$0^h\ 35^m\ 51^s$	+41° 14′.2	Andromeda	105	V 18	44	El.	152	IV*a*
278	0 47 23	+47 6.0	Cassiopeia	158	I 159	71	Spl.	168	IV*b*
650–1	1 37 4	+51 9.2	Perseus	385–6	I 193, M 76	.....	Irr.	57, 150, 151, 170	.....
895	2 17 29	− 5 54.3	Cetus	529	II 438	219	Spl.	281	.....
955	2 26 20	− 1 28.6	Cetus	551	II 278	229	Spe.	229	.....
972	2 29 20	+28 56.9	Aries	560	II 211	232	El.	231	IV*e*
1023	2 35 12	+38 42.5	Perseus	575	I 156	242	El.	171	.....
1068	2 38 26	− 0 21.9	Cetus	600	M 77	262	Spl.	49, 51, 53	IV*c*, *d*
1186	3 0 4	+42 30.2	Perseus	639	IV 43	281	Spl.	244, 245	.....
1501	3 59 50	+60 41.9	Camelopardus	801	IV 53	.....	Plan.	174, 178	I*a*
1535	4 10 23	−12 56.9	Eridanus	826	IV 26	2618	Plan.	163, 182	I*b*
1579	4 24 46	+35 6.0	Perseus	853	I 217	315	Irr.	227	III*a*
1931	5 25 55	+34 11.0	Auriga	1137	I 263	355	Irr.	277, 278	.....
2022	5 37 33	+ 9 2.7	Orion	1225	IV 34	365	Plan.	183	I*c*
2366	7 20 7	+69 11.5	Camelopardus	1515	III 748	.....	Irr.	279	.....
2371–2	7 20 20	+29 39.1	Gemini	1519–20	II 316–17	444–5	Irr.	257	I*d*
2392	7 24 16	+21 5.0	Gemini	1532	IV 45	450	Plan.	187, 189, 190, 191, 255	I*e*, *f*
2403	7 28 49	+65 46.9	Camelopardus	1541	V 44	.....	Spl.	169	V*c*
2681	8 47 36	+51 37.7	Ursa Major	1711	I 242	530	Spl.	179	IV*f*
2825	9 14 21	+34 5.1	Lynx	1806	.....	581	Spe.	246, 247	.....
2826	9 14 22	+33 58.0	Lynx	1807-1809	.....	.....	Spe.	246, 247	.....
2827	9 14 23	+34 16.7	Lynx	1808	.....	.....	El.	246, 247	.....
2828	9 14 33	+34 17.2	Lynx	1810	.....	.....	El.	246, 247	.....
2829	9 14 39	+34 0.8	Lynx	1804	.....	.....	Neb. star	246, 247	.....
2830	9 14 44	+34 6.0	Lynx	1811	I 113	582	Spe.	246, 247	.....
2831	9 14 45	+34 6.6	Lynx	1812	.....	.....	Neb. star	246, 247	.....
2832	9 14 46	+34 6.9	Lynx	1813	.....	.....	El.	246, 247	.....
2834	9 15 3	+34 3.3	Lynx	1815	.....	.....	Neb. star	246, 247	.....
2839	9 15 36	+33 59.2	Lynx	1821	.....	.....	Neb. star	246, 247	.....
2841	9 16 18	+51 19.7	Ursa Major	1823	I 205	584	Spl.	58	V*a*
2976	9 40 24	+68 17.9	Ursa Major	1905	I 285	625	Spl.	175	V*b*
3115	10 1 6	− 7 18.9	Sextans	2008	I 163	668	Spe.	50	VI*a*
3593	11 10 17	+13 16.0	Leo	2347	I 29	840	Spl.	185	VI*b*
3666	11 20 8	+11 47.9	Leo	2405	I 20	882	Spl.	248	.....
3938	11 48 31	+44 35.4	Ursa Major	2597	I 203	1002	Spl.	249	.....
4206	12 11 6	+13 30.5	Virgo	2795	II 165	.....	Spl.	192	.....
4216	12 11 40	+13 36.4	Virgo	2806	I 35	1148	Spl.	192	VI*c*
4222	12 12 10	+13 48.0	Virgo	2841	II 109	.....	Spe.	192	.....
4236	12 12 48	+69 56.0	Draco	2825	V 51	1163	Irr.	201	.....
4374	12 20 52	+13 20.8	Virgo	2930	M 84	1237	Neb. spot	234	.....
4387	12 21 30	+13 16.0	Virgo	2955	II 167	1250	El.	234	.....

4388	12	21	35	+13	7.2	Virgo	2949-2956	II	168	1244	El.	234	
4402	12	21	55	+13	34.8	Virgo	2965				El.	234	
4406	12	21	59	+13	24.3	Virgo	2961	M	86	1253	Neb. spot	234	
4407	12	22	4	+13	6.0	Virgo	2968			1255	El.	234	
4425	12	23	1	+13	11.7	Virgo	2983	II	170	1267	Spe.	234	
4449	12	24	11	+44	33.0	Canes Venatici	3002	I	213	1281	Irr.	198	IIIb
4564	12	32	15	+11	53.6	Virgo	3105	II	68	1356	Spe.	235, 237	
4567–8	12	32	20	+11	42.9	Virgo	3108–9	IV	8–9	1358–9	Spl.	235, 237	VId
4594	12	35	40	−11	10.0	Virgo	3132	I	43	1376	Spl.	256, 262	VIe
4736	12	46	59	+41	34.3	Canes Venatici	3258	M	94	1456	Spl.	60, 3093P, 3094P	VIIa,b,c,d,e
4900	12	56	28	+	2 56.5	Virgo	3356	I	143	1509	Spl ?	188	
5005	13	7	3	+37	30.2	Canes Venatici	3437	I	96	1547	Spl.	59	
5308	13	44	15	+61	23.5	Ursa	3362	I	255	1674	Spe.	196	
5383	13	53	41	+42	14.9	Canes Venatici	3723	I	181	1717	Spl.	195, 199	VIIIa, b
5544–5	14	13	33	+36	57.3	Boötes	3833–4	II	419	1771	Spl.	127, 261	VIIIc
5560	14	15	54	+	4 22.3	Virgo	3845	II	579	1778	Spl.	250	
5566	14	16	10	+	4 19.8	Virgo	3846	I	144	1779	Spl.	250	
5569	14	16	22	+	4 20.1	Virgo	3848				Spl.	250	
5740	14	40	21	+	2 2.0	Virgo	3985	II	538	1872	Spl.	236	
5746	14	40	43	+	2 18.3	Virgo	3937	I	126	1874	Spl.	236	VIIId
5866	15	4	12	+56	5.0	Boötes	4058	I	215	1909	Spe.	129	VIIIe
5907	15	13	44	+56	38.0	Draco	4087	II	759	1917	Spl.	197	
6070	16	5	45	+	0 55.7	Serpens	4164	III	553	1947	Spl.	265, 267	IXa
6210	16	41	1	+23	57.2	Hercules	4234	Σ	5	1970	Plan.	139	
6217	16	36	32	+78	22.0	Ursa Minor	4236	I	280		Spl.	200	
6309	17	9	24	−12	48.9	Ophiuchus	5851				Plan.	252, 263	IIa
6412	17	32	4	+75	46.6	Draco	4321	VI	41		Spl.	128	
6478	17	46	41	+51	11.6	Draco		SW	III		Spl.	135	
6543	17	58	35	+66	38.2	Draco	4373	IV	37		Plan.	9, 10, 11, 20, 34, 238	IIb
6555	18	3	28	+17	35.3	Hercules	4383	II	902		Spl.	268	IXb
6702	18	44	33	+45	36.7	Lyra	5931				Neb. spot	269, 270	
6703	18	44	55	+45	27.5	Lyra	5932				Plan.?	269, 270	
6804	19	27	37	+	9 2.9	Aquila	4499	VI	38	2043	Plan.	120	
6818	19	39	17	−14	21.1	Sagittarius	4510	VI	51	2047	Plan.	115, 116, 137	IIc
6826	19	42	34	+50	19.4	Cygnus	4514	IV	73	2050	Plan.	130, 131, 132	
6894	20	13	3	+30	18.6	Cygnus	4565	IV	13	2072	Plan.	4, 7	
6905	20	18	42	+19	50.3	Delphinus	4572	IV	16	2075	Plan.	145, 147, 149	
7008	20	58	8	+54	13.5	Cepheus	4627	I	192	2099	Irr.	243	IId
7009	20	59	39	−11	41.6	Aquarius	4628	IV	1	2098	Plan.	138, 140	IIe
7023	21	0	35	+67	50.3	Draco	4634	IV	74		Irr.	12	
7026	21	3	30	+47	30.8	Cygnus		Burnham			Plan.	156	
7027	21	3	56	+41	54.0	Cygnus		Webb			Plan.	142	
7129	21	41	4	+65	43.3	Cepheus	4702	IV	75	2131	Irr.	273, 274	
7177	21	56	44	+17	20.4	Pegasus	4734	II	247	2139	Spl.	126	
7217	22	4	10	+30	57.2	Pegasus	4760	II	207	2149	Spl.	216	IXc
7662	23	21	54	+42	4.8	Andromeda	4964	IV	18	2241	Plan.	29, 148, 157, 172, 173, 177	IIf

NOTES

N.G.C. 2825–2829, 2831, 2832, 2834, 2839, see text description of N.G.C. 2830.
N.G.C. 4206, 4222, see text description of N.G.C. 4216.
N.G.C. 4374, 4387, 4388, 4402, 4407, 4425, see text description of N.G.C. 4406.
N.G.C. 4564, see text description of N.G.C. 4567–8.
N.G.C. 5566, 5569, see text description of N.G.C. 5560.
N.G.C. 5740, see text description of N.G.C. 5746.
N.G.C. 6702, see text description of N.G.C. 6703.

a different shading on one side of the major axis from that on the other, one side being soft while the other is more knotted and of stronger contrast, the latter resembling the effect produced by the sun shining through an irregular bank of clouds. All illustrations are placed with north (N) at the top and west (W, preceding) at the right.

All catalogued nebulae showing on any of the photographs here discussed have been inserted in the list; but those which appear only incidentally are described in the text under the *N.G.C.* number of the object for which the plate was primarily taken (see notes to Table I). A number of uncatalogued nebulae and nebulous stars are also shown. Mention of such is made in the text description of *N.G.C.* 1186, 2681, 2830, 2841, 4406, 5308, 5383, 6555, and 6703.

I am indebted to Mr. Ellerman for the preparation of the positives for the half-tones.

N.G.C. 205 Andromeda

$\alpha = 0^h 35^m 51^s$, $\delta = +41°14'.2$ (1917); $\lambda = 89°$, $\beta = -22°$
Plate No. 152, 1912, October 9, 230^m. Images large
Illustrated Plate IV*a*

This is the bright nebula lying on the N*p* side of the great nebula of Andromeda 36'.4 distant. On a diffuse ellipse $10' \times 4'$, $p = 172°$, gradually fading away at the edge, lies centrally a brighter patch about $1'.5 \times 1'$. Besides the sharp nucleus there is detail in the bright central part, and dark patches of irregular shape, similar in character to that surrounding the nucleus of the great nebula, lie one on the S end and the other on the N*f* end. The nebula is possibly spiral, but the exposure is not long enough to show detail in the outer nebulosity. Huggins[1] assigns it a continuous spectrum.

N.G.C. 278 Cassiopeia

$\alpha = 0^h 47^m 23^s$, $\delta = +47°6'$ (1917); $\lambda = 92°$, $\beta = -16°$
Plate No. 168, 1912, November 8, 240^m. Fine plate.
Illustrated Plate IV*b*

This fine left-handed spiral is seen in plan. Four or five whorls emanating from the nucleus make about a half-revolution before

[1] *Philosophical Transactions*, **156**, 388, 1866.

fading suddenly to a very much less intensity, thus forming a bright center irregularly round, 50″ in diameter. One arm, however, is interrupted, but again continues strong and forms a wing to the bright patch on the northern side. Along these arms lie many bright nebulous knots and condensations. Outside this the arms continue faint, and they fade out at 85″ diameter. The nucleus is irregular and appears to be a number of knots bunched together, each forming the starting-point of an arm.

N.G.C. 650–651 Persei

$\alpha = 1^h 37^m 4^s$, $\delta = +51°9'$ (1917); $\lambda = 99°$, $\beta = -11°$
Plate No. 57, 1912, February 19, 105^m. Poor plate
Plate No. 150, 1912, October 7, 180^m. Poor plate
Plate No. 151, 1912, October 8, 360^m. Poor plate
Plate No. 170, 1912, December 6, 15^m. Poor plate

The shape of this gaseous nebula reminds one of a moth; a strong, irregular, elliptical mass with diaphanous extension on either side. The body is about $1'.6 \times 1'$, $p = 41°$, with wings extending about $1'$ either side. The whole forms the central zone of a circle of $3'$ diameter, the wing periphery being tangent to the circle. On the E side a faint wisp extends beyond this; at the center of the circle lies a faint star. The brightest spot in the nebula, forming the S*p* portion, is N.G.C. 650; N.G.C. 651 is the N*f* portion. The spectrum of the nebula shows bright lines.[1]

N.G.C. 895 Cetus

$\alpha = 2^h 17^m 29^s$, $\delta = -5°54'.3$ (1917); $\lambda = 140°$, $\beta = -58°$
Plate No. 281, 1916, November 28, 75^m. Weak exposure

This is a right-handed spiral $3'.5 \times 2'$, $p = 120°$. Two prominent arms emerge from the faint nucleus, one of which, as is often the case, is interrupted only to fork out into two branches. This, however, may be merely an effect of contrast caused by an overlapping streamer. Quite away from the nucleus the arms are apparently strings of knotted nebulosity. N.G.C. 894 blends with the spiral.

[1] *Astrophysical Journal*, 33, 59, 1911.

N.G.C. 955 Cetus

$\alpha = 2^h 26^m 20^s$, $\delta = -1°28'.6$ (1917); $\lambda = 138°$, $\beta = -54°$

Plate No. 229, 1913, November 25, 90^m. Images elongated

This is a spindle nebula, almost certainly spiral, about $80'' \times 7''$, $p = 20°$, with a stellar nucleus W of the center. At one time it was thought to be variable, but Dreyer has doubted this. The strong part of the nebula forms a rhombus $45'' \times 7''$.

N.G.C. 972 Aries

$\alpha = 2^h 29^m 20^s$, $\delta = +28°56'.9$ (1917); $\lambda = 116°$, $\beta = -28°$

Plate No. 231, 1913, November 26, 195^m. Good plate

Illustrated Plate IV*e*

This object has the shape of an irregular ellipse of greatly varying intensity, about $2' \times 1'.9$, $p = 152°$, almost certainly a left-handed spiral. The strong region E of the major axis is somewhat elliptical in shape, $40'' \times 15''$, with its axis parallel to the general figure of the nebula. Its detail is knotted and full of contrast, with a very strong knot at the N end. W of the major axis, except for the knots described below, the nebulosity consists of large softer wisps mingled with dark lanes. At 28″ N*p* the nucleus is a strong triple condensation and at 26″ S*f* the nucleus is a strong knot, both lying on the major axis. There are two more condensations beyond the N one, both surrounded by a dark ring except for a wisp on the rear side as met traveling along the arm from the center and a fine strong thread on the front side.

N.G.C. 1023 Perseus

$\alpha = 2^h 35^m 12^s$, $\delta = +38°42'.5$ (1917); $\lambda = 112°$, $\beta = -18°$

Plate No. 171, 1915, December 7, 240^m. Bad seeing

A bright nucleus 15″ in diameter lies on an ellipse $90'' \times 45''$, $p = 70°$. From this extend faint wings in either direction along the major axis, forming an ellipse $5' \times 1'$, $p = 85°$.

Fath[1] found for the nebula a spectrum of the solar type, and Slipher's[2] value of radial velocity is roughly +200 km.

[1] *Astrophysical Journal*, 37, 199, 1913.

[2] *Popular Astronomy*, 23, 36, 1915.

N.G.C. 1068 Cetus

$\alpha = 2^h38^m26^s$, $\delta = -0°21'.9$ (1917); $\lambda = 141°$, $\beta = -51°$

Plate No. 49, 1911, December 22, 120^m. Illustrated Plate IV*d*
Plate No. 53, 1911, December 25, 22^m. Illustrated Plate IV*c*
Good plates

This left-handed spiral is viewed in plan, with three striking gradations of intensity centrally superimposed. Surrounding the bright central nucleus, elongated in $p = 40°$, is a strong, distinct spiral forming an ellipse $40'' \times 25''$, $p = 50°$, consisting mainly of two arms emanating from the ends of the nucleus, which extend a little more than a half-revolution. Distinct nebulous condensations lie along these arms. Outside this strong center is a fainter annulus $130'' \times 110''$, $p = 10°$, still holding the spiral form. Two of the arms are continuations of the central branches, but there are others besides, all softly mottled in appearance. Beyond this lie two immense and very faint arms, starting at about $p = 30°$, and extending to an ellipse $6' \times 5'$, $p = 60°$. These are so faint that it is difficult to say more than that they appear mottled. On the plate showing this external faint material the entire central spiral form is so overexposed that no detail shows. The spectrum[1] obtained with the focal-plane slit gives a value for the radial velocity of +765 km, while Slipher's[2] value is +1100 km. Fath[3] found an absorption spectrum with bright lines.

N.G.C. 1186 Perseus

$\alpha = 3^h0^m4^s$, $\delta = +42°30'.2$ (1917); $\lambda = 115°$, $\beta = -13°$

Plate No. 244, 1914, November 13, 75^m. Good plate
Plate No. 245, 1914, November 14, 130^m. Good plate, grain a little coarse

This supposedly variable nebula lies 2° north of Algol. It is a faint left-handed spiral $2' \times 0'.5$, $p = 120°$, with faint stellar nucleus. A star several magnitudes brighter than the nucleus lies directly on one of the arms at $p = 230°$, $12''$. There is a knot N of the nucleus at $p = 330°$, $12''$. There are 15 faint nebulae lying within a radius of $15'$.

[1] *Publications of the Astronomical Society of the Pacific*, **27**, 134 and 192, 1915.
[2] *Popular Astronomy*, **23**, 36, 1915.
[3] *Astrophysical Journal*, **33**, 60, 1911.

N.G.C. 1501 Camelopardus

$\alpha = 3^h 59^m 50^s$, $\delta = +60°41'.9$ (1917); $\lambda = 112°$, $\beta = +7°$

Plate No. 174, 1912, December 10, 60^m

Plate No. 178, 1913, January 7, 120^m. Illustrated Plate I*a*

Good plates

This is a fine planetary of regular elliptical shape, $60'' \times 45''$, $p = 120°$, with protuberances at each end of the minor axis making the total breadth $53''$. The nebula is irregularly mottled, bearing a resemblance to the convolutions of the brain. Its periphery is in general denser than its center, and is twice as dense at the ends of the minor axis as at the extremities of the major axis. There is a bright central stellar nucleus. The spectrum shows bright lines.

N.G.C. 1535 Eridanus

$\alpha = 4^h 10^m 23^s$, $\delta = -12°56'.9$ (1917); $\lambda = 174°$, $\beta = -39°$

Plate No. 163, 1912, November 5, 60^m. 100-foot focus

Plate No. 182, 1913, February 4, 85^m. 25-foot focus. Illustrated Plate I*b*

This is a planetary of almost uniform intensity $46'' \times 40''$, $p = 23°$, on which lie a strong ring, a strong stellar nucleus, and a faint star. The ring is irregularly round, $18''$ in diameter, elongated in the same direction as the disk, quite sharp on the outer edge, but softer on the inner edge with branches running to the nucleus. The star is at $p = 320°$, $17''$. The spectrum shows bright lines; Keeler's[1] value of the radial velocity is -10.4 km.

N.G.C. 1579 Perseus

$\alpha = 4^h 24^m 46^s$, $\delta = +35°6'.0$ (1917); $\lambda = 133°$, $\beta = -8°$

Plate No. 227, 1913, October 29, 30, 31, 420^m. Illustrated Plate III*a*

This is an irregular nebula of the dispersive type; the dark lanes call to mind the Trifid nebula, and the outer faint nebulosity, that of the Orion nebula. The most prominent bit of nebulosity is a broad arrowhead adjoining the principal dark lane on the N and pointing due E; it is mottled in appearance and full of detail. Directly S of the arrowhead in the dark lane is a very faint star.

[1] W. W. Campbell, *Stellar Motions*, p. 210.

The principal part of the nebula lies within a circle of 5′ diameter, while faint patches extend Np to a distance of 10′ from the center. There are four stars which form nuclei for patches of nebulosity. Their positions with respect to the faint central star are as follows:

a.....	35°12′.8	10	mag. (very rough)
b.....	213° 6.5	11	mag.
c.....	251°10.0	11	mag.
B.D.+34°883.....	346° 3.1	9.5	mag.

N.G.C. 1931 Auriga

$\alpha = 5^h25^m55^s$, $\delta = +34°11'.0$ (1917); $\lambda = 143°$, $\beta = +1°$

Plate No. 277, 1916, October 27, 15^m
Plate No. 278, 1916, October 28, 60^m

This group of small stars, one of which is double, is here apparently superimposed upon an irregular, patchy, nebulous mass contained within a circle 1′.5 in diameter. Several loops appear in the nebulosity, and there are two prominent dark spots. At 3′.7 S of the nebula lies another star with a nebulous wing to the SW. The region is rich in stars, though the nebula lies in one of the so-called dark lanes, where the stars are much fewer than in the adjacent parts.

N.G.C. 2022 Orion

$\alpha = 5^h37^m33^s$, $\delta = +9°2'.7$ (1917); $\lambda = 164°$, $\beta = -9°$

Plate No. 183, 1913, February 4, 60^m. Good plate. Illustrated Plate I*c*

This is a fairly bright planetary with a disk of almost uniform intensity, on which lies a ring and nucleus. The nebula is sharply outlined, and may best be described as the central zone of a circle 30″ in diameter; equator lies in $p = 115°$, the distance between the sides being 27″; the S side is a little convex outward. The ring is very much stronger in intensity than the disk. It is elliptical, 20″×15″, $p = 13°$ (median line), and on the average about 4″ wide. There is a condensation in the ring at each end of the axis in $p = 30°$, making the axis 23″ long. There is an interruption in the N side of the ring and a wisp running toward the nucleus from the S knot. The spectrum shows bright lines.

N.G.C. 2366 Camelopardus

$\alpha = 7^h 20^m 7^s$, $\delta = +69°11'.5$ (1917); $\lambda = 113°$, $\beta = +29°$

Plate No. 279, 1916, October 30, 60^m. Very weak

This is the same general character as N.G.C. 4449, composed of nebulous knots and soft nebulosity. Very irregular in shape, $3' \times 1'$, $p = 30°$, with the brightest star or knot near the S end; $1'$ E of this star lies a group irregularly $30''$ in diameter.

N.G.C. 2371–2 Gemini

$\alpha = 7^h 20^m 20^s$, $\delta = +29°39'.1$ (1917); $\lambda = 157°$, $\beta = +21°$

Plate No. 257, 1916, March 6–7, 221^m. Bad seeing. Images large

Illustrated Plate I*d*

This gaseous nebula comprises an irregularly round, patchy mass of nebulosity lying within $33''$ radius of a stellar nucleus; two wisps on opposite ends of an axis in $p = 120°$, each $1'$ distant from the nucleus. The striking parts of the nebula are two strong condensations in the central part, diametrically opposite each other on an axis in $p = 60°$, each about $15''$ in size and $15''$ from the nucleus. In the *f* condensation is a faint star, and on the W edge of the *p* one a hazy nucleus. Faint wisps extend from the central mass to points halfway between the nucleus and the outer condensations, the W ones forming a loop, a feature seen also in N.G.C. 7026. Each of the outer wisps is $10'' \times 45''$ and lies perpendicular to the line joining them, being slightly convex outward with streamers turned inward.

N.G.C. 2392 Gemini

$\alpha = 7^h 24^m 16^s$, $\delta = +21°5'.0$ (1917); $\lambda = 165°$, $\beta = +19°$

Plate No. 187, 1913, March 6, 180^m. 25-foot focus
Plate No. 189, 1913, March 7, 10^m. 25-foot focus
Plate No. 190, 1913, March 7, 30^m. 25-foot focus
Plate No. 191, 1913, March 7, 60^m. 25-foot focus
Plate No. 255, 1915, December 8–9, 120^m. 80-foot focus

Illustrated Plate I*e*, and I*f*

Plate No. 258, 1916, April 1, 30^m. 25-foot focus

This bright planetary can best be described as the pupil of an eye with the surrounding iris. The iris varies only a few seconds from a mean outside diameter of $46''$ and consists of a uniform

annulus with about 20 bright knots non-uniformly distributed along its median line. The knots are sharply bounded on the side toward the pupil and stringy toward the outside. There are several interruptions in the string of knots, notably at $p=144°$, where two lie diametrically opposite. The brighter knots are on the S side along $p=189°$, where four or five of them form an almost continuous mass. Opposite these is another continuous set, but not so bright. Between the ends of these two series the knots stand more apart. W of the "pupil," between it and the ring of knots, is an elongated condensation lying in a NS position. A 3^h exposure does not extend the disk any, but 3 threads spring from as many knots of the iris on the E side and curve out over the edge of the disk a distance of $5''$. The pupil is stirrup-shaped, $19''\times17''$, with axis $p=5°$, and has a strong central nucleus. The N periphery is bright; the E has two bright knots, the W two, and the S one that reaches almost to the nucleus, and half-way between the nucleus and the N side is another; between this latter and the N side is a vacant space. The nucleus is listed as B.D. $+21°$ 1609, $9^m.1$. A focal-plane spectrum shows a continuous band crossed by projecting bright lines. Campbell and Moore[1] found internal motion in the nebula. Both illustrations are from the same negative, the one to show central detail, the other the external ring.

N.G.C. 2403 Camelopardus

$\alpha=7^h28^m49^s$, $\delta=+65°46'.9$ (1917); $\lambda=118°$, $\beta=+30°$

Plate No. 169, 1912, November 8, 210^m. Good plate. Illustrated Plate V*c*

This fine right-handed spiral nebula resembles M 33. The bright part is contained within an ellipse roughly $9'\times5'$, $p=126°$. Faint knots and arms extend as far as $10'$ from the center. It does not possess the wealth of detail of M 33, but it has the same sharp stellar images, the nebulous stars, the bunching of these into knots, and the dark streaks where one can imagine one looks completely through the nebula to the sky beyond. While M 33 has two strong arms running out from the center, this nebula has but one, which starts from the central mass at the S*p* side, the opposite side being

[1] *Publications of the Astronomical Society of the Pacific*, **28**, 119, 1916.

a continuous sheet of nebulosity, not separable into arms. There is no distinct central nucleus.

N.G.C. 2681 Ursa Major

$\alpha = 8^h47^m36^s$, $\delta = +51°37'.7$ (1917); $\lambda = 134°$, $\beta = +41°$

Plate No. 179, 1913, January 7, 190^m. Good plate. Illustrated Plate IV*f*

This right-handed spiral is seen in plan. There is a strong central nucleus out of which springs at $p = 35°$ a single arm which wraps itself concentrically around the nucleus at a mean radius of 20″ and stops in the NE quadrant. It is possible that this arm is really continued inward in the ring of nebulosity which entirely surrounds the nucleus at a mean radius of 8″. In the SW quadrant of this ring, however, are two strong condensations, which appear as if they might be very short arms, and a third fine wisp that starts at $p = 185°$ and runs into the outer arm. Traces of the W half of a ring of 40″ radius appear with ends forming elongated knots at $p = 25°$ and 205°, and at a mean radius of 1′.25 is an almost continuous faint broad ring. A long exposure is necessary to determine whether the two outer rings really form part of the spiral arms. Five small faint nebulae appear on the plate.

N.G.C. 2830 Lynx

$\alpha = 9^h14^m44^s$, $\delta = +34°6'.0$ (1917); $\lambda = 158°$, $\beta = +46°$

Plate No. 246, 1914, November 15, 150^m
Plate No. 247, 1914, November 16, 60^m

This is a spindle nebula 50″×6″, $p = 106°$, with faint stellar nucleus.

The ends of the nebula bend counter-clockwise, giving it a resemblance to the integral sign. The traces of detail show that it is almost certainly a spiral.

On this photograph 36′×36′ are 28 nebulous spots or stars, 6 spindles with nucleus, and 3 without; among them are the following:

N.G.C. 2825—A spindle about 40″×4″, $p = 83°$, of about the same intensity as N.G.C. 2830. It has a stronger nucleus than N.G.C. 2830 and a knot N*f* the nucleus.

N.G.C. 2826—A rhombus about 1′×6″, $p = 143°$, with nucleus and nebulosity much stronger than N.G.C. 2830.

N.G.C. 2827—Faint nucleus in elongated nebulosity in $p=8°$.
N.G.C. 2828—Nebulous star in very faint elongated nebulosity $p=45°$.
N.G.C. 2829—Nebulous star.
N.G.C. 2831—Nebulous star.
N.G.C. 2832—Strong nucleus surrounded by strong nebulosity that fades rapidly to about 14″ diameter, then gradually to 30″ diameter. The whole is elongated, $p=150°$.
N.G.C. 2834—Nebulous star.
N.G.C. 2839—Nebulous star.

N.G.C. 2841 Ursa Major

$\alpha=9^h16^m18^s$, $\delta=+51°19'.7$ (1917); $\lambda=135°$, $\beta=+45°$

Plate No. 58, 1912, February 19, 120^m. Good plate. Illustrated Plate V*a*

This is a fine left-handed spiral nebula $6'.5\times2'.2$, $p=150°$. The strong nucleus lies in an almost uniform glow of nebulosity, but the fine sweeping arms are streamers of nebulous knots. This nebula shows very nicely the difference in the nebulosity on the two sides of the major axis. The W side is softened and permeated with a glow, lacking in the E side, which is of marked contrast. In a field $36'\times36'$, 16 faint nebulae appear.

N.G.C. 2976 Ursa Major

$\alpha=9^h40^m24^s$, $\delta=+68°17'.9$ (1917); $\lambda=111°$, $\beta=+42°$

Plate No. 175, 1912, December 10, 180^m. Good negative
Illustrated Plate V*b*

This bright elliptical nebula $3'.2\times1'$, $p=142°$, is full of condensations and dark lanes, with faint extensions 25″–30″ at each end. The arrangement of some of the patches and dark lanes gives it somewhat the appearance of a spiral, but one cannot be certain. There is no nucleus, but at the center are three bright stellar knots and a fourth elongated knot. There are 11 more of these knots scattered about the nebula, together with many that range from small nebulous spots to areas barely distinguishable from the general nebulosity.

N.G.C. 3115 Sextans

$\alpha=10^h1^m6^s$, $\delta=-7°18'.9$ (1917); $\lambda=216°$, $\beta=+38°$

Plate No. 56, 1911, December 25, 100^m. Good plate. Illustrated Plate VI*a*

This is a bright spindle with an oblate center, which measures about 30″×25″. The disk lies in $p=45°$, is about 6″ wide, and

strong and continuous for about 45″ either side of the nucleus; then come several interruptions and knots. The whole lies within an elliptical halo of nebulosity 3′×1′. Slipher's[1] value for the radial velocity is roughly +400 km.

N.G.C. 3593 Leo

$\alpha = 11^h10^m17^s$, $\delta = +13°16'.0$ (1917); $\lambda = 210°$, $\beta = +64°$

Plate No. 185, 1913, March 5, 210^m. Good plate. Illustrated Plate VI*b*

This nebula has more or less of the spiral characteristics, but it cannot be said for certain that it is a spiral. On a faint patchy elliptical ground of nebulosity 4′.5×1′, $p = 89°$, lies centrally a bright patch 60″×13″. The E 15″ of this ellipse is not much brighter than the fainter nebulosity; the W end is crossed by two straight dark lanes, the one nearest the center running in $p = 39°$ to 219°, the other in $p = 178°$ to 358°, thus forming two isolated bright spots. At the E end of the bright central part are two stellar condensations. At the E end of the faint nebulosity there are a number of dark wisps or tongues curved left-handed. An irregular dark lane runs N of the bright center almost the length of the major axis.

N.G.C. 3666 Leo

$\alpha = 11^h20^m8^s$, $\delta = +11°47'.9$ (1917); $\lambda = 215°$, $\beta = +66°$

Plate No. 248, 1915, February 12, 150^m. Weak plate

This is a faint left-handed spiral 3′.5×0′.7, $p = 100°$, the central part 80″×20″ being brighter, and having a number of nebulous knots scattered through it, the brightest of which is the nucleus. At one time it was suspected of variability, but Dreyer's conclusions are opposed to this.

N.G.C. 3938 Ursa Major

$\alpha = 11^h48^m31^s$, $\delta = +44°35'.4$ (1917); $\lambda = 118°$, $\beta = +70°$

Plate No. 249, 1915, March 12, 39^m. Poor plate

The photograph is a very weak exposure, but sufficient to show a right-handed open spiral 4′ in diameter, having a small bright nucleus and resembling M 74 or M 101, with most of the material in the well-separated arms.

[1] *Popular Astronomy*, 23, 36, 1915.

N.G.C. 4216 Virgo

$\alpha = 12^h11^m40^s$, $\delta = +13°36'.4$ (1917); $\lambda = 243°$, $\beta = +73°$

Plate No. 192, 1913, March 7, 90^m. Illustrated Plate VI*c*

Good plate, but needs longer exposure

This is a left-handed spiral $6' \times 1'$, $p = 21°$. The nucleus and the arm starting from it are bright; there is a condensation $1'$ N of the nucleus. The *p* side is soft, while the *f* side shows the marked contrast usual in inclined nebulae. There are many nebulous spots scattered over the plate and $10'$ *p*, $2'$ N of the nucleus of 4216 lies a left-handed nebula about $30''$ diameter. The two following nebulae also appear on the plate:

N.G.C. 4206—Faint spiral, $4' \times 30''$, $p = 1°$.
N.G.C. 4222—Faint spindle, $2'.5 \times 10''$, $p = 59°$.

N.G.C. 4236 Draco

$\alpha = 12^h12^m48^s$, $\delta = +69°56'.0$ (1917); $\lambda = 95°$, $\beta = +47°$

Plate No. 201, 1913, May 7, 180^m. Poor plate

This nebulosity lies S*p* the variable star SW Draconis. It is an irregular cloud of nebulous stars and nebulous haze roughly scattered about a region $15' \times 4'$, $p = 160°$. The strongest parts are a mixed group in the N*p* corner and a wisp extending from the N end a little to the E of southward for about $7'$.

N.G.C. 4406 Virgo

$\alpha = 12^h21^m59^s$, $\delta = +13°24'.3$ (1917); $\lambda = 251°$, $\beta = +75°$

Plate No. 234, 1914, March 18, 90^m

The photograph shows a nebulous spot, having a bright nucleus, gradually decreasing in brightness until it fades away at a mean radius of $35''$. It is slightly elongated in $p = 130°$. Besides a number of faint nebulae and spots the following nebulae appear:

N.G.C. 4374—Practically the same type and size as N.G.C. 4406. The nucleus is possibly a little larger, but the nebula lies near the edge of the plate.

N.G.C. 4387—Of the same type as N.G.C. 4406, $40'' \times 15''$. Elongated in $p = 140°$.

N.G.C. 4388—An elliptical nebula $3'.5 \times 30''$, $p = 90°$, lying near the S edge of the plate. A bright T-shaped knot, base to the N, cuts across

the center, with a dark spot on either side. A second bright elongated knot lies just W of the base of the T. Probably spiral.

N.G.C. 4402—A faint elongated nebula $3' \times 35''$, $p = 89°$, dark elongated central space, bright periphery, soft outside and indented inside; probably spiral.

N.G.C. 4407—An elongated nebulous spot lying near the S edge of the plate, $20'' \times 8''$, $p = 10°$.

N.G.C. 4425—A spindle consisting of nucleus 8″ diameter in uniform nebulosity about $90'' \times 22''$, $p = 30°$.

N.G.C. 4449 Canes Venatici

$\alpha = 12^h24^m11^s$, $\delta = +44°33'.0$ (1917); $\lambda = 96°$, $\beta = +72°$

Plate No. 198, 1913, April 7, 300^m. Illustrated Plate III*b*

This is an irregular nebulous mass in which many nebulous stars are distributed unevenly. The greater part of the nebula is roughly rectangular, about $4'.5 \times 2'.5$, $p = 40°$, there being an assemblage of some dozen nebulous stars W of the SW corner. On the original negative there are 230 nebulous stars or patches, about 40 appearing bright and 190 faint, though the gradation is very uniform. Two-thirds of them are in the N half. The nebulosity proper is weak toward the edge, gradually increases inward, and culminates along a central ridge, where it is as strong as the stars themselves. A number of dark irregular rifts appear here and there in it. Wolf[1] found an absorption spectrum similar to that of the Andromeda nebula, with possible bright lines.

N.G.C. 4567–8 Virgo

$\alpha = 12^h32^m20^s$, $\delta = +11°42'.9$ (1917); $\lambda = 264°$, $\beta = +73°$

Plate No. 235, 1914, March 19–20, 180^m

Plate No. 237, 1914, April 24, May 19, 360^m. Illustrated Plate VI*d*

The plate shows two fine overlapping spirals; one, N.G.C. 4567, seen more nearly in plan than N.G.C. 4568.

N.G.C. 4567 is a right-handed spiral $2' \times 1'.5$, $p = 75°$, having a small bright nucleus and two arms consisting chiefly of nebulous stars. The nebulosity is weak and irregular in intensity with a number of dark lanes, notably one following the concave side of

[1] *Sitzungsberichte der Heidelberger Akad.*, August 26, 1912.

the p arm. There is evidence of much disturbance in the nebula, as the W arm is broken off and forked and the E arm offset.

N.G.C 4568 is a right-handed spiral $4' \times 1'.5$, $p = 29°$, having a small nucleus which is fainter than that of N.G.C. 4567. It is hard to trace the arms distinctly about the nucleus, as the nebulous knots are irregularly placed. At their extremities the arms are much broken, especially on the N side, which is crossed with several great rifts; there is no question, however, as to the general trend. The dark rift at the apparent contact line of the two nebulae may really belong to N.G.C. 4568, which apparently lies beyond N.G.C. 4567.

N.G.C. 4564 appears on the plate as a spindle $90'' \times 20''$, $p = 49°$, with strong nebulous nucleus, $15''$ diameter. There are 6 or more very small faint nebulous spots or spindle nebulae on the plate.

N.G.C. 4594 Virgo

$\alpha = 12^h 35^m 40^s$, $\delta = -11° 10'$ (1917); $\lambda = 269°$, $\beta = +52°$

Plate No. 256, 1916, February 12, 55^m
Plate No. 259, 1916, April 6, 120^m
Plate No. 262, 1916, May 3, 132^m. Illustrated Plate VI*e*
Plate No. 264, 1916, May 26, 90^m. Seed 27 bathed Wallace 3 dye. Red screen

This fine spiral nebula, $7' \times 1'$, $p = 89°$ is seen almost edge-on, the convolutions being so nearly concentric that it is not possible to state whether it is right- or left-handed. It is crossed by a dark streak which lies at the periphery, being possibly an outer ring of cooler material, or perhaps the unilluminated edge of the thin disk of nebulous matter surrounding the brilliant nucleus. The streak is $9''$ wide except near the ends, where it gradually broadens to twice this width. A trace of nebulosity runs almost centrally along the dark streak. A strong halo $2'$ in diameter surrounds the nucleus, and the first ring is much stronger than the surrounding ones. A test for possible differences in temperature, by exposures made on a Seed 23 plate and on a red-sensitive plate with a screen transmitting λ 5650–7600, showed no certain difference.

An 80-hour exposure with the focal-plane spectrograph, the slit parallel to the major axis and across the nucleus, showed that: (*a*) the spectrum is F5; (*b*) the velocity-curve is sensibly linear, $V = -278x + 1180$, the radial velocity accordingly being 1180 km

and the rotation, at a distance of 2′, 330 km, the W side approaching and the E side receding from the observer.

N.G.C. 4736 Canes Venatici

$\alpha = 12^h46^m59^s$, $\delta = +41°34'.3$ (1917); $\lambda = 85°$, $\beta = +76°$

Plate No. 60, 1912, February 20, 225m. Illustrated Plate VII*e*
Plate No. 3093P, 1916, May 8, 5m. Illustrated Plate VII*b*
Plate No. 3093P, 1916, May 8, 10m. Illustrated Plate VII*a*
Plate No. 3094P, 1916, May 8, 20m. Illustrated Plate VII*d*
Plate No. 3094P, 1916, May 8, 40m. Illustrated Plate VII*c*

This fine right-handed spiral has three regions of very marked difference in brightness. From a very bright, sharp stellar nucleus spring branches of smooth nebulosity, which after a turn about the nucleus break into a series of nebulous knots forming the periphery of an ellipse $2' \times 1'.5$, $p = 126°$. Here the intensity suddenly diminishes while the arms continue in fine sweeping curves of faint smooth nebulosity, devoid of knots save for two or three small patches, to such an extent as to fill an ellipse $5' \times 4'$, $p = 105°$. The nebulosity for a distance of 30″ diameter around the nucleus is very strong. Plates 3093–4 P, taken by Mr. Seares, show the central parts well. The nebula has a solar-type spectrum,[1] with possible Wolf-Rayet bands. Its radial velocity[2] is roughly +200 km.

N.G.C. 4900 Virgo

$\alpha = 12^h50^m28^s$, $\delta = +2°56'.5$ (1917); $\lambda = 280°$, $\beta = +66°$

Plate No. 188, 1915, March 5, 210m. Elongated images

The type of this interesting nebula cannot definitely be stated, though the lines are such as are followed by a left-handed spiral. It is irregularly round, 1′.5 in diameter, patchy in appearance, with a number of nebulous stars, a single row around the N rim and a double row on the S side. There is a faint central stellar nucleus crossed by a bright patch of nebulosity $15'' \times 6''$, $p = 145°$. A star much brighter than the nucleus lies on the S*f* point of the rim.

[1] *Astrophysical Journal*, **37**, 199–200, 1913.

[2] *Popular Astronomy*, **23**, 36, 1915.

N.G.C. 5005 Canes Venatici

$\alpha = 13^h 7^m 3^s$, $\delta = +37° 30'.2$ (1917); $\lambda = 64°$, $\beta = +78°$

Plate No. 59, 1912, February 19, 50^m

This left-handed spiral $3'.5 \times 1'.3$, $p = 69°$, has a stellar nucleus surrounded by strong nebulosity which gradually fades toward the edge. The N half shows contrast, and the S half is smooth.

N.G.C. 5308 Ursa Major

$\alpha = 13^h 44^m 15^s$, $\delta = +61° 23'.5$ (1917); $\lambda = 76°$, $\beta = +55°$

Plate No. 196, 1913, April 4, 180^m. Good plate

This is a spindle with oblate center $2' \times 0'.25$, $p = 60°$, having almost no detail. On either side of the bright nucleus the major axis appears as a bright line, gradually fading toward the rim and apparently interrupted at the nucleus on the p side. Several nebulous spots appear on the plate.

N.G.C. 5383 Canes Venatici

$\alpha = 13^h 53^m 41^s$, $\delta = +42° 14'.9$ (1917); $\lambda = 48°$, $\beta = +69°$

Plate No. 195, 1913, April 3, 180^m. Images elongated. Illustrated Plate VIII*b*

Plate No. 199, 1913, May 5, 6, 360^m. Good plate. Illustrated Plate VIII*a*

This right-handed spiral resembles a pinwheel lying about a very bright multiple nucleus within a circle $2'.25$ diameter. Some disturbance has altered the regularity of distribution of the typical form. On the f side much of the nebulosity has been swept into a broad band running in a SE direction to a row of bright nebulous knots lying along the rim at right angles to it; enough nebulosity remains, however, to show the spiral form. In the p arm there are no traces of the spiral form, everything being swept into a broad band running in a NW direction from the nucleus for some distance, when it suddenly turns counter-clockwise in a bright ridge diametrically opposite and similar to that of the E arm. A dark streak runs from between the central and S parts of the nucleus and separates the p band into two arms; opposite this another dark interrupted streak emanating from between the central and the N members of the nucleus, runs E and S following the line of the spiral. The nucleus consists of 3 almost parallel bright condensations 15″ to 20″

long, elongated in $p=100°$, their central lines separated about 6″.5, the northernmost slightly *f*, and the southernmost *p* the central one. A dark streak cuts across the three members of the nucleus, running almost due NS.

S of N.G.C. 5383, 3′.25, lies a faint S-shaped left-handed spiral about 1′ in diameter.

N.G.C. 5544–5 Boötes

$\alpha=14^h13^m33^s$, $\delta=+36°57'.3$ (1917); $\lambda=32°$, $\beta=+68°$

Plate No. 127, 1912, June 13, 180^m

Plate No. 261, 1916, May 1, 2, 3, 4, 5, 360^m. Illustrated Plate VIII*c*

Good negatives

These are two overlapping spirals, the E one in plan, the W one very much inclined to the line of sight.

N.G.C. 5544 is a left-handed spiral 70″×15″, $p=60°$, its *f* end just tangent to the NW point of the nucleus of N.G.C. 5545. The nucleus is faint and stellar. The arms are about equal in intensity where they start from the nucleus, but that on the E side continues bright for a much greater distance, being interrupted, however, at several points.

N.G.C. 5545 consists of a bright stellar nucleus, a nebulous ring 28″ outside diameter, a fainter diametral streak crossing the nucleus in $p=130°$, and another ring about the same intensity as the inner one, irregularly round, 45″ outside diameter, both being slightly elongated $p=120°$.

In N.G.C. 5545 the nebulosity is entirely soft; in N.G.C. 5544 several knots and condensations appear.

N.G.C. 5560 Virgo

$\alpha=14^h15^m54^s$, $\delta=+4°22'.3$ (1917); $\lambda=318°$, $\beta=+57°$

Plate No. 250, 1915, April 11, 200^m

This right-handed spiral is very much inclined to the line of sight. It has a weak nucleus, several knots in nebulosity near the nucleus, and two arms that make a half-revolution, then sweep outward very rapidly and fade away. It is 3′×0′.3, $p=105°$.

N.G.C. 5566 is a right-handed spiral, with a bright nucleus, 18″×8″, $p=30°$. Surrounding the nucleus is faint nebulosity from

which the arms emerge. More exposure is needed to bring out the arms well, but they sweep outward so as practically to fill an ellipse $6'\times1'.5$, $p=32°$. An elliptical ring of nebulosity $90''\times45''$, $p=20°$, gives the appearance of overlapping arms.

N.G.C. 5569 is a faint right-handed spiral in plan.

N.G.C. 5746 Virgo

$\alpha=14^h40^m43^s$, $\delta=+2°18'.3$ (1917); $\lambda=323°$, $\beta=+52°$

Plate No. 236, 1914, March 20, 21, 22, 360^m. Good plate

Illustrated Plate VIII*d*

This fine right-handed spiral is seen almost edge-on, having the characteristic oblate center surrounding the bright nucleus. It is crossed by a dark streak parallel to the major axis; nebulosity full of contrast occurs on the W side, the E side being smooth. The spiral form measures $7'.5\times0'.75$, $p=170°$, and the oblate halo projects to a semi-minor axis of $30''$.

N.G.C. 5740 lies near the S edge of the plate. It is a left-handed spiral $3'\times1'.25$, $p=160°$, with bright nucleus, and arms gradually weakening toward the edge. An asteroid trail appears (March 20) $p=234°$, $19'$, S*p* the nucleus, the trail lying in $p=158°$. Through the kindness of Dr. Leuschner, Miss Levy identified this as (304) Olga.

N.G.C. 5866 Boötes

$\alpha=15^h4^m12^s$, $\delta=+56°5'.0$ (1917); $\lambda=58°$, $\beta=+52°$

Plate No. 129, 1912, June 14, 165^m. Illustrated Plate VIII*e*

This nebula is lenticular, $2'.5\times0'.75$, $p=126°$, with no apparent nucleus, but with a bright center gradually decreasing in intensity toward the edge. Lying across the center and making an angle of 3° with the major axis is a narrow dark streak, $p=123°$, about $1'$ long. Overlapping this at either end, and extending along the major axis to a distance of $45''$ in either direction from the center, lies a streak as bright as the central nebulosity, which gradually fades out toward the end. Slipher's[1] value for the radial velocity is +600 km.

[1] *Popular Astronomy*, **23**, 36, 1915.

N.G.C. 5907 Draco

$\alpha = 15^h 13^m 44^s$, $\delta = +56°38'$ (1917); $\lambda = 57°$, $\beta = +51°$

Plate No. 197, 1913, April 4, 90^m. Weak plate

This nebula is a spiral seen edge-on, similar to N.G.C. 5746 in having a longitudinal absorption streak lying just to one side of the nucleus. It measures $11' \times 0'.7$, $p = 156°$.

N.G.C. 6070 Serpens

$\alpha = 16^h 5^m 45^s$, $\delta = +0°55'.7$ (1917); $\lambda = 340°$, $\beta = +35°$

Plate No. 265, 1916, May 26, 75^m
Plate No. 267, 1916, May 27, 150^m. Illustrated Plate IX*a*

This is a right-handed spiral $3' \times 1'.3$, $p = 59°$. Several arms dotted with nebulous stars make a full turn or more; those ending on the *f* side are well defined, those on the S*p* side diffused and free of knots. Directly *f* the nucleus two arms of the same curvature appear to overlap. There is a small stellar nucleus in an elongated nebulous knot. In a line a little to E of N of the nucleus the arms are much reduced in intensity.

N.G.C. 6210 Hercules

$\alpha = 16^h 41^m 1^s$, $\delta = +23°57'.2$ (1917); $\lambda = 11°$, $\beta = +36°$

Plate No. 139, 1912, July 13, 60^m. 100-foot focus

This is the well-known bright planetary nebula, Struve No. 5. The negative is overexposed, but one can see a bright central nucleus, bright nebulous streaks, fainter short curves bowed outward, some of them fading before returning, and several faint extensions, all of which give the nebula an angular appearance. The focal-plane slit spectrum is continuous for the star and crossed by bright lines projecting on either side. Keeler's[1] value of the radial velocity is -34.3 km and Campbell and Moore[2] have found internal motion.

[1] W. W. Campbell, *Stellar Motions*, p. 210.

[2] *Publications of the Astronomical Society of the Pacific*, **28**, 120, 1916.

N.G.C. 6217 Ursa Minor

$\alpha = 16^h36^m32^s$, $\delta = +78°22'$ (1917); $\lambda = 79°$, $\beta = +33°$

Plate No. 200, 1913, May 6, 60^m. Weak plate

This right-handed spiral has a stellar nucleus. Nebulosity is noticeably absent near nucleus. There are nebulous knots along the arms. It measures $1'.5 \times 1'$, $p = 160°$.

N.G.C. 6309 Ophiuchus

$\alpha = 17^h9^m24^s$, $\delta = -12°48'.9$ (1917); $\lambda = 337°$, $\beta = +13°$

Plate No. 252, 1915, May 10, 90^m. Illustrated Plate II*a*

Plate No. 263, 1916, May 5, 10^m

The plate shows a nebulous spot with a well-defined arrowhead at the S end, a blunt arrowhead at the N end, both pointing outward, the two connected by faint nebulosity. A faint stellar nucleus lies at the base of the N head a little N of the center of the nebula. It measures $22'' \times 12''$, $p = 162°$. Keeler's[1] value of the radial velocity is -51.5 km.

N.G.C. 6412 Draco

$\alpha = 17^h32^m4^s$, $\delta = +75°6'.6$ (1917); $\lambda = 74°$, $\beta = +31°$

Plate No. 128, 1912, June 13, 80^m. Weak plate

This is a faint left-handed spiral $90'' \times 70''$, $p = 160°$, having a faint stellar nucleus, with respect to which there is a knot of about the same brightness, $p = 350°$, $36''$.

N.G.C. 6478 Draco

$\alpha = 17^h32^m4^s$, $\delta = +51°11'.6$ (1917); $\lambda = 46°$, $\beta = +29°$

Plate No. 135, 1912, July 11, 270^m

This is a right-handed spiral, $90'' \times 30''$, $p = 32°$, having a stellar nucleus. A star a little brighter than the nucleus lies at $p = 10°$, $14''$. It is surrounded by a dark space $5''$ to $6''$ in diameter, the arms being cut off sharply. Does the star have an absorbing atmosphere? The detail is stronger in contrast on the p side. There are over a dozen very small and faint nebulae on this plate.

[1] W. W. Campbell, *Stellar Motions*, p. 210.

N.G.C. 6543 Draco

$\alpha = 17^h58^m35^s$, $\delta = +66°38'.3$ (1917); $\lambda = 63°$, $\beta = +9°$

Plate No.	9, 1911, July	23, 10^m.	25-foot focus
Plate No.	10, 1911, July	23, 20^m.	25-foot focus
Plate No.	11, 1911, July	23, 6^m.	25-foot focus
Plate No.	20, 1911, July	25, 90^s.	25-foot focus
Plate No.	34, 1911, October	18, 50^m.	100-foot focus

Illustrated Plate II*b*

Plate No.	238, 1914, May	17, 90^m.	80-foot focus

This is the well-known planetary nebula in Draco. The long exposures show a sharply outlined ellipse $24'' \times 18''$, $p = 40°$, without detail, beyond which project ansae $2''$ to $3''$ on an axis in $p = 20°$. On the shorter exposures the brighter nebulosity has the appearance of a curved thread which crosses itself several times, the ansae forming the ends. Its continuity is more or less disturbed in several places. Overlapping points are of greater brightness. At two points the thread approaches the bright stellar nucleus, giving almost the appearance of arms starting therefrom, but in neither case do they connect directly with the nucleus. The focal-plane slit spectrum appears as a continuous band corresponding to the nucleus, crossed by bright lines which project on either side. Keeler's[1] value for the radial velocity is -64.7 km, and Campbell and Moore[2] have found internal motion.

N.G.C. 6555 Hercules

$\alpha = 18^h3^m28^s$, $\delta = +17°35'.3$ (1917); $\lambda = 12°$, $\beta = +16°$

Plate No. 268, 1916, May 28–29, 360^m. Illustrated Plate IX*b*

This left-handed spiral $1'.5 \times 1'$, $p = 111°$, is in a rich field of stars. There is a star which might be taken for the nucleus, but the real nucleus is a slightly elongated knot a few seconds N. The brightest part of the nebula is a double knot at $p = 240°$, $13''$, with respect to star. A number of small faint nebulae appear on the plate.

[1] W. W. Campbell, *Stellar Motions*, p. 210.

[2] *Lick Observatory Bulletin*, No. 278, 1916.

N.G.C. 6703 Lyra

$\alpha = 18^h44^m53^s$, $\delta = +45°27'.5$ (1917); $\lambda = 42°$, $\beta = +18°$

Plate No. 269, 1916, July 1, 60^m
Plate No. 270, 1916, July 1, 180^m

A long exposure is necessary to show whether this is a ring nebula of a type very different from that usually met with, or whether a spiral, though indications point toward the former. The central nucleus lies in a bright nebulous spot which gradually fades out at 30″ diameter. The surrounding ring is very faint and narrow and about 80″ diameter.

N.G.C. 6702 appears as a nebulous spot very similar to, but fainter and smaller than, the central part of 6703. It is slightly elongated in $p = 60°$.

There are six additional small faint nebulae on the plate, three being nebulous spots and three spindles, the brightest two of the latter with respect to N.G.C. 6703 being at $p = 177°$, 8′.9, elongated in $p = 120°$, and $p = 132°$, 9′.8, elongated in 129°.

N.G.C. 6804 Aquila

$\alpha = 19^h27^m37^s$, $\delta = +9°2'.9$ (1917); $\lambda = 13°$, $\beta = -6°$

Plate No. 120, 1912, June 11, 60^m. Weak

The plate shows the nebula as a faint annulus with an irregularly shaped ring 5″ to 10″ in width and about 32″×25″, $p = 60°$. It has the typical central star and another of about the same magnitude lying directly upon the ring at the W end of the major axis. As in many planetaries, the nebulosity is stronger near the ends of the minor axis than near the ends of the major axis. Huggins[1] found that it had a bright-line spectrum.

Plate 294, 1917, June 24–25, 5^h25^m exp., shows a planetary nebula with uniform disk 65″×55″, $p = 165°$, on which lies the ring described above. The Np and S points of the rim are strengthened while the f side is missing.

[1] *Philosophical Transactions*, **166**, 386, 1866.

N.G.C. 6818 Sagittarius

$\alpha = 19^h39^m17^s$, $\delta = -14°21'.1$ (1917); $\lambda = 353°$, $\beta = -19°$

Plate No. 115, 1912, June 10, 5^m. 25-foot focus
Plate No. 116, 1912, June 10, 2^m. 25-foot focus
Plate No. 137, 1912, July 12, 75^m. 100-foot focus. Illustrated Plate II*c*

This bright planetary nebula is about 25″ in diameter and contains a small faint nucleus and much detail. Upon the faint uniform disk lies a moderately bright elliptical ring 25″×16″, $p = 9°$, and varying in width and intensity, the N end almost fading into the disk and the other end crossed by a dark streak. From each of two strong knots, about 8″ apart and equidistant from the nucleus in the W limb of the ring, a wisp runs inward to the major axis, the two wisps being parallel. A thread runs from the nucleus NE to the E limb. The spectrum has bright lines; Keeler's[1] value for the radial velocity is −16.7 km.

N.G.C. 6826 Cygnus

$\alpha = 19^h42^m34^s$, $\delta = +50°19'.4$ (1917); $\lambda = 52°$, $\beta = +12°$

Plate No. 130, 1912, June 14, 10^m
Plate No. 131, 1912, June 14, 5^m
Plate No. 132, 1912, June 14, 25^m
Bathed-process plate and red screen; Pan-Iso developer

This is a bright planetary nebula 30″×27″, $p = 127°$. The central nucleus is bright, sharply defined, and about 10″ in diameter. A knot appears at each end of the major axis, otherwise the disk is uniform. On the red-sensitive plate the nucleus is about 5″ in diameter and lies in a faint nebulous haze that fades out at about 18″ diameter. The Cassegrain short-focus camera gives a spectrum strongly continuous for the star, crossed by bright lines, some projecting but a slight distance beyond the nucleus, others clear across the disk. Values obtained for the radial velocity are −5.3[2] and −8[3] km.

[1] W. W. Campbell, *Stellar Motions*, p. 210.

[2] *Ibid.*

[3] *Publications of the Astronomical Society of the Pacific*, **27**, 239, 1915.

N.G.C. 6894, Cygnus

$\alpha = 20^h 13^m 3^s$, $\delta = +30°18'.6$ (1917); $\lambda = 37°$, $\beta = -3°$

Plate No. 4, 1911, July 2, 60^m
Plate No. 7, 1911, July 3, 14^m

This is a well-defined ring; on the outside there is a haze, particularly on E and W sides; and on the inside, many protrusions toward the center giving an internal-toothed appearance. The strongest thread of the ring measures $42'' \times 32''$, $p = 45°$. The central nucleus is stellar and small. In the Np section of the ring is a star with a very faint companion partly surrounded by a dark ring. A. Searle[1] found the spectrum to show bright lines.

N.G.C. 6905 Delphinus

$\alpha = 20^h 18^m 42^s$, $\delta = +19°15'.3$ (1917); $\lambda = 29°$, $\beta = -11°$

Plate No. 145, 1912, August 16, 180^m. 100-foot focus
Plate No. 147, 1912, September 5, 175^m. 100-foot focus
Plate No. 149, 1912, September 6, 205^m. 100-foot focus
All plates weak

This is a planetary nebula $47'' \times 34''$, $p = 175°$, containing much detail, strongest on E and W sides and weak along the NS line. Huggins[2] found it to have a bright-line spectrum.

N.G.C. 7008 Cepheus

$\alpha = 20^h 58^m 8^s$, $\delta = +54°13'.5$ (1917); $\lambda = 61°$, $\beta = +5°$

Plate No. 243, 1914, July 22, 180^m. Illustrated Plate II*d*

This planetary nebula is elliptical in shape, $95'' \times 75''$, $p = 5°$, containing much detail. The strongest bits of nebulosity are two condensations just E of the N end of the major axis. On the S*f* side the elliptical form seems eaten away, but traces of nebulosity may be seen connecting with a star which lies $p = 156°$, $53''$. A number of stars a magnitude or two fainter than the nucleus appear in the nebula. Except for one, they are surrounded by a dark ring which in turn opens directly on a dark region. As the nucleus

[1] *Harvard Annals*, **33**, 145.

[2] *Philosophical Transactions*, **156**, 385, 1866.

itself presents this appearance, it is suggested that these stars lie within the nebula. One of these stars, $p=240°$, $23''$, appears elongated; it may be a double star or a very bright bit of nebulosity. One star at $p=65°$, $29''$, with respect to the nucleus, is but partly surrounded by the dark ring. Huggins[1] found the spectrum to be gaseous.

N.G.C. 7009 Aquarius

$\alpha=20^h59^m39^s$, $\delta=-11°41'.6$ (1917); $\lambda=5°$, $\beta=-36°$

Plate No. 138, 1912, July 12, 90^m. 100-foot focus
Plate No. 140, 1912, July 13, 210^m. 100-foot focus. Illustrated Plate II*e*

This is a most striking planetary, owing to its resemblance to Saturn. The brightest nebulosity is in the form of an elliptical ring, outside diameter $30''\times13''$, $p=78°$. A second ring, more or less complete in outline, lying across the nucleus and in $p=160°$, almost at right angles to the first, shows as a condensed knot on the N side, broadening out as it approaches the S side. Another feature is the rhomboid-shaped uniform mass with the E and W edges, approximately $18''$ long lying parallel to a NS line, and with the N and S sides, $23''$ long, slightly convex outward and running parallel to the major axis of the bright ellipse. The faint ansae are about $51''$ apart and connect with the central parts of the nebula through a bar lying in $p=78°$. Other knots and threads besides those described also show. The reproduction has been prepared with a view to detail rather than to relative intensities. The focal-plane slit spectrograph shows a bright-line spectrum. The radial velocity is $+10.1$ km,[2] and Campbell and Moore have found internal motion.[3]

N.G.C. 7023 Draco

$\alpha=21^h0^m35^s$, $\delta=+67°50'.3$ (1917); $\lambda=72°$, $\beta=+14°$

Plate No. 12, 1911, July 23, 149^m

This large nebula contains a great wealth of detail and is intimately connected with a star of the seventh magnitude lying in it.

[1] *Philosophical Transactions*, **156**, 387, 1866.

[2] W. W. Campbell, *Stellar Motions*, p. 210.

[3] *Lick Observatory Bulletin*, No. 278.

It occupies one of those dark regions which appear devoid of stars and which have been explained in several ways: the stellar material is at present in the nebula, or the nebula, containing both dark and bright material, lies this side of the stars and cuts off their light. Traces of the nebula extend as far as 9′ from it, but only in those regions that are starless. The nebulosity surrounding the star is strongest and projects on its S*p* side. Several bright filaments run S*p* from the star, and there are two more S of the star running in an EW direction. The spectra of both the star and the nebulosity 13.″6 N of the nucleus photographed with the focal-plane spectrograph are continuous with absorption lines. The velocity of the nucleus is +0.7 km.[1]

N.G.C. 7026 Cygnus

$\alpha = 21^h 3^m 30^s$, $\delta = +47°30'.8$ (1917); $\lambda = 57°$, $\beta = 0°$

Plate No. 156, 1912, October 10, 120^m. 100-foot focus

This bi-nuclear planetary is formed by two nebulous knots of about the same intensity, elongated NS, one lying 6″ almost due E of the other. They are connected by a bar but there is no central star. There are traces of two loops, one on the N and another on the S, so connecting the knots that the whole forms an ellipse, 27″×11″, $p = 10°$. The spectrum shows bright lines and Campbell and Moore[2] have found internal motion.

N.G.C. 7027 Cygnus

$\alpha = 21^h 3^m 56^s$, $\delta = +41°54'.0$ (1917); $\lambda = 53°$, $\beta = -5°$

Plate No. 142, 1912, August 15, 30^m. 100-foot focus

This is Webb's bright planetary, a bright starlike patch with faint wings extending 3″ to 4″ to the N and E. A second condensation of about the same intensity as the wing, elongated in $p = 80°$, and of about the same size as the star lies at $p = 130°$, 5″. The focal-plane spectrum shows very strong bright lines with practically no continuous background. Internal motion has been detected[3] by Campbell and Moore.

[1] *Publications of the Astronomical Society of the Pacific*, **27**, 239, 1915.

[2] *Ibid.*, **29**, 55, 1917. [3] *Ibid.*, **28**, 119, 1916.

N.G.C. 7129 Cepheus

$\alpha = 21^h41^m4^s$, $\delta = +65°43'.3$ (1917); $\lambda = 73°$, $\beta = +9°$

Plate No. 273, 1916, August 31, 150^m
Plate No. 274, 1916, September 3, 25^m

This nebula lies in one of the vacant Milky Way regions in which one or more bright stars are involved in nebulosity, faint traces of which may be followed over a large part of the dark area. Seven stars are involved in nebulosity, their positions with respect to the brightest, *a*, being as follows:

ab	$p = 298°$, 58″	*ac*	$p = 50°$, 62″	*ad*	$p = 15°$, 60″
ae	$p = 355°$, 4′.5	*af*	$p = 346°$, 4′.9	*ag*	$p = 63°$, 5′.9

The nebulosity about *a* for a distance of 12″ is very strong, completely masking the star; beyond it is fainter and more or less interrupted by dark patches up to a distance of 30″, where the curve begins. From *a* the nebulosity sweeps N*f*, just passes *c* and *d* on the N, and sweeps backward to the W underneath *b*. Fainter clouds appear S*p* as far as 4′.5 from *a*. Not including *e*, *f*, and *g* the nebula lies within a circle 6′ in diameter, the center of which is about 1′.5 S*p* *a*. Two stars lie near this center, but do not seem involved in the nebula; *e*, *f*, and *g* are each centers of nebulosity of medium intensity and irregular form about 1′.5 to 2′ in diameter. A long exposure will probably show all these stars connected by nebulosity.

N.G.C. 7177 Pegasus

$\alpha = 21^h56^m44^s$, $\delta = +17°20'.4$ (1917); $\lambda = 43°$, $\beta = -30°$

Plate No. 126, 1912, June 12, 75^m

This nebula is a right-handed spiral with moderately bright nucleus, arms fairly strong over roughly 30″ diameter. Outside of this are traces of arms filling an ellipse 2′.5 × 1′.5, $p = 75°$. One arm starts from the nucleus and branches in two, the arm opposite being deformed or missing altogether.

N.G.C. 7217 Pegasus

$\alpha = 22^h 4^m 10^s$, $\delta = +30°57'.2$ (1917); $\lambda = 54°$, $\beta = -21°$

Plate No. 216, 1913, September 2, 330^m. Illustrated Plate IX*c*

This nebula is a fine right-handed spiral seen in plan. It meaures $3' \times 2'.5$, $p = 80°$. For one turn about the nucleus the nebulosity is quite bright; then it drops in intensity over a space $75'' \times 60''$ where it fades away, to increase again in brightness so as to form a ring, at the periphery $20''$ to $30''$ wide, almost as bright as the second stage. Instead of two separate arms there seem to be many small ones composed of fine, knotted, and stringy nebulosity lying closely parallel. It lies in a region rich in stars. Huggins[1] found the spectrum to be continuous.

N.G.C. 7662 Andromeda

$\alpha = 23^h 21^m 54^s$, $\delta = +42°4'.8$ (1917); $\lambda = 74°$, $\beta = -18°$

Plate No. 29, 1911, October 17, 90^m. 100-foot focus, 44-inch aperture
Illustrated Plate II*f*
Plate No. 148, 1912, September 5, 60^m. 100-foot focus
Plate No. 157, 1912, October 10, 60^m. 100-foot focus. Seed 27 plate
Plate No. 172, 1912, December 10, 1^m, 3^m, 6^m, 10^m
Plate No. 173, 1912, December 10, 7^m, 30^m
Plate No. 177, 1913, January 7, 4^m, 7^m
Plate No. 275, 1916, September 3, 1^m, 4^m, 10^m

This is the well-known planetary in Andromeda with sharp bright nucleus and a mottled disk $31'' \times 27''$, $p = 40°$, on which lies a very bright elliptical ring, $2''$ to $3''$ wide, whose median line is $15'' \times 9''$, $p = 45°$, weakened on the minor axis. The E edge is tipped with a bright line of nebulosity. The longer exposures show a considerable number of knots on the rim, and from two of these at opposite ends of a diagonal in $p = 200°$ threads appear which project over the edges and form ansae. The spectrum with focal-plane slit has bright lines, with practically no continuous background. Keeler's[2] value of the radial velocity is -11.4 km.

MOUNT WILSON SOLAR OBSERVATORY
April 1917

[1] *Philosophical Transactions*, **156**, 391, 1866.

[2] W. W. Campbell, *Stellar Motions*, p. 210.

LIGHT-CURVES AND ORBITAL ELEMENTS OF TT LYRAE AND Y CAMELOPARDALIS

By MARTHA BETZ SHAPLEY

Photographic light-curves of the eclipsing variables TT Lyrae and Y Camelopardalis have been obtained recently by Miss Harwood, and the observations, in advance of their publication, have been kindly sent to me for a discussion of the orbits. Miss Harwood's paper, which will appear shortly in *Harvard Annals*, **84**, contains a detailed treatment of the observations and reductions. The present note is devoted to a brief statement of the orbital computations, and gives the elements and the related data derived from them.

Provisional orbits for both stars have been published,[1] but because of additional and more accurate observations the new orbits entirely replace the ones computed on the basis of the visual estimates by Nijland. The observations upon which the computations in this paper are based are of considerable accuracy and can be satisfactorily represented by the theoretical curves.

The light-elements derived from the new observations are:

TT Lyrae Min. = J.D. 2410000.757 + $5^d.243708 \cdot E$
Y Camelopardalis Min. = J.D. 2410002.642 + $3.305568 \cdot E$

To the period of Y Camelopardalis was applied a small correction read from a curve to be published in Miss Harwood's paper. The positions of the stars for 1900 are as follows:

	R.A.	Dec.	Gal. Lat.	Gal. Long.
TT Lyrae	$19^h24^m.3$	$+41°30'$	$+11°$	$42°$
Y Camelopardalis	7 27.6	+76 71	+30	105

The solution for orbital elements follows the methods outlined in *Astrophysical Journal*, **35** and **36**, and in *Princeton Contributions*, No. 3. The light-curves were assumed symmetrical. The observa-

[1] *Contributions from the Princeton University Observatory*, No. 3, p. 90, 1915.

tions with positive and negative phases, counted from minimum, were plotted as a single branch, and theoretical curves were computed which would best fit the observations so plotted.

TT LYRAE

The variation at the principal minimum of TT Lyrae is two and a half magnitudes—one of the dozen largest ranges known among eclipsing variables. The maximum light-observations give positive evidence (1) of a shallow secondary minimum, (2) of a light-variation due to the ellipsoidal form of the components, and (3) of an unusually large "reflection" effect that may be wholly a conspicuous differential interradiation phenomenon, or a normal condition of reflection enhanced by periastron brightening. The latter alternative demands an eccentric orbit with periastron passage occurring at or near the time of secondary minimum. The observations are not sufficient to show orbital eccentricity through differences in the widths of the two minima. Accordingly, the orbit has been assumed circular, and the increase of maximum light around secondary minimum is attributed to interradiation. On this interpretation one hemisphere of the faint star (the one that always faces the bright companion) is eleven times as bright as the other. Since only a small part of the light of the bright star remains visible at the deepest phase of principal minimum, a large fraction of the total loss of light at that time, when measured in magnitudes, is due merely to the rotation of this unequally illuminated faint companion. The reflection-constant computed from the photographic curve is more than twice that derived for any eclipsing star heretofore. A further observational study of the maximum light would be of much interest.

The observations of TT Lyrae are from photographic plates made at Harvard. For the purpose of the orbital computations it was found convenient to bring zero phase to the mid-point of the minimum by adding $+0^d.004$ to the phases derived by Miss Harwood. Table I gives the deviations of the normal points from the theoretical curve, together with other data concerning the observations. The data referring to the principal minimum, from the fourth and sixth columns of the table, are plotted in Fig. 1.

The first orbit computed for this star was based upon the assumption that the stellar disks are uniformly luminous, except for the reflection, the effect of which is eliminated from the light-curve

TABLE I

NORMAL PLACES FOR TT LYRAE

Harwood Number	Number of Observations	Phase	sin θ	Observed Magnitude	Observed Magnitude Rectified	O−C Uniform
1– 4.....	34	$0^d.810$	+0.825	9.24	9.14	$+0^M.03$
5– 8.....	39	1.200	+ .991	9.205	9.13	+ .02
9–12.....	26	1.601	+ .939	9.19	9.11	.00
13–16.....	47	2.016	+ .667	9.20	9.13	+ .02
17–19.....	28	2.353	+ .317	9.16	9.11	− .02
20–22.....	27	2.663	− .049	9.23	9.20	.00
23–26.....	27	3.004	− .441	9.185	9.12	+ .01
27–30.....	25	3.396	− .800	9.16	9.09	− .02
31–34.....	32	3.808	− .989	9.20	9.12	+ .01
35–38.....	35	4.213	− .945	9.18	9.09	− .02
39–42.....	51	4.592	− .705	9.23	9.11	.00
43–45.....	9	4.878	− .428	9.28	9.13	+ .02
46.....	4	4.978	− .314	9.40	9.23	+ .02
47.....	2	5.032	− .252	9.66	9.44	+ .03
48.....	7	5.079	− .198	9.97	9.69	+ .01
49.....	5	5.141	− .125	10.54	10.10	.00
50.....	6	5.174	− .086	10.98	10.37	.00
51.....	6	5.222	− .028	11.59	10.67	− .01
52.....	7	0.039	+ .045	11.46	10.62	.00
53.....	7	0.083	+ .098	10.85	10.30	.00
54.....	5	0.133	+ .157	10.23	9.88	.00
55.....	7	0.176	+ .208	9.82	9.57	− .03
56.....	2	0.237	+ .278	9.59	9.39	+ .08
57.....	4	0.290	+ .339	9.34	9.17	.00
58.....	2	0.345	+ .401	9.27	9.12	+ .01
59–63.....	16	0.488	+0.552	9.22	9.09	−0.02

by rectification. Another orbit was computed for disks completely darkened at the edge. The principal elements of these solutions are as follows:

Solution	Semi-Duration of Eclipse	k	a_0	L_b	cos i
U.....	$0^d.331$	0.62	0.97	0.799	0.109
D.....	0.352	0.73	0.90	0.850	0.122

A solution intermediate between U and D is the one adopted.[1] It is given in detail in Table III. For this the darkening coefficient

[1] For an application of the method of computing orbits for intermediate degrees of darkening, see *Mt. Wilson Contr.*, No. 86; *Astrophysical Journal*, 40, 219, 1914.

chosen is $x=0.75$, a value comparable with that observed photographically on the sun.[1] The orbital inclination has been corrected for the probable polar flattening of the stars; and the densities have been corrected for polar flattening as well as for unequal mass distribution by means of the approximate relation

$$\rho=\frac{b\bar{\rho}}{c}(0.4+1.2L),$$

where b and c are the middle and shortest axes of the ellipsoidal stars, $\bar{\rho}$ is the "equal mass" density, and L is the luminosity in terms of the combined light of both components.

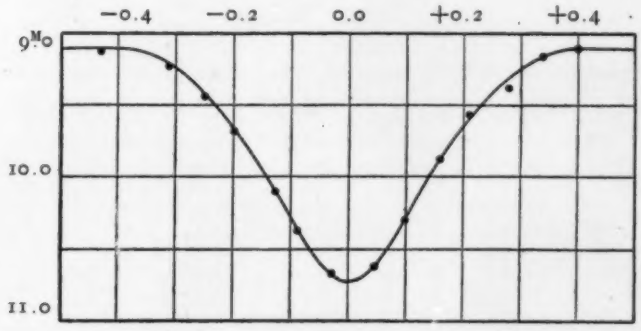

FIG. 1.—Observations and theoretical light-curve of TT Lyrae at principal minimum. Abscissae are sines of phase-angles; ordinates are magnitudes rectified for ellipticity and reflection.

Y CAMELOPARDALIS

The other eclipsing star treated in this paper, Y Camelopardalis, also has a large range, losing 78 per cent of its light at principal eclipse. Though the surface intensities of the components in this system are very unequal, there is an indication that the spectra are quite similar, for the variation is practically the same in visual and photographic light. Observations of maximum light give some evidence of a secondary minimum of a tenth of a magnitude.

Two series of observations are available—measures of photographic plates from the Harvard College Observatory and visual

[1] *Mt. Wilson Contr.*, No. 99; *Astrophysical Journal*, 41, 292, 1915.

photometric observations at Harvard by Wendell.[1] The latter are used for the orbital computations because the photographic observations at primary eclipse are relatively few in number and are derived generally from single-exposure plates taken at widely separated intervals; the phases, therefore, may be effected to some extent by the recognized irregularities of the period. Wendell's observations extend over a much shorter period of time and are exceptionally accurate and homogeneous. To the phases published in *Harvard Annals*, **69**, in addition to the correction (mentioned above) depending on the epoch, it was found necessary to apply a constant correction of $+0^{d}.011$ in order to bring the mid-point of minimum to zero phase.

TABLE II

Y CAMELOPARDALIS

No.	Phase	Obs. Mag.	O−C "Uniform"	No.	Phase	Obs. Mag.	O−C "Uniform"
1.....	$3^{d}.087$	10.70	$-0^{M}.04$	26.....	$3^{d}.357$	11.86	$-0^{M}.04$
2.....	3.140	10.86	− 1	27.....	3.358	11.92	+ 3
3.....	3.160	10.96	− 4	28.....	3.363	11.86	+ 1
4.....	3.184	11.20	+ 3	29.....	3.370	11.77	+ 1
5.....	3.192	11.23	0	30.....	3.374	11.66	− 5
6.....	3.205	11.42	+ 6	31.....	3.383	11.39	− 22
7.....	3.208	11.44	+ 5	32.....	3.384	11.63	+ 2
8.....	3.220	11.47	− 4	33.....	3.397	11.42	− 4
9.....	3.240	11.72	0	34.....	3.417	11.38	+ 11
10.....	3.245	11.69	− 10	35.....	3.434	11.20	+ 8
11.....	3.254	11.92	+ 3	36.....	3.442	11.04	− 2
12.....	3.266	12.14	+ 11	37.....	3.450	11.05	+ 4
13.....	3.269	12.03	− 3	38.....	3.451	10.98	− 3
14.....	3.271	12.08	0	39.....	3.452	11.05	+ 5
15.....	3.274	11.98	− 12	40.....	3.463	10.98	+ 5
16.....	3.290	12.30	+ 6	41.....	3.464	10.98	+ 6
17.....	3.300	12.27	0	42.....	3.476	10.83	− 3
18.....	3.308	12.33	+ 5	43.....	3.479	10.81	− 3
19.....	3.311	12.22	− 5	44.....	3.480	10.87	+ 4
20.....	3.323	12.16	− 6	45.....	3.491	10.73	− 5
21.....	3.325	12.21	0	46.....	3.495	10.72	− 4
22.....	3.347	12.06	+ 4	47.....	3.499	10.78	+ 4
23.....	3.348	11.92	− 3	48.....	3.506	10.69	− 3
24.....	3.349	12.03	+ 4	49.....	3.527	10.63	−0.03
25.....	3.352	11.98	+0.02	.....	.....	.....	.....

For Y Camelopardalis the observations were not combined into normals but are plotted singly in Fig. 2, together with the "uniform" computed curve. The adopted range at secondary minimum

[1] *Harvard Annals*, **69**, 151, 1914.

is $0^{M}.10$. There is one "uniform" and one "darkened" solution, with elements as shown in the following table:

Solution	Semi-Duration of Eclipse	k	a_0	L_b	$\cos i$
U.....	$0^{d}.245$	0.694	0.968	0.812	0.103
D.....	0.258	0.78	0.92	0.854	0.116

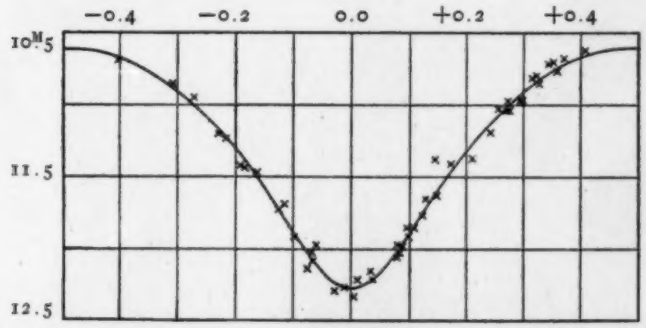

FIG. 2.—Observations and computed uniform light-curve of Y Camelopardalis. Abscissae are sines of phase-angles; ordinates are visual magnitudes.

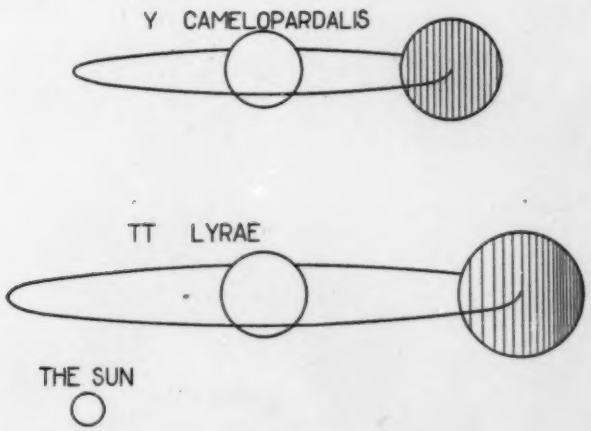

FIG. 3

The orbit adopted and given in Table III is intermediate for $x=0.6$, the value of the darkening coefficient which has been found to be

in best agreement with solar observations at the wave-length corresponding to mean visual light. Table II gives Wendell's observations during minimum, together with the phase (corrected as explained above) and the residuals from the computed curve.

TABLE III

ORBITAL ELEMENTS

Elements and Other Data		TT Lyrae	Y Camelopardalis
Period	P	5^d2437	3^d3056
Spectrum		A	A–F
Maximum	m_0	9^M17	10^M61
Depth of primary minimum	m_1-m_0	2^M48	1^M67
Depth of secondary minimum	m_2-m_0	0^M08	0^M10
Adopted coefficient of darkening	x	0.75	0.6
Semi-duration of eclipse	t'	0^d347	0^d253
Nature of eclipse		Partial, large star in front at primary	Partial, large star in front at primary
Ratio of radii	k	0.703	0.745
Fraction of light lost at primary eclipse	a_0	0.92	0.944
Light of bright star	L_b	0.835	0.832
Light of faint star, brighter end	L_f	0.165	0.168
Light of faint star, fainter end	L_f-2b	0.015	.....
Major semi-axis of bright star	a_b	0.175	0.202
Minor semi-axis of bright star	b_b	0.172	.....
Major semi-axis of faint star	a_f	0.249	0.271
Minor semi-axis of faint star	b_f	0.244	.....
Probable ratio of polar axis to major axis	c/a	0.970	.....
Cosine of inclination	$\cos i$	0.118	0.111
Ratio of surface brightness of the bright ends of the two stars	J_b/J_f	10.2	8.9
Ratio of surface brightness of the ends of the faint star	$L_f/(L_f-2b)$	11.	.....
Most probable density of bright star	ρ_b	0.067	0.11
Most probable density of faint star	ρ_f	0.010	0.02
Maximum radius of bright star in terms of sun	$\bar{a}_b$	2.80	2.36
Maximum radius of faint star in terms of sun	$\bar{a}_f$	3.98	3.18
Hypothetical absolute magnitude of bright star	M_b	−0.4	+0.7
Hypothetical parallax	π	$+0''.0011$	$+0''.001$

Fig. 3 contains a graphical representation of the two systems at greatest elongation, and below to the left the sun is drawn to scale.

SUMMARY

1. Orbits of two eclipsing binaries, TT Lyrae and Y Camelopardalis, have been computed on the basis of curves derived by Miss Harwood from Harvard observations.

2. The theoretical curves represent the observations well within their probable errors. For both variables shallow secondary minima have been observed.

3. In the system of TT Lyrae the stars are slightly ellipsoidal, and the "reflection" effect is peculiarly large.

4. The two systems are remarkably alike in many respects (see Table III and Fig. 3). Both are estimated to be more than 3000 light-years distant from the earth.

5. The densities of the brighter components are normal for the spectral types to which they belong.

PASADENA, CAL.
April 1917

STUDIES BASED ON THE COLORS AND MAGNITUDES IN STELLAR CLUSTERS

By HARLOW SHAPLEY

FIFTH PAPER: COLOR-INDICES OF STARS IN THE GALACTIC CLOUDS[1]

The interpretation of the color-results[2] for Messier 11 has involved a more thorough investigation of the general stellar fields of that part of the sky than can be made on the basis of the stars shown on the photographs of the cluster. In this system the presence of faint stars that are conspicuously bluer than those found in Messier 67 and other open clusters of high galactic latitude opens the question of the relation of color to galactic latitude and necessitates an inquiry into the frequency of color-classes in the dense galactic clouds, one of the richest of which surrounds Messier 11. The present paper is concerned with the results for color and magnitude in four fields in the immediate neighborhood of the cluster.

The position of the center of each field is given in Table I. Fields I and II are respectively southwest and northwest of

TABLE I

GALACTIC CLOUD FIELDS NEAR MESSIER 11

Field	Central Star	R.A. 1900	Decl. 1900
I.....	B.D.−7°4736	$18^h45^m\ 6^s$	−7° 8′
II.....	B.D.−6°4913	18 43 18	−6 7
III.....	.....	18 46 10	−6 28
IV.....	.....	18 45 42	−6 17

Messier 11, each nearly a degree distant, and in the denser parts of the galactic clouds, as may be seen by referring to Barnard's photographs of the Milky Way.[3] The photographic and photo-

[1] *Contributions from the Mount Wilson Solar Observatory*, No. 133.

[2] *Mt. Wilson Contr.*, No. 126; *Astrophysical Journal*, **45**, 164, 1917.

[3] *Publications of the Lick Observatory*, **11**, Plates 62–65, 1915.

visual magnitudes in these two fields were determined by direct comparison with the stars in Messier 11, and those for Field I were also derived through Polar comparisons. Table II contains a list and description of the plates used for the first two fields.

TABLE II

OBSERVATIONS ON FIELDS I AND II

Plate Number	Date	G.M.T.	Kind of Plate	No. Exp.	Exp. Time	Hour-Angle	Remarks
3201....	1916 July 6	18^h56^m	Iso	3	15^m, 2^m	10° E	I and M 11
3202....	6	19 28	Seed 27	3	3	2° E	I and M 11
3219....	7	18 52	Seed 27	3	3	11° E	I and M 11
3220....	7	19 2	Iso	3	15	8° E	I and M 11
3221....	7	20 10	Seed 27	1	7	9° W	I, for chart
3402....	Aug. 25	16 4	Iso	6	1–10	4° E	II, exp.-ratio
3403....	25	16 34	Iso	5	0.4–4	4° W	II, exp.-ratio
3404....	25	16 52	Seed 27	3	2	8° W	II and M 11
3407....	25	17 59	Iso	6	1–10	25° W	I, exp.-ratio
3431....	Sept. 6	16 4	Iso	3	5	8° W	II and M 11
3463....	24	15 23	Seed 27	3	2	16° W	II and M 11
3464....	24	15 52	Seed 27	3	2	22° W	II and M 11
3465....	24	16 0	Iso	3	10	24° W	II and M 11
3563....	Nov. 22	13 57	Iso	5	3	51° W	I and N.P.
3564....	22	14 3	Seed 27	5	1	53° W	I and N.P.

Field III is about 9′ southeast, and Field IV 7′ north of the cluster. The magnitudes were determined directly from the plates used for the study of Messier 11, which are described in the first table of the preceding paper of this series. A further partial check of the colors in all fields was obtained by the method of exposure-ratios.[1]

The fifty stars in Field I for which final results appear in Table III were selected at random from the several hundred within the measurable limits of the plates. Details concerning the measures and reductions can be omitted. It will suffice to note that the average deviation from the mean of one determination of a photographic magnitude is ±0.10; for a photo-visual magnitude the average deviation is ±0.06. The average probable error of a color-index is about ±0.08. In this field the exposure-ratios for a hundred stars give an independent determination of the colors, and, though the reduction-curve now available is provisional, the

[1] F. H. Seares, *Mt. Wilson Communications*, No. 33; *Proceedings of the National Academy of Sciences*, 2, 521, 1916.

TABLE III

MAGNITUDES AND COLORS IN FIELD I

Star	$\Delta\alpha \cos\delta$	$\Delta\delta$	Photographic Magnitude	Photo-visual Magnitude	Color-Index
1	−188″	−196″	15.46	13.88	$+1^{M}58$
2	−177	+448	15.54	14.28	+1.26
3	−154	− 33	14.78	13.65	+1.13
4	−154	+418	14.84	14.59	+0.25
5	−153	− 46	15.42	15.00	+0.42
6	−129	− 56	14.94	13.64	+1.30
7	−128	−149	13.26	12.93	+0.33
8	−119	− 1	15.12	14.62	+0.50
9	−118	+428	15.57	14.61	+0.96
10	−114	+372	14.95	14.53	+0.42
11	−103	−221	14.40	13.77	+0.63
12	− 81	− 20	14.32	14.46	−0.14
13	− 69	+174	15.41	14.43	+0.98
14	− 68	+ 95	15.38	14.86	+0.52
15	− 63	+145	16.24	15.04	+1.20
16	− 55	+330	14.42	13.81	+0.61
17	− 47	− 60	15.49	14.30	+1.19
18	− 44	+319	13.70	12.64	+1.06
19	− 38	+ 72	13.98	13.72	+0.26
20	− 37	+ 12	15.37	13.83	+1.54
21	− 35	+ 18	14.54	13.84	+0.70
22	− 34	− 67	15.31	14.43	+0.88
23	0	+189	15.07	14.64	−0.43
24	+ 25	+146	15.19	14.16	+1.03
25	+ 35	+417	14.45	13.17	+1.28
26	+ 43	+123	15.25	14.58	+0.67
27	+ 44	+196	11.45	11.34	+0.11
28	+ 49	+205	14.99	14.53	+0.46
29	+ 53	+401	14.40	12.64	+1.76
30	+ 59	+231	14.85	14.12	+0.73
31	+ 70	+223	14.77	14.37	+0.40
32	+ 80	+297	15.01	13.05	+1.96
33	+ 83	+ 14	14.96	14.05	+0.91
34	+ 87	+ 66	15.58	14.22	+1.36
35	+ 88	+ 72	13.73	12.57	+1.16
36	+ 93	+234	12.78	12.30	+0.48
37	+106	+119	14.46	14.14	+0.32
38	+116	+ 89	14.36	13.98	+0.38
39	+145	+ 22	14.36	13.83	+0.53
40	+174	+197	13.89	12.93	+0.96
41	+200	+ 79	15.39	14.56	+0.83
42	+220	+138	13.17	13.11	+0.06
43	+229	+109	13.04	12.71	+0.33
44	+244	+188	14.61	13.98	+0.63
45	+351	+216	13.29	11.48	+1.81
46	+253	+154	15.32	14.02	+1.30
47	+358	+133	14.89	13.80	+1.09
48	+361	+126	15.17	14.10	+1.07
49	+363	+169	14.89	14.57	+0.32
50	+367	+113	13.20	12.12	+1.08

results from the different methods are in satisfactory agreement. The positions given in Tables III–VI, which are intended to serve only for identification, were determined, with the aid of a reseau, from enlargements of the original negative, the orientation and scale being derived from catalogue stars.

Table IV contains results for Field II. The average deviation of a magnitude from one plate is $\pm 0^{M}.07$, giving an average probable

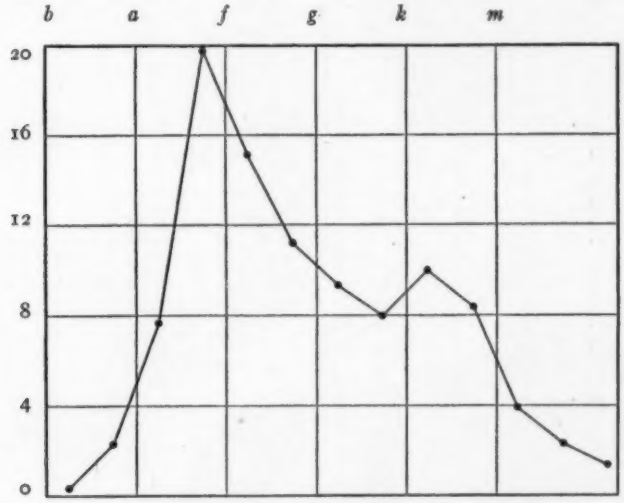

FIG. 1.—Frequency of color-classes in galactic clouds
Abscissae are color-classes; ordinates are percentages

error for a color-index of less than $\pm 0^{M}.06$. This value is independent of the accidental errors in the magnitudes in Messier 11, as thirty or forty of the cluster stars were used in the intercomparison, but it is not free from possible systematic errors in those magnitudes. From the results of the Polar comparisons for Field I and from the colors derived by exposure-ratios, this latter source of error is found to be unimportant.

The errors in the magnitudes for Fields III and IV are essentially the same as those given previously for the stars in Messier 11. Stratonoff's catalogue of stars in and near the cluster[1] includes a number of these outlying objects, and, when available, his numbers are given in the second column of Tables V and VI.

[1] *Publications de l'Observatoire astronomique et physique de Tachkent*, No. 1, 1899.

TABLE IV

MAGNITUDES AND COLORS IN FIELD II

Star	$\Delta\alpha \cos\delta$	$\Delta\delta$	Photographic Magnitude	Photo-visual Magnitude	Color-Index
1	−484″	+ 76″	12.89	12.48	$+0^{M}41$
2	−481	+144	15.68	14.50	+1.18
3	−474	+ 1	14.01	13.81	+0.20
4	−468	+ 19	13.99	13.61	+0.38
5	−467	+155	14.82	13.84	+0.98
6	−466	+ 10	16.58	14.35	+2.23
7	−463	−436	12.92	12.75	+0.17
8	−450	+ 42	14.72	14.28	+0.44
9	−449	−431	13.86	13.83	+0.03
10	−445	+ 15	15.12	14.52	+0.60
11	−440	−477	12.64	12.34	+0.30
12	−427	−500	15.84	15.01	+0.83
13	−422	− 25	15.16	13.61	+1.55
14	−411	+147	14.72	14.55	+0.17
15	−389	− 45	14.77	13.48	+1.29
16	−388	− 68	14.24	14.02	+0.22
17	−377	−521	14.47	13.45	+1.02
18	−376	+ 33	15.19	13.28	+1.91
19	−367	−353	15.30	14.97	+0.33
20	−367	−371	16.29	14.83	+1.46
21	−365	−445	14.88	13.28	+1.60
22	−364	+ 90	14.18	12.45	+1.73
23	−356	−316	15.17	14.85	+0.32
24	−354	−327	15.64	15.00	+0.64
25	−353	−526	14.50	14.50	0.00
26	−352	+107	16.69	14.69	+2.00
27	−336	−379	13.99	13.85	+0.14
28	−330	−307	15.40	13.96	+1.44
29	−325	−447	15.05	13.83	+1.22
30	−325	+ 90	16.01	14.61	+1.40
31	−322	+ 60	16.61	14.98	+1.63
32	−318	+256	14.34	14.25	+0.09
33	−315	+198	14.03	12.82	+1.21
34	−315	−373	12.66	11.82	+0.84
35	−314	−366	14.79	14.55	+0.24
36	−314	−323	14.45	14.23	+0.22
37	−303	+239	15.12	14.79	+0.33
38	−302	−208	15.20	14.66	+0.54
39	−299	−317	15.17	14.08	+1.09
40	−294	+127	14.69	14.40	+0.29
41	−292	−350	15.88	15.02	+0.86
42	−292	−199	14.99	13.98	+1.01
43	−289	+280	15.68	14.27	+1.41
44	−288	−330	14.82	14.55	+0.27
45	−283	+ 69	14.41	13.94	+0.47
46	−282	−254	14.21	13.94	+0.27
47	−281	−301	14.79	14.33	+0.46
48	−279	+120	16.64	14.56	+2.08
49	−278	+470	15.63	15.03	+0.60
50	−265	−217	15.13	14.81	+0.32
51	−260	+298	15.57	14.98	+0.59
52	−259	−249	14.74	14.30	+0.44

TABLE IV—*Continued*

Star	$\Delta\alpha \cos\delta$	$\Delta\delta$	Photographic Magnitude	Photo-visual Magnitude	Color-Index
53.....	−258″	+330″	15.16	14.63	+0^{M}53
54.....	−255	+107	14.69	14.35	+0.34
55.....	−254	+469	13.91	13.83	+0.08
56.....	−248	+178	14.82	13.28	+1.54
57.....	−245	+240	15.32	14.81	+0.51
58.....	−244	+302	16.03	14.56	+1.47
59.....	−243	+348	16.01	14.87	+1.14
60.....	−243	+372	13.78	12.03	+1.75
61.....	−238	+128	13.75	13.55	+0.20
62.....	−237	+236	14.52	14.18	+0.34
63.....	−233	−290	14.38	14.16	+0.22
64.....	−232	+241	14.15	13.85	+0.30
65.....	−228	−246	15.48	14.30	+1.18
66.....	−225	+295	14.40	13.34	+1.06
67.....	−224	−336	13.49	12.83	+0.66
68.....	−224	+146	14.79	13.94	+0.85
69.....	−221	+270	14.27	13.85	+0.42
70.....	−218	+469	15.00	14.74	+0.26
71.....	−211	+252	14.90	14.43	+0.47
72.....	−211	+470	13.63	12.39	+1.24
73.....	−210	+319	14.32	12.50	+1.82
74.....	−210	+386	14.77	14.55	+0.22
75.....	−210	+139	16.57	14.52	+2.05
76.....	−207	−259	16.50	14.57	+1.93
77.....	−200	−314	14.80	13.51	+1.29
78.....	−197	−280	15.40	14.23	+1.17
79.....	−195	+242	16.13	14.66	+1.47
80.....	−195	−445	12.27	11.43	+0.84
81.....	−186	+405	15.48	14.52	+0.96
82.....	−171	−475	15.78	14.48	+1.30
83.....	−166	−476	15.78	15.04	+0.74
84.....	−163	−482	16.08	15.09	+0.99
85.....	−155	−189	15.65	14.51	+1.14
86.....	−146	+376	16.04	14.79	+1.25
87.....	−141	−215	15.59	14.92	+0.67
88.....	−134	+411	14.77	14.90	−0.13
89.....	−125	+354	15.53	14.23	+1.30
90.....	−122	−480	14.31	13.96	+0.35
91.....	−119	−249	15.80	14.55	+1.25
92.....	−116	+429	15.40	14.80	+0.60
93.....	− 92	−268	14.87	14.42	+0.45
94.....	− 86	−514	14.69	13.58	+1.11
95.....	− 85	+401	15.56	14.15	+1.41
96.....	− 81	−492	16.08	14.72	+1.36
97.....	− 79	−479	14.72	14.52	+0.20
98.....	− 77	+282	14.85	13.96	+0.89
99.....	− 75	−534	15.49	14.95	+0.54
100.....	− 67	−282	14.90	14.86	+0.04
101.....	− 67	−493	15.12	14.85	+0.27
102.....	− 52	+299	16.18	14.77	+1.41
103.....	− 49	−482	13.46	13.39	+0.07
104.....	− 45	+283	15.56	14.35	+1.21
105.....	− 24	−265	16.26	14.88	+1.38
106.....	− 10	+315	14.72	14.23	+0.49

TABLE IV—*Continued*

Star	$\Delta\alpha \cos\delta$	$\Delta\delta$	Photographic Magnitude	Photo-visual Magnitude	Color-Index
107.....	− 7″	−237″	12.93	12.18	+0.M75
108.....	+ 2	+301	14.54	14.48	+0.06
109.....	+ 30	+332	14.45	13.05	+1.40
110.....	+ 31	+291	14.50	14.13	+0.37
111.....	+ 73	+289	15.20	14.66	+0.54
112.....	+ 89	−354	15.12	14.61	+0.51
113.....	+ 94	−349	16.61	14.74	+1.87
114.....	+100	+339	13.26	12.33	+0.93
115.....	+100	+150	15.20	14.86	+0.34
116.....	+100	−165	15.35	14.53	+0.82
117.....	+101	− 31	13.13	12.36	+0.77
118.....	+101	+247	15.68	14.37	+1.31
119.....	+101	− 59	12.36	11.35	+1.01
120.....	+105	−194	16.11	14.58	+1.53
121.....	+107	−320	13.91	12.68	+1.23
122.....	+108	−142	14.80	14.50	+0.30
123.....	+110	− 69	14.93	13.46	+1.47
124.....	+118	−424	14.77	14.50	+0.27
125.....	+121	−218	15.33	14.83	+0.50
126.....	+127	−350	14.03	13.94	+0.09
127.....	+130	−353	13.93	13.61	+0.32
128.....	+144	−177	16.22	14.86	+1.36
129.....	+150	−347	14.65	14.20	+0.45
130.....	+154	−424	15.99	14.55	+1.44
131.....	+155	+281	16.10	14.66	+1.44
132.....	+163	+ 79	15.94	14.27	+1.67
133.....	+163	−401	13.56	12.82	+0.74
134.....	+167	−120	16.07	14.76	+1.31
135.....	+174	−108	14.99	14.39	+0.60
136.....	+179	−328	14.90	14.46	+0.44
137.....	+180	+293	14.86	13.40	+1.46
138.....	+183	+145	15.17	13.22	+1.95
139.....	+187	−322	15.83	14.80	+1.03
140.....	+193	−321	15.50	14.80	+0.70
141.....	+195	+ 93	15.91	14.48	+1.43
142.....	+210	−453	15.88	14.50	+1.38
143.....	+214	−432	12.41	11.93	+0.48
144.....	+216	−155	15.75	14.27	+1.48
145.....	+219	−443	14.91	14.97	−0.06
146.....	+229	−481	13.27	13.32	−0.05
147.....	+241	−435	14.91	14.25	+0.66
148.....	+248	−180	14.92	14.02	+0.90
149.....	+249	−186	13.19	12.19	+1.00
150.....	+278	−187	16.54	14.86	+1.68
151.....	+297	−278	15.54	15.01	+0.53
152.....	+306	−497	12.46	11.50	+0.96
153.....	+310	−291	15.58	14.20	+1.38
154.....	+311	−195	16.87	15.25	+1.62
155.....	+313	−517	12.89	13.06	−0.17
156.....	+333	−491	13.78	14.20	−0.42
157.....	+334	−224	13.38	11.99	+1.39

TABLE V

MAGNITUDES AND COLORS IN FIELD III

Star	Stratonoff Number	R.A. 1900	Decl. 1900	Photographic Magnitude	Photo-visual Magnitude	Color-Index
1.....	697	$18^h45^m55^s.8$	$-6°\ 28'\ 26''$	14.45	14.14	$+0^M.31$
2.....	698	56.3	27 37	13.14	11.98	+1.16
3.....	.....	56.7	27 42	16.03	14.83	+1.20
4.....	710	57.6	28 27	13.23	12.84	+0.39
5.....	713	58.1	28 43	14.50	14.17	+0.33
6.....	730	59.9	28 46	14.46	14.21	+0.25
7.....	.....	46 0.2	27 32	15.07	14.74	+0.33
8.....	.....	0.5	28 20	15.38	15.06	+0.32
9.....	738	0.7	29 2	13.52	11.84	+1.68
10.....	.....	0.9	27 44	15.04	14.58	+0.46
11.....	740	1.1	28 25	12.02	11.96	+0.06
12.....	.....	2.0	27 56	15.22	14.85	+0.37
13.....	.....	2.1	28 54	15.12	15.18	−0.06
14.....	.....	2.5	28 5	15.04	14.71	+0.33
15.....	748	2.5	29 20	14.30	14.17	+0.13
16.....	.....	2.7	28 55	14.72	14.24	+0.48
17.....	.....	5.0	28 28	15.02	14.02	+1.00
18.....	.....	5.4	30 35	14.88	13.80	+1.08
19.....	.....	5.4	29 34	14.80	14.74	+0.06
20.....	769	6.9	27 57	14.21	14.06	+0.15
21.....	770	6.9	30 18	13.23	12.91	+0.32
22.....	.....	9.1	30 29	15.07	14.95	+0.12
23.....	.....	9.3	30 24	15.27	14.40	+0.87
24.....	780	9.4	29 10	11.60:	10.67	+0.93
25.....	.....	9.6	27 22	14.84	14.55	+0.29
26.....	.....	9.7	27 35	15.55	14.55	+1.00
27.....	.....	9.8	27 16	14.97	14.55	+0.42
28.....	782	10.1	30 32	13.76	12.47	+1.29
29.....	783	10.1	26 28	13.15	11.61	+1.54
30.....	786	10.3	27 12	13.76	13.64	+0.12
31.....	.....	10.8	25 37	14.76	13.89	+0.87
32.....	788	10.9	25 54	14.59	13.64	+0.95
33.....	789	11.2	28 57	14.11	13.84	+0.27
34.....	.....	13.2	28 52	14.93	14.68	+0.25
35.....	.....	13.3	28 42	14.93	14.48	+0.45
36.....	.....	13.6	25 39	15.98	14.55	+1.43
37.....	795	14.0	25 50	13.93	13.68	+0.25
38.....	.....	14.1	29 43	14.34	12.73	+1.61
39.....	796	14.2	29 57	13.89	13.49	+0.40
40.....	.....	15.3	27 18	15.55	14.93	+0.62
41.....	804	15.9	27 16	13.64	13.56	+0.08
42.....	809	16.6	27 34	13.52	13.36	+0.16
43.....	811	17.3	28 22	13.80	13.70	+0.10
44.....	814	17.9	26 13	14.42	14.17	+0.25
45.....	.....	19.0	27 38	14.80	13.84	+0.96
46.....	823	19.3	27 18	13.19	11.64	+1.55
47.....	.....	20.5	27 47	14.93	14.21	+0.72
48.....	.....	21.5	28 15	15.46	13.98	−1.48
49.....	.....	21.9	28 2	14.88	14.10	+0.78
50.....	.....	22.3	28 49	14.80	14.48	+0.32
51.....	.....	23.1	28 41	14.84	14.21	+0.63
52.....	831	23.2	28 29	13.56	12.82	+0.74

TABLE VI

MAGNITUDES AND COLORS IN FIELD IV

Star	Stratonoff Number	R.A. 1900	Decl. 1900	Photographic Magnitude	Photo-visual Magnitude	Color-Index
1.....	177	$18^h45^m26^s.7$	$-6°16'38''$	13.98	13.68	$+0^M.30$
2.....	.....	27.1	16 24	15.32	15.00	+0.32
3.....	.....	28.4	17 30	15.84	15.16	+0.68
4.....	.....	28.5	17 1	16.56:	14.97	+1.59:
5.....	195	28.7	18 0	14.74	13.24	+1.50
6.....	196	28.7	16 29	14.86	14.65	+0.21
7.....	.....	30.6	16 30	16.94:	14.58	+2.36:
8.....	.....	30.8	17 4	15.26	14.83	+0.43
9.....	.....	31.2	17 42	15.50	14.17	+1.33
10.....	220	31.5	17 37	13.85	12.99	+0.86
11.....	.....	32.3	18 32	14.93	14.52	+0.41
12.....	241	33.2	15 7	13.37	12.82	+0.55
13.....	.....	33.4	16 29	15.80	14.06	+1.74
14.....	246	33.5	15 13	13.85	13.33	+0.52
15.....	255	33.9	18 34	14.89	14.58	+0.31
16.....	.....	34.8	15 22	14.78	14.14	+0.64
17.....	.....	35.0	17 5	16.38	14.71	+1.67
18.....	.....	35.2	17 2	14.86	14.17	+0.69
19.....	.....	35.3	15 12	15.46	14.85	+0.61
20.....	.....	35.6	17 35	15.92	14.58	+1.34
21.....	304	36.8	15 56	12.67	11.63	+1.04
22.....	312	37.0	16 30	14.86	14.24	+0.62
23.....	326	37.7	14 59	14.51	14.17	+0.34
24.....	339	38.1	18 31	13.30	12.77	+0.53
25*.....	340	38.1	16 2	12.74	12.04	+0.70
26.....	367	39.2	16 26	14.03	13.49	+0.54
27.....	371	39.3	16 38	14.10	13.88	+0.22
28.....	382	39.8	16 49	13.36	12.64	+0.72
29.....	.....	40.0	16 28	15.35	14.91	+0.44
30.....	.....	40.0	16 35	15.42	14.21	+1.21
31.....	388	40.1	17 50	14.51	14.21	+0.30
32.....	.....	42.4	16 46	15.92	15.20	+0.72
33.....	.....	42.6	16 16	14.86	13.42	+1.44
34.....	463	42.8	18 25	14.07	13.76	+0.31
35.....	.....	43.2	16 52	15.01	13.72	+1.29
36.....	473	43.2	15 34	14.24	13.72	+0.52
37.....	479	43.3	15 58	13.72	13.42	+0.30
38.....	.....	44.0	15 30	15.39	15.00	+0.39
39.....	.....	45.0	18 41	14.97	14.62	+0.35
40.....	530	45.4	18 36	13.81	13.08	+0.73
41.....	549	46.2	18 30	13.02	12.15	+0.87
42.....	575	47.5	18 26	14.48	14.06	+0.42
43.....	578	47.5	17 43	14.26	14.02	+0.24
44.....	587	48.1	17 50	12.45	11.95	+0.50
45.....	595	48.6	18 18	14.55	14.44	+0.11
46.....	605	49.1	18 30	14.93	14.62	+0.31
47.....	626	50.5	18 30	13.18	12.39	+0.79
48.....	627	50.7	18 3	13.74	13.24	+0.50
49.....	632	51.0	17 44	14.32	13.49	+0.83
50.....	641	51.8	16 53	13.02	12.15	+0.87
51.....	646	52.2	17 26	14.97	14.48	+0.49
52.....	665	53.3	18 14	13.06	12.39	+0.67
53.....	673	53.8	18 37	14.44	14.06	+0.38
54.....	683	54.4	17 26	14.07:	14.10	−0.03:

*This star apparently varies through six-tenths of a magnitude.

The results for the four fields are collected in Tables VII and VIII, the former showing the distribution of the stars among the various color-classes,[1] the latter giving statistical data bearing on the relation of average color-index to luminosity. A wide range in color is immediately apparent; and the plot of the relative frequency of color-classes in Fig. 1 indicates that the distribution of spectral types among the fourteenth-magnitude stars is much the same in this distant galactic region as in the immediate vicinity of the sun.

TABLE VII

PERCENTAGE FREQUENCY OF COLORS IN GALACTIC CLOUDS

FIELD	COLOR-CLASS												NUMBER OF STARS
	*b*0	*b*5	*a*0	*a*5	*f*0	*f*5	*g*0	*g*5	*k*0	*k*5	*m*0	*m*5	
I*.....	0	2	6	12	18	12	12	16	12	4	2	4	50
II.....	1	3	7	17	13	8	8	8	12	12	5	6†	157
III.....	0	2	17	29	10	10	10	8	4	8	4	0	52
IV.....	0	0	2	27	24	22	10	0	8	4	4	0	51
All fields..	0.3	2	8	20	15	11	9	8	10	8	4	4‡	310

*The corresponding numbers for Field I from the 100 provisional exposure-ratio color-determinations are 0, 6, 22, 17, 11, 6, 8, 10, 7, 9, 3, 1.

† 2.5 per cent have color-indices greater than +2.00.

‡ 1.3 per cent have color-indices greater than +2.00.

A small but probably real increase of mean color with brightness is suggested by Table VIII. In Messier 11 the corresponding change is very striking,[2] the average color-index decreasing a whole magnitude as the brightness decreases three magnitudes. An examination of the individual values for the fields in the galactic clouds shows that in Table VIII, for all cases, the average deviation of the color-index from the means is large. In other words, stars of all colors are included in each interval of magnitude; and, so far as color is an index of intrinsic luminosity, this may be accepted as an indication of considerable difference in the distances of such stars. Herein the galactic clouds apparently differ from the stellar

[1] Under *b*0 are included stars with color-indices between $-0^{M}.40$ and $-0^{M}.20$; under *b*5 those between $-0^{M}.20$ and $0^{M}.00$, etc.

[2] *Mt. Wilson Contr.*, No. 126, Table VIII and Fig. 3.

group comprising the nucleus of Messier 11. There the color-phenomenon is reasonably explained, in the light of results for globular clusters as well as for moving groups of stars, as the characteristic of a relatively condensed physical group whose distances from the sun are sensibly the same.[1] These cluster-stars are probably giants in luminosity, and accordingly the distance of the group must be of the order of 15,000 light-years.

TABLE VIII

RELATION OF COLOR INDEX IN GALACTIC CLOUDS TO PHOTO-VISUAL MAGNITUDE

Field I...	Mean mag....	12.08	13.02	13.81	14.14	14.50	14.80
	Mean color...	+ 1.07	+ 0.91	+ 0.87	+ 0.78	+ 0.59	+ 0.67
	No. stars.....	6	8	10	10	10	6
Field II...	Mean mag....	12.05	13.13	13.82	14.27	14.67	15.01
	Mean color...	+ 0.96	+ 1.07	+ 0.63	+ 0.75	+ 0.93	+ 0.69
	No. stars.....	15	19	21	36	51	15
Field III..	Mean mag....	11.62	13.02	13.78	14.15	14.54	14.89
	Mean color...	+ 1.15	+ 0.62	+ 0.68	+ 0.46	+ 0.61	+ 0.37
	No. stars.....	6	8	9	11	9	9
Field IV..	Mean mag....	12.10	13.01	13.62	14.14	14.56	14.96
	Mean color...	+ 0.78	+ 0.74	+ 0.64	+ 0.72	+ 0.44	+ 0.66
	No. stars.....	7	8	9	11	8	8
All fields..	Mean mag....	11.99	13.07	13.77	14.21	14.62	14.94
	Mean color...	+ 0.98	+ 0.90	+ 0.69	+ 0.70	+ 0.80	+ 0.60
	No. stars.....	34	43	49	68	78	38

The wide dispersion in magnitude of both blue and red stars indicates a similarly great distance for the neighboring galactic clouds. It suggests that the extent of the stellar clouds in the line of sight is relatively very great—in fact, the depth may be as great as, or greater than, the distance to the nearer boundary.

Fainter than the fourteenth photo-visual magnitude the average color-index in Messier 11 begins to increase (see Fig. 3 of the preceding paper). These faint stars might perhaps be considered as at the head of the series of dwarf stars in a stellar system that includes all the grades of luminosity found among the stars at large;

[1] The correction of the cluster-results (if it were rigorously possible) for the stars not belonging to the physical group would not affect these conclusions.

but a preferable interpretation is that the physical group in Messier 11, containing chiefly stars of high luminosity, has but a few stars fainter than the fourteenth apparent magnitude. The increasing redness, then, is due to the increasing predominance of the members of the star-clouds, which we now find are of all color-classes with an average index, between the fourteenth and fifteenth magnitudes, of +0.70.

SUMMARY

1. Magnitudes and colors have been determined for three hundred stars in four fields in the vicinity of the open galactic cluster Messier 11. Twenty-three plates have been used in the discussion, and the various errors are satisfactorily small.

2. As in Messier 11, a wide range of color is present; but the change of color with brightness is hardly perceptible. The magnitudes of the blue stars seem to indicate the remoteness of the star-clouds and also their great dimensions. Similar results have been obtained in a number of other galactic fields,[1] all pointing to a diameter of the galactic system considerably greater than generally supposed.

3. The cluster Messier 11 proves to be a physical group in the midst of the star-clouds, which on their own part have the general appearance and some of the properties of an enormous but definitely outlined physical system. There is no certain evidence as yet of the existence of dwarf stars, either in Messier 11 or in the galactic clouds.

MOUNT WILSON SOLAR OBSERVATORY
April 1917

[1] *Mt. Wilson Communications*, No. 44; *Proceedings of the National Academy of Sciences*, 3, 269, 1917.

EFFECT OF A LONGITUDINAL MAGNETIC FIELD UPON GLOW-DISCHARGE

By R. F. EARHART and C. B. JOLLIFFE

A relation probably exists between variation in solar activity and magnetic phenomena. This is the general conclusion reached from observations on sun-spots and recorded variation in terrestrial magnetism. The application of the Zeeman effect to magnetic variations in the sun-spots made by Professor Hale and colaborers at Mount Wilson bears out this connection. The authors' information, while exceedingly incomplete, may be briefly summarized.

Accompanying variations in the solar activity which are observed visually, there are magnetic disturbances on the earth. These magnetic disturbances are probably due to change in the magnetization of the sun itself, the magnetic field in the surrounding region being disturbed thereby. Our terrestrial observations are records of this general change. It has never been made clear to the authors which is the cause and which the effect—that is, whether the luminous solar variations are due to magnetic changes or whether variations in the streams of luminous and possibly electrified matter cause the magnetic variations. Possibly both are effects of some more fundamental cause. Any relation between variation of the magnetic field and variation of the luminous glow-discharge will have at least a bearing in the general subject.

The senior author of this paper has previously made some experiments on the effect of a magnetic field on glow-discharge in a vacuum tube.[1]

In the former experiment the discharge took place between flat plates, and the current-density was small. It was found that for a pressure less than the critical pressure (low pressure) the longitudinal field tended to suppress the discharge, while for higher pressure the current-density was increased with increasing field-strengths, but that a maximum value of the field was attained beyond which increase in field no longer increased the discharge.

[1] *Physical Review*, 3, 103, 1914.

The intent of the present experiment is to extend the measurements to larger currents. The method of controlling, measuring the current passing through the discharge-chamber, and determining the potential-difference between the terminals is precisely as in the former experiment, save that all electrical measurements

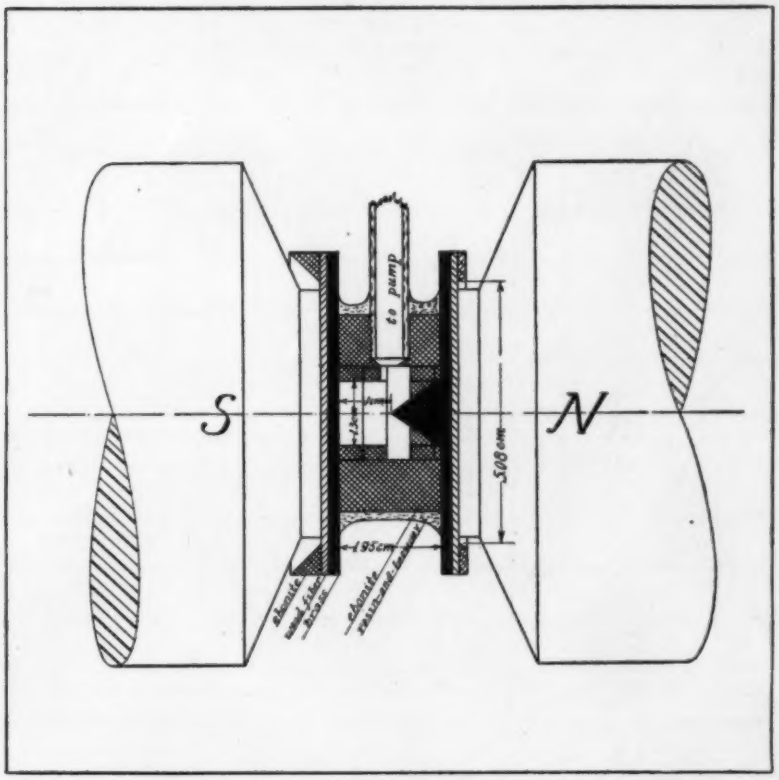

FIG. 1

were made with direct-reading voltmeters and millimeters. The discharge-chamber indicated in Fig. 1 was a cylindrical tube closed at one end by a flat plate and at the other by a conical electrode. The tube was coaxial with the poles of a large electromagnet. The pole-pieces of the magnet measured 5.08 cm across the face. Exploration with a flip-coil showed a uniform magnetic field to exist in the central region. The intent was to produce a

discharge with the electric and magnetic lines of force parallel. This was accomplished, barring the distortion of the electric field due to the shape of the conical electrode. It will be noted later that this distortion greatly modifies the result where the cone was the cathode.

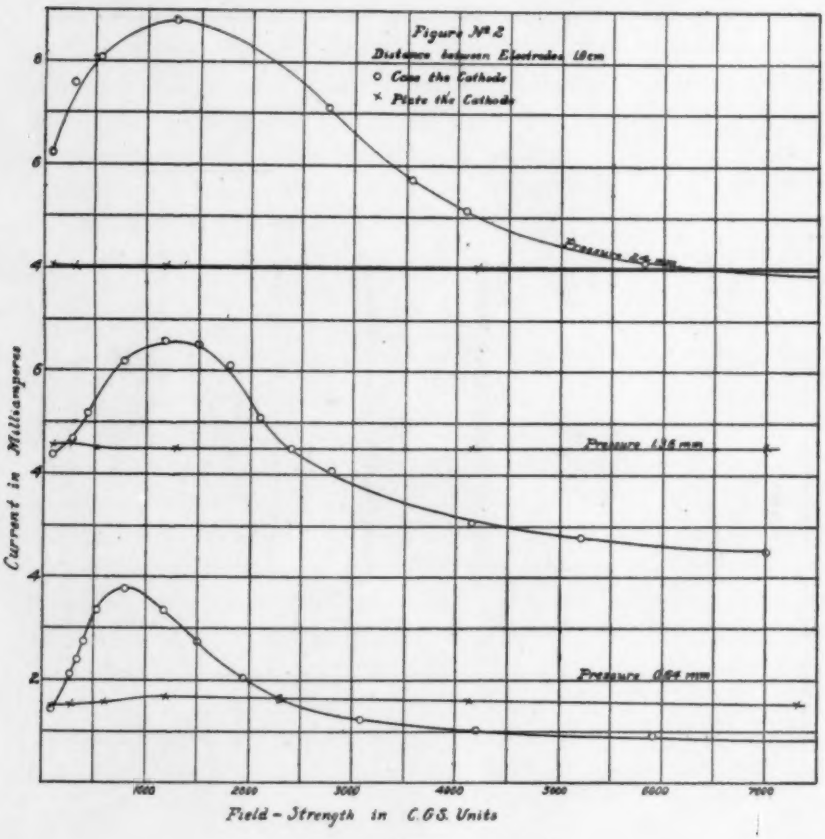

FIG. 2

The plan adopted was to produce a current through a circuit consisting of a set of storage cells, a controlling device, an ammeter, and the discharge-chamber; then, without altering any other control factor, to make readings of the current simultaneously with variation in the magnetic field. Measurements of pressure were made with a McLeod gauge. Dry air was the only dialectric used.

A large number of curves showing relation between current and field-strength were obtained. The various factors altered in obtaining these results were pressure, length of gap, area of electrodes, polarity, and potential-difference. A few typical results are reproduced. Fig. 2 shows three members of a family of curves obtained

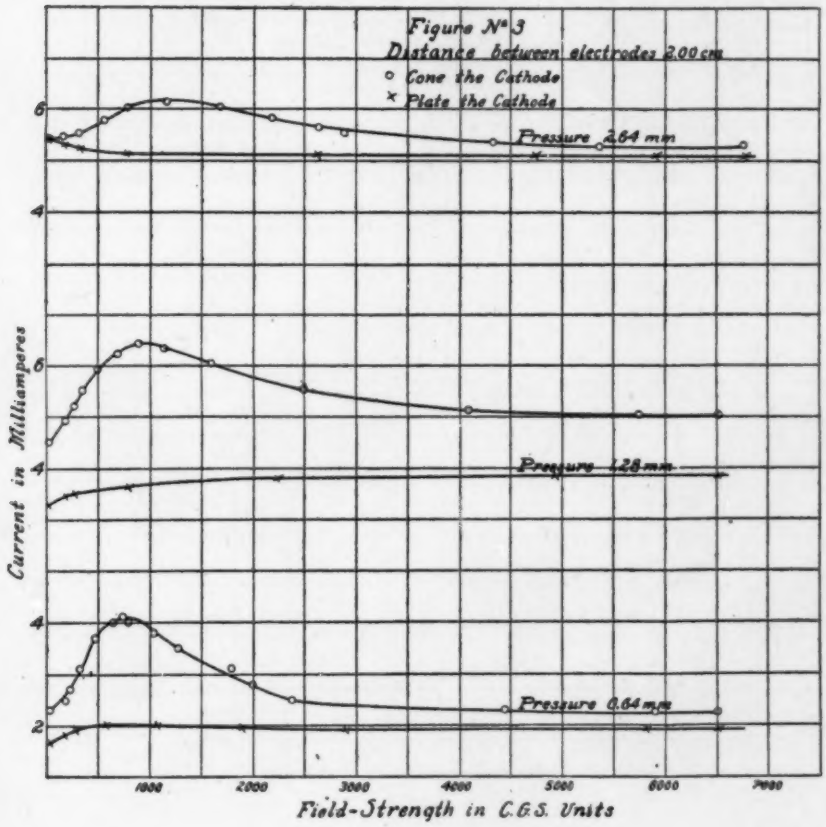

FIG. 3

when the gap was 1 cm. Circles (o) represent values when cone is cathode; crosses (X) give values when plate is cathode. Similar families were obtained for distances of 0.5 cm, 1.5 cm, and 2 cm. The results obtained in the last case are shown in Fig. 3. Finally, the effect of concentrating the discharge from one electrode, leaving the other undiminished, was studied by covering one-half of the

cone by a ring of insulating material, leaving the point projecting. Similarly the plate electrode was reduced one-half, the original area of the cone being restored at the same time. The results are indicated in Fig. 4. It may be noted that when the cone is made

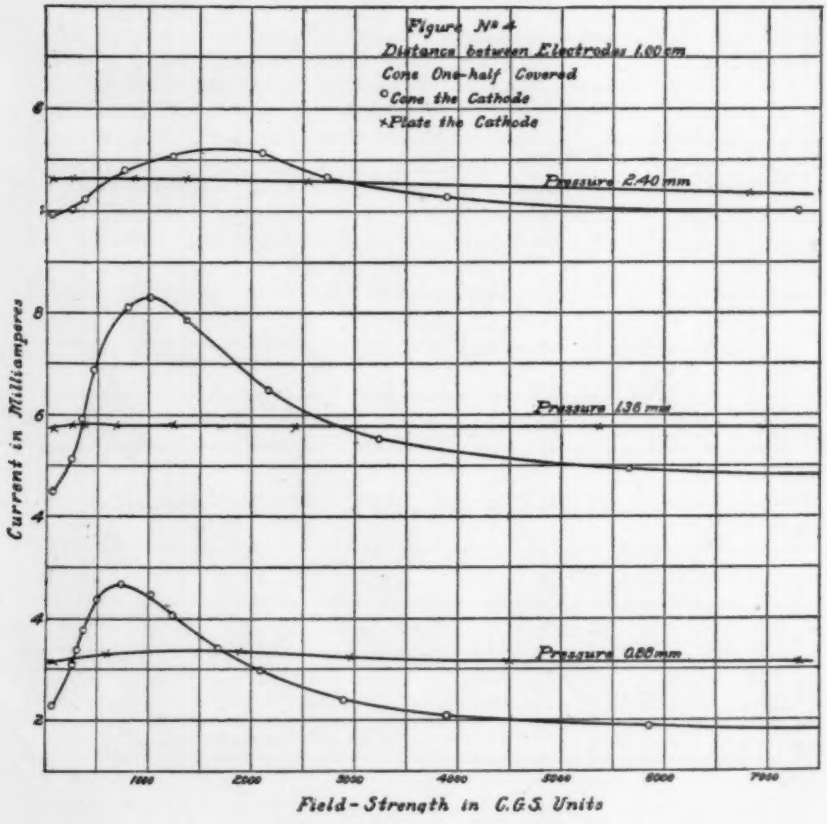

FIG. 4

the cathode an increase in field causes a rapid increase in current up to a well-defined maximum, which is best defined at low pressures. A further increase causes a rapid decrease in current, followed by a more gradual decrease. The final values in many cases are less than the original value. Increase in pressure causes a shift in maximum toward higher fields. The omitted curves bear out this statement completely. Lengthening the discharge-gap, as well

as decreasing the area of the electrodes, serves to flatten the peaks, which means that the variations due to magnetic fields are less abrupt, thus making the wider area more sensitive to small changes in the critical region. When the flat plate is made cathode, the

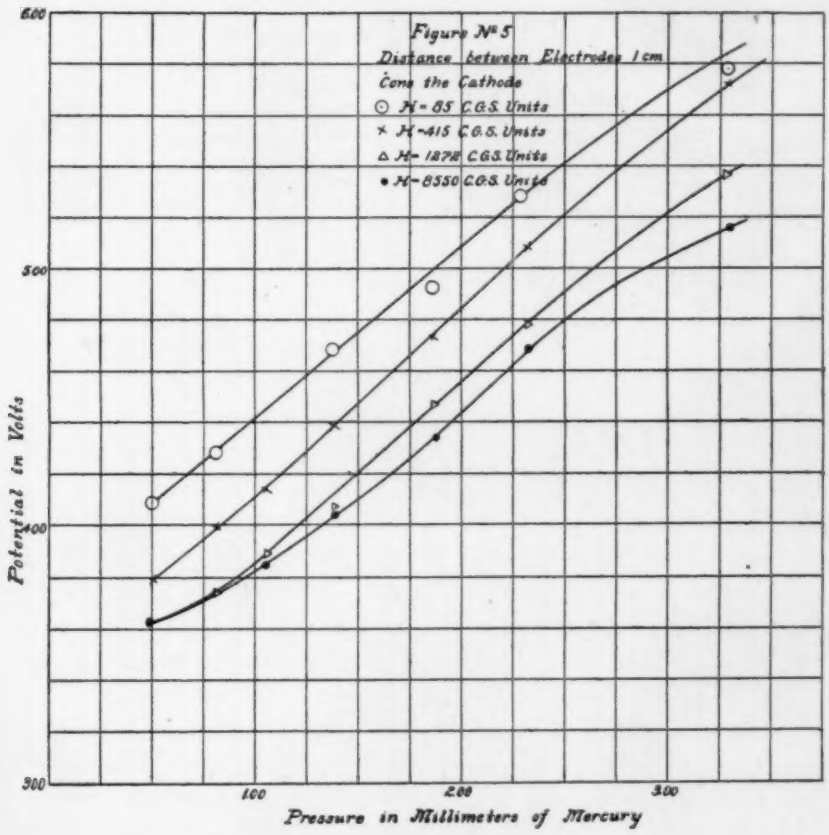

FIG. 5

shape of the curves is different. Changes due to field-strength are not great, and no well-defined maximum appears.

SPARK-POTENTIALS

Measurements were made on the potentials required to start a discharge, using the apparatus shown in Fig. 1. The spark-length chosen was 1 cm. Pressures were varied from 0.5 mm to

3 mm of mercury. The cone was made cathode and the minimum potential required to produce a discharge was determined. The pressure remaining constant, the field was varied from 85 to 8550 c.g.s. units in eleven steps. The value 85 represents the

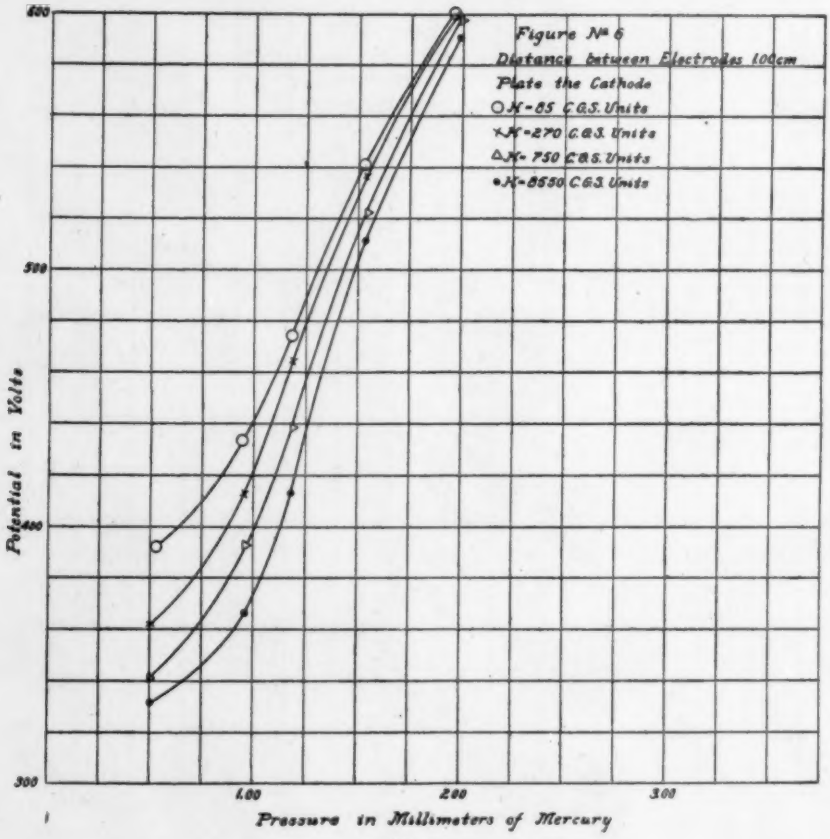

FIG. 6

residual magnetism, i e., the field-strength with zero current in the coils of the magnet.

Fig. 5 indicates the results for several pressures with the cone as cathode. A reduction of spark-potential with increase in fields up to 1300 c.g.s. units is quite marked. Above such values changes are small. Fig. 6 shows values secured with the polarity reversed.

PHYSICAL LABORATORY
OHIO STATE UNIVERSITY
COLUMBUS, OHIO
June 2, 1917

Minor Contributions and Notes

NOTE ON THE SOUTHERN TAIL OF HALLEY'S COMET SEEN MAY 17 AND 18, 1910

In a paper printed in the *Astrophysical Journal*, **39**, 373, 1914, I gave two drawings of the tail or tails of Halley's comet on the nights of May 17 and 18, 1910. Below the long bright tail a luminous region is shown in each drawing, extending to the south-eastern horizon, with a definite dark rift between it and the bright tail. On the original drawing this dark rift is more strongly marked, and the lower illumination is quite definitely bounded at its upper part, where it makes the lower edge of the dark rift. In the paper referred to, this lower illumination is attributed to a second tail (which I now think was probably the main tail) of the comet, which perhaps blended into the zodiacal light, since this tail extended along the ecliptic.

This second tail is an interesting factor in the study of the close approach of Halley's comet to the earth at that time and the probability of the earth having passed through a part of the tail. It is therefore important to know just how much of this object belonged to the comet and how great a part the zodiacal light played in the phenomenon.

The southern observers (among them Perrine at Cordoba, who has given a good account of the two tails in the *Astronomical Journal*, **26**, 145, 1910, and Innes at the Union Observatory, South Africa), who saw the comet under better conditions, unhesitatingly describe it as having two tails—a northern tail and a southern one much broader and only one-half as bright. Their location of these tails among the stars agrees closely with the drawings given in the *Astrophysical Journal* referred to (Plate X). The question with me was not whether the comet had two tails, for this fact was evident from the definite northern boundary of the southern branch, which is not a characteristic of the edges of the zodiacal light, but how much of the phenomenon belonged to the comet and how much to the zodiacal light. Fortunately this is a question that can be

decided by an actual observation of the region of the comet under similar atmospheric conditions on or about May 18 of any year.

In the present year the smoky condition of the sky prevented any observations of this kind here until the night of May 22, at which time the conditions were good and the sky was certainly as clear as on the nights of May 17 and 18, 1910. At frequent intervals on the night above mentioned, while working with the Bruce telescope, I carefully examined the region of the drawings of 1910 from 12^h30^m to 15^h0^m, Central Standard Time, or later, for traces of the zodiacal light. The effect of this light was not visible at any time. The sky was free from any illumination where the supposed southern tail was seen. The dawn came up as usual with a uniform illumination rising from the horizon, and was not specially noticeable until after 14^h45^m. As late as 14^h50^m the arch of dawn was only beginning to whiten the horizon, though the sky was beginning to whiten generally.

From these observations it is clear to me that as seen from this latitude the zodiacal light could not have entered at all into the phenomenon of 1910. It is also clear that the brightness along the southeastern horizon in 1910 before 14^h45^m C.S.T. was due entirely to the second branch of the tail of Halley's comet. This is a fact that can be substantiated at the Yerkes Observatory any year in the latter half of May under proper conditions of the sky. This fact may be of interest in connection with the observations in 1910 made in the Southern Hemisphere, where the large angle made by the ecliptic with the horizon may have introduced an effect from the zodiacal light.

In the *Astronomical Journal*, **26**, 140, 1910, there is a report by Professor Mary Whitney, of Vassar College Observatory, where the second tail was seen but was attributed to the zodiacal light. Doubtless similar observations of this tail were made elsewhere in the Northern Hemisphere with the same inference.

So far as the observations at the Yerkes Observatory are concerned, the phenomenon of 1910 was in no way due to the zodiacal light, but belonged entirely to the comet.

E. E. BARNARD

YERKES OBSERVATORY
May 24, 1917